# IDENTIFICATION OF SOURCE REGIONS AFFECTING CHEMICAL COMPOSITION OF ATMOSPHERIC PARTICLES IN EASTERN MEDITERRANEAN USING TRAJECTORY STATISTICS

A THESIS SUBMITTED TO
THE GRADUATE SCHOOL OF NATURAL AND APPLIED SCIENCES
OF
THE MIDDLE EAST TECHNICAL UNIVERSITY



BY

CANAN GAMZE (EMRE) GUNAYDIN

IN PARTIAL FULFILLMENT OF THE REQUIREMENTS FOR THE DEGREE OF
MASTER OF SCIENCE
IN
THE DEPARTMENT OF ENVIRONMENTAL ENGINEERING



OCTOBER 2000

Approval of the Graduate School of Natural and Applied Sciences

Prof. Dr. Tayfur Öztürk
Director

I certify that this thesis satisfies all the requirements as a thesis for the degree of Master of Science.

Prof. Dr. Ülkü Yetiş
Head of Department

This is to certify that we have read this thesis and that in our opinion it is fully adequate, in scope and quality, as a thesis for the degree of Master of Science.

Prof. Dr. Gürdal Tuncel
Supervisor

Examining Committee Members

Prof. Dr. Kahraman Ünlü

Prof. Dr. Gürdal Tuncel

Prof. Dr. Celal Gökçay

Prof. Dr. Selçuk Soyupak

Assoc. Prof. Dr. Gülen Güllü

## ABSTRACT

# IDENTIFICATION OF SOURCE REGIONS AFFECTING CHEMICAL COMPOSITION OF ATMOSPHERIC PARTICLES IN EASTERN MEDITERRANEAN USING TRAJECTORY STATISTICS

Günaydın (Emre), Canan Gamze

M.S., Department of Environmental Engineering

Supervisor: Prof. Dr. Gürdal Tuncel

October 2000, 123 pages

Three backtrajectory models, namely, Branching Atmospheirc Transport, National Oceanic and Atmospheric Administration (Hyslpit) and European Centre Medium Range Weather Forecast trajectory models were compared by both qualitatively and quantitatively for the purpose of investigating the differences between the trajectories calculated by different models .

The trajectories of each model passing through Istanbul were selected to be able to differentiate the ones better relating high pollutant concentrations at Antalya. BAT trajectories performed better than ECMWF trajectories in relating high Pb concentrations and Hysplit trajectories were better than ECMWF trajectories to relate high $SO_4^{2-}$ and $NO_3$ concentrations observed at the receptor site.

The residence time of air masses over the study area and percentage flow contributions from wind sectors were calculated. The ECMWF trajectories differed from BAT trajectories greatly, whereas, ECMWF and Hysplit trajectories were displayed an approximate residence time distribution and percent flow contributions from each wind sectors.

The single and three layer Potential Source Contribution Function; Concentration and Redistributed Concentration Fields approaches used in trajectory statistics were applied to Antalya using $SO_4$, Al and Pb as test elements and 3D ECMWF trajectories during March 1992 and December 1993. The source regions identified by each approach showed a general agreement. Each method identified the sources that are close to the receptor site, however, the distant sources were heavily weighted in redistributed concentration fields and three layer PSCF.

To understand the air mass transport patterns to eastern Mediterranean, western Mediterranean and Black Sea basins, flow climatology analysis was performed for the receptor sites selected in each basin. The backtrajectories for the years 1992, 1993, 1994 and 1995 were calculated daily by 3D ECMWF trajectory model for each receptor site. This treatment indicated that the air mass flow to the each of the basin were from North, Northwest, Northeast and West sectors.

The potential source regions of pollutants affecting each basin were calculated by residence time - emission intensity product and PSCF analysis using the experimental concentration data. The differences observed between theoretical and experimental source regions was found out to be scavenging of particles during transport.

Keywords: Mediterranean, Backtrajectory, Trajectory statistics, Potential Source Contribution Function, Concentration Fields, Redistributed Concentration Fields

# ÖZ

## DOĞU AKDENİZ ATMOSFERİNDEKİ PARTİKÜLLERİN KOMPOZİSYONUNU ETKİLEYEN POTANSİYEL KAYNAK BÖLGELERİNİN TRAJEKTORİ İSTATİSTİĞİ İLE BELİRLENMESİ

Günaydın (Emre), Canan Gamze
Yüksek Lisans, Çevre Mühendisliği Bölümü
Tez Yöneticisi: Prof. Dr. Gürdal Tuncel

Ekim 2000, 123 sayfa

Dallandırılmış Atmosferik Taşınım, Ulusal Okyanus ve Atmosfer Yönetimi ve Avrupa Orta Ölçekli Hava Tahminleri Merkezi trajektori modelleri kalitative ve kantitative olarak karşılaştırıldı. Bu karşılaştırmadaki amaç, farklı trajektöri modelleri ile hesaplanan trajektöriler arasındaki farklılıkları incelemekti.

Kalitative karşılaştırma sonucunda, İstanbul'dan geçen BAT trajektorilerinin reseptör noktasında gözlemlenen yüksek Pb konsantrasyonu ve Hysplit trajektorilerinin yüksek $SO_4^{2-}$ ve $NO_3$ konsantrasyonları ile ECMWF trajektorilerinden daha yüksek oranda bağlantılı olduğu görüldü. Trajektori modellerinin kantitative olarak karşılaştırılması için hava kütlelerinin ülkeler üzerinde geçirdiği zaman ve % olarak her bir rüzgar sektörünün katkısı analiz edildi. Bunun sonucunda, ECMWF trajektorileri ile hesaplanan hava kütlelerinin çalışma

alanı üzerinde geçirdiği zaman ve sektörel katkıların, BAT trajektorileri ile hesaplananlardan büyük ölçüde farklılıklar gösterdiği, Hysplit ile yapılan hesaplarla oldukça yakın sonuçlar verdiği görüldü.

Trajektori istatistiğinde kullanılan tek ve üç boyutlu potansiyel kaynak katkı fonksiyonları, Konsantrasyon alanı ve tekrar dağıtılmış konsantrasyon alanı metotları Mart 1992 ile Aralık 1993 tarihleri arasında Antalya'da sonuçlanan ECMWF geri trajektorileri ile uygulandı. Her bir yaklaşımla $SO_4^{2-}$, Al ve Pb için belirlenen potansiyel kaynak bölgeleri birbirine yakın sonuçlar verdi. Her yöntem, reseptör noktasına yakın olan kaynak bölgelerini belirlerken, uzak kaynak bölgeleri daha çok üç boyutlu PKKF ve tekrar dağıtılmış konsantrasyon alanı metotları ile belirlenmiştir.

Hava kütlelerinin Doğu Akdeniz, Batı Akdeniz ve Karadeniz'e taşınım yollarını anlamak için her bir havzada seçilen reseptör noktası için akış klimatolojisi analizi yapıldı. Her reseptör noktasında 1992,1993,1994 ve 1995 yılları boyunca günlük 3 boyutlu ECMWF geri trajektorileri hesaplandı. Akış klimatolojisi çalışması her bir havzaya hava kütlelerinin taşınıcının Kuzey, Kuzeybatı, Kuzeydoğu ve Batı sektörlerinden olduğunu gösterdi.

Her havzayı etkileyen kirleticilerin potansiyel kaynak bölgeleri hem hava kütlelerinin seçilen alt bölgelerde geçirdikleri süre ile alt bölgelerdeki emisyon değerlerinin çarpımı ile, hem de deneysel konsantrasyon verilerinin kullanıldığı PKKF yöntemi ile hesaplandı. Teorik ve deneysel olarak elde edilen potansiyel kaynak bölgelerinde gözlenen farklılıkların partiküllerin taşınım sırasında uzaklaştırılmasından kaynaklandığı belirlendi.

Anahtar Kelimeler: Akdeniz, Geri trajektori, trajektori istatistiği, Potansiyel Kaynak Katkı Fonksiyonu, Konsantrasyon Alanı, Tekrar Dağıtılmış, Konsantrasyon Alanı

*To my dear husband Hakan*

*and my parents Nadire and Murat Emre*

## ACKNOWLEDGMENT

I would like to express my sincere appreciation to Prof. Dr. Gürdal Tuncel for his great guidance, support and encouragement throughout this study.

I am also grateful to Assoc. Prof. Gülen Güllü for her valuable helps at every step of my study. I would also like to thank Dr. Duran Karakaş, Dr. Omar El-Agha for their guidance and Dr. Saleh Abdalla for helping me for getting backtrajectories.

I would like to thank to all my friends in Atmospheric Chemistry Research Group for their moral support and valuable suggestions at every step of this study.

Finally I am deeply grateful to my parents Nadire and Dr. Murat Emre, my dear sister Şahika Gaye Tacal and to my dear husband Hakan Salih Günaydın for their endless support and faith in me both during this study and throughout my life.

## TABLE OF CONTENTS

## LIST OF TABLES

TABLE

## LIST OF FIGURES

FIGURE

## LIST OF ABBREVIATIONS

| | |
|---|---|
| ECMWF | European Centre for Medium Range Weather Forecast |
| HYSPLIT | Hybrid Single Particle Lagrangian Transport |
| BAT | Branching Atmospheric Transport |
| PSCF | Potential Source Contribution Function |
| CF | Concentration Fields |
| RCF | Redistributed Concentration Fields |

# CHAPTER 1

# INTRODUCTION

## *1.1. Framework*

The long-range transport of pollutants has come under scrutiny in the last decade. In the late 1980's three problems have aroused associated with longer live pollutants and the pollutants that are transported through the atmosphere. These problems are acid rain, ozone layer destruction and build up of greenhouse gases in the atmosphere.

The pollutants that are emitted to the atmosphere can be transported over long distances and influence both ecosystems and human health adversely. It has been also recognised that, the atmosphere is an important route for the transport of pollutants from continents to the oceans. The pollutant flux via transport through the atmosphere may lead to severe pollution of inland water bodies such as Mediterranean and Black Sea.

The Mediterranean and Black Sea are of special importance since industrialised regions, which are the sources of continuous flux of anthropogenic substances, surround them. Additionally, the population increase in the bordering countries of these water bodies resulted in continuously increasing pollution due to the high amount of waste disposal, atmospheric transport and deposition of pollutants.

As a result of the recognition of the global nature of the transport of pollutants, the co-operative action of bordering countries was become obligatory.

The first international action was adopted by an international meeting in 1975, convened by United Nations Environment Programme (UNEP), which was accepted by 16 bordering countries of Mediterranean Sea. The measures necessary to protect the Mediterranean Sea and to control of pollution were discussed in this conference.

Although extensive data are now available concerning pollution of the specific locations in Mediterranean, the data collection methodologies are not comparable enough. Therefore, the utilisation of databases is not effective and it is necessary to set up evaluation criteria, which can highlight the gaps in knowledge and allow a better data gathering methodology. This problem was addressed in the framework of a study performed in cooperation of Mediterranean Action Plan (MAP) by European Environment Agency (EEA) and European Topic Centre on the Marine and Coastal Environment (ETC/MCE). The data for the assessment were taken from UNEP/MAP database and MEDPOL (Mediterranean Pollution Assessment and Control Programme). The results of this study were presented in a report "State and pressures of the marine and coastal Mediterranean environment", edited by G. Izzo and S. Moretti in 1997. Various interactions between human activities and environment, and also the political actions to reduce the damage to Mediterranean environment were described in this report.

The first international coordinated plan of the protection of Black Sea was the "Convention for the Protection of the Black Sea Against Pollution" and signed in Bucharest, 1992, by six Black Sea countries. The "Bucharest Convention" contained a framework of agreement and three specific protocols, which are based on; (1) the control of land based sources of pollution, (2) waste dumping (3) joint action in the case of accidents.

### *1.2. Scope of the Study*

In this study, the atmospheric long range transport patterns of major natural and anthropogenic pollutants to the receptor site located in eastern Mediterranean basin was investigated by several statistical methods using the back trajectory modelling. The purposes of this investigation were to determine the source regions of major pollutants and their transport mechanisms, and also to make a comparison of the source locations determined by different statistical methods applied.

The main objectives of this thesis are stated below:

**1.Comparison of three back trajectory models:** Trajectory models are helpful in determining the source regions of pollutants as they give information about the history of an air parcel before arriving the sampling site. There exists several trajectory models based on different assumptions and procedural designs. Therefore, it will be beneficial to make a comparison between them. In this study, using the three different back trajectory models, namely BAT, HYSPLIT and ECMWF, the transport patterns to the Eastern Mediterranean Basin, and the residence time of air masses over the source locations are determined. By this way, it could be possible to make a comparison.

**2.Determination of the regional sources of pollutants affecting the Eastern Mediterranean atmosphere:** Up to now, a limited number of studies were performed to identify the potential source regions of pollutants affecting Mediterranean atmosphere, most of which were involving the western part of the basin.

Identification of source regions affecting eastern Mediterranean atmosphere was studied by Güllü (1996) by one of the trajectory statistics method, named

previous study performed in our group, the flow patterns to receptor locations at eastern Mediterranean, western Mediterranean and Black Sea basins were also investigated (Güllü, 1996). However, the reliability of the model used to calculate back trajectories was reported to be low in the literature and therefore the atmospheric flow patterns to these sites were calculated using a more recent back trajectory model.

The flow frequency to the receptor sites Antalya (eastern Mediterranean), Corsica (western Mediterranean) and Bartın (Black Sea) were investigated by classification of back trajectories according their transport sectors.

In the following chapter of this thesis one can find a survey of existing works related to the atmosphere, and specifically to the Mediterranean Basin. This chapter first gives brief information about sources of trace elements in the atmosphere, the climatology and transport regimes of Mediterranean and Black Sea basins and reviews trajectory modelling.

The three different trajectory models and their basics are discussed in the third chapter. In addition, the statistical methods available to identify the source locations of pollutants are explained.

The obtained results are discussed in the following chapter. The source regions determined by different statistical approaches and back trajectory models are compared in this section.

In the fifth chapter of this study, concluding remarks together with the suggestions for future research on this subject are given.

# CHAPTER 2

# BACKGROUND

## *2.1. Atmospheric Trace Elements, Ionic Species and Their Sources*

Aerosol is a mixture of particles and gases that exhibit stabilization in gravitational field. Aerosols consist of both solid and liquid particles that are suspended in air.

The aerosols originate from both natural (pollen, salt spray, soil erosion) and anthropogenic (soot, fly ash, metal oxides) activities in the atmosphere. The presence of aerosols in the atmosphere may result in the visibility reduction and threatens the public health. They are also responsible for the changes in the radiant energy reaching the earth's surface and modify the climate since the atmospheric processes like light scattering and absorption are influenced by the presence of aerosols.

The particle size is the most important characteristics of aerosols in the ambient atmosphere. Particles range in size from approximately 0.005 to 500 μm. Atmospheric aerosols are accepted to have a trimodal distribution as shown in Figure 2.1. These modes are (1) nuclei (diameter,d < 0.1 μm); (2)accumulation (0.1μm < d< 0.2 μm) and (3) coarse (0.2 μm< d).

The nuclei mode is produced by combustion or other high temperature processes. The particles in this mode can coagulate to form accumulation mode particles. Mechanical processes such as grinding usually produce the coarse particles.

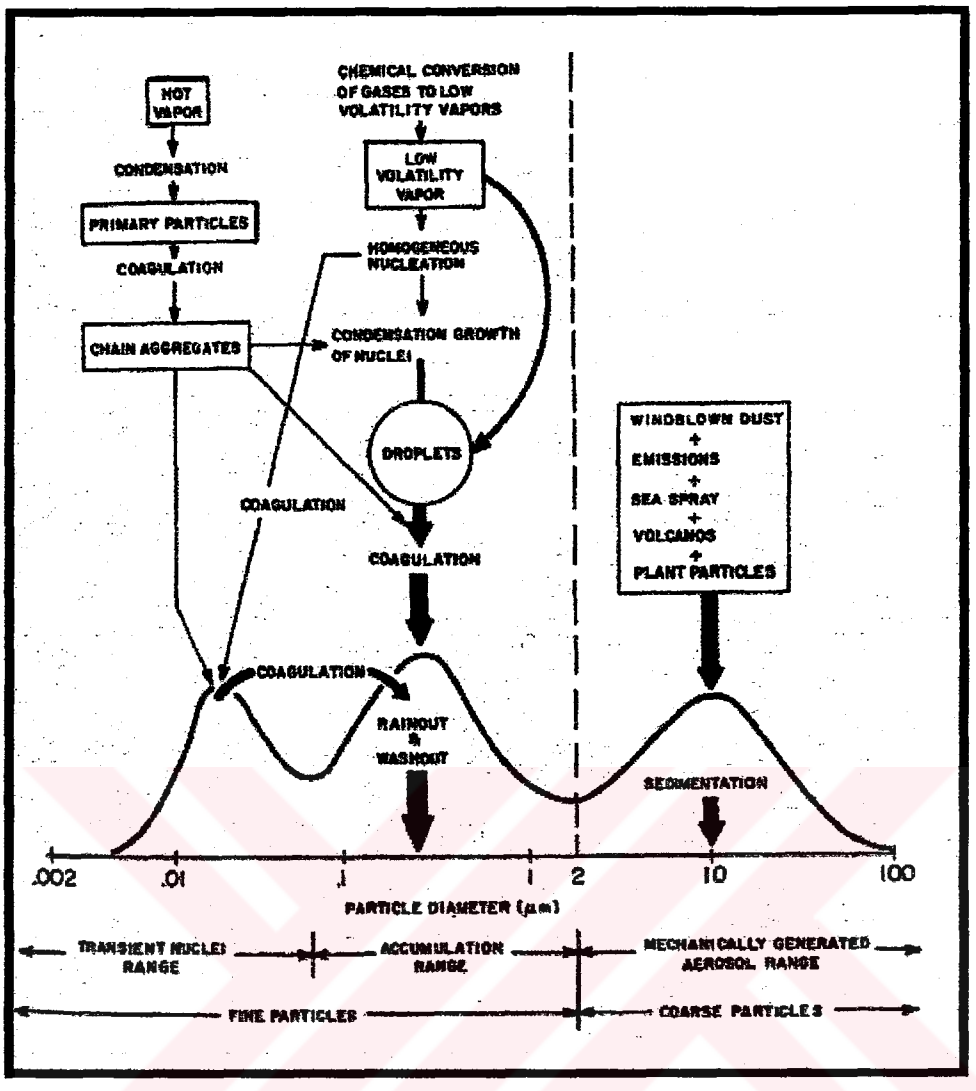


**Figure 2.1.** Schematic representation of atmospheric aerosol surface area distribution

Trace elements that are introduced into the atmosphere from both natural and anthropogenic sources. The most common sources of crustal substances are wind-blown dust, bubble bursting, forest fires, volcanoes and biogenic emissions. The anthropogenic emission sources are mainly combustion, industrial processes, solid waste incineration, and various miscellaneous activities like forest fires, slash burning, fertilizer usage, etc.

### *2.2. Long Range Transport of Atmospheric Pollutants*

The horizontal and vertical distributions of aerosols are important factors in determination of the effect of aerosols on the earth's radiation budget and atmospheric chemistry. Most atmospheric aerosols exist within the boundary layer and have short atmospheric residence times due to wet deposition processes. Having short residence time in the atmosphere, they have only regional influences. Aerosols that can reach the free troposphere have longer lifetimes, and therefore, can be transported over regional boundaries.

The long range transport of air pollutants have become an important concern due to the adverse impacts that the air pollutants induce far from the areas they have been emitted, and perception of the problem resulted co-operative actions.

The Convention on Long Range Transboundary Air Pollution (LRTAP), was signed in 1979 by 32 European countries, Eastern European nations (EEC), Canada and the US and to establish a framework for the co-operative action to reduce the impacts of air pollution and to control air pollutant emissions by legally binding protocols. The objective of this programme for Monitoring and Evaluation of the Long-Range Transmission of Air pollutants in Europe is to give qualified scientific information to the governments and to support the development of the international protocols related with the emission reductions.

Several activities have been initiated to protect the ecosystem from the possible adverse impacts of substances. In this manner, The UN/ECE Convention of Long-Range Transboundary Air Pollution (CLRTAP) protocol on heavy metals and persistent organic pollutants are being prepared and the long-range transport of substances is determined to be a significant criterion in the selection of the substances for the protocol. Nowadays, the EMEP programme has also focused on the assessment of the long-range transport of heavy metals and persistent organic pollutants (POPs).

The studies involved in long-range transport of pollutants were attempted to determine the transport and removal processes which affect the atmospheric concentrations and the amount pollutant deposition. The long-range transport of pollutants to western Mediterranean basin (Dulac et al., 1987; Plaisance at el., 1996; Sandroni and Migon, 1997) and eastern Mediterranean basin (Katsoulis and Whelpdale, 1993;Al-Momani, 1995; Güllü, 1996; Kubilay et al., 2000) were studied in the past in numerous studies. These studies showed that the Mediterranean Basin is under the influence of anthropogenic sources mainly Europe, as well as natural sources from Sahara.

### *2.3. Geography, Climatological Regimes and Transport Patterns of Mediterranean Basin*

The Mediterranean Sea located between 30° N 46° N to 5.5° W and 36°E. The length from east to west is 4000 km and north to south is 800 km in average.

The Mediterranean region has a distinctive climate. The eastern parts of the basin has sub-tropical summer-dry weather regime, in contrast to northern and western parts, where weather regime is described as transitional zones between Mediterranean and Continental weather systems.

The Mediterranean Basin is located in the subtropical latitudes, surrounded by high mountains and the ground properties of the basin such as wetness, albedo, etc., show large annual variations.

The topography of the basin is highly complicated. The major mountain ranges, which are Pyrenees, Alps and Balkans, act as barriers and constrain the north-south flow of air masses. Strong winds which are tunnelled through gaps in the mountain ranges which are surrounding the Mediterranean Basin are among the best known meteorological features of the basin: (1) the north-westerly mistral through Alps-

Pyrenees gap; (2) the north-easterly bora through Trieste gap; (3) the easterly levanter and westerly vendaval through the strait of Gibraltar; (4) the warm south-easterly to south-easterly sirocco, ghibli, or khamsin from Africa.

These topographic features give rise to the atmospheric motions in Mediterranean Basin, which are highly local, showing strong seasonal variations, and influence the horizontal transport to the basin and vertical mixing of pollutants.

The classification of synoptic weather patterns is useful tool to understand the flow climatology of the Mediterranean Basin The five main synoptic weather patterns and their descriptions (Dayan and Miller, 1989) are as follows:

Type A: An anticyclone or ridge of high pressure lies over the north-eastern Atlantic or the British Isles. During the presence of this blocking anticyclone, a quasi-permanent low pressure through in the mid-troposphere (about 500 hpa) extends along the axis of the Mediterranean Basin. The trough line leads to cyclogenesis when vorticity maxima move into its region of influence. This cyclogenesis constitute the major pattern in winter. (Miller et al., 1987)

Type B: Northern Europe is dominated by an anticyclone. Pressure is relatively low over Mediterranean.

Type C: Westerly type. A deep depression dominates in the middle latitudes of Europe, and westerly winds prevail over most of the Mediterranean.

Type D: Easterly type. An anticyclone dominates central and southern Europe, giving easterly ends over most of the Mediterranean. Pressure is relatively low over northern Europe.

Type E: Anticyclone type. An anticyclone or ridge of high pressure covers the greater part of the Mediterranean area, giving generally light winds, mainly westerly

in the north, easterly in the south, and northerly in the east. Pressure is relatively low over central or northern Europe.

Among these synoptic weather patterns, type A, B and C are commonly occur in winter and D and E are frequently observed during summer.

The flow patterns to eastern Mediterranean (Dayan, 1986) and western Mediterranean (Miller et al., 1987) regions were studied in the past. The major conclusions drawn were; (1) the most frequent flow patterns to eastern Mediterranean (33 °°N 35 E) were from northwestern Europe during winter, and (2) northeast continental flow passing through Asia Minor during summer season. The dominating flow patterns to western Mediterranean (40° N 6° E) were found out to be from west and northern Europe.

### *2.4. Geography, Climatological Regimes and Transport Patterns of Black Sea Basin*

The Black Sea is an inland sea in the east of Europe. The length of Black Sea is 1200 km from east to west in average, and the width is 610 km maximum.

The region is affected by high pressure systems located over Siberia during winter and under the influence of high pressure systems over North Africa and Basra low during summer. As a result of these systems, easterly flows are observed in Black Sea Basin during whole year.

The main paths of depression observed in Black Sea are (1) moving northeast from the Mediterranean Sea over Marmara Sea, (2) moving in east and southeast from Bulgaria and Romania. The meteorological features of the region strongly affect the transport form Europe and Russia (Hacısalihoğlu et al., 1990).

The Black Sea is surrounded by six coastal countries, which are the main pollution sources. These countries are Romania, Bulgaria, Russia and Turkey, Georgia and Ukraine.

The long-range transport patterns to Black Sea basin were first studied for the receptor site Bartın (41.78° N 32.48° E) by our group (Karakas, 1999).

### *2.5. Trajectory Models*

Trajectory is the time integration of an air parcel's position while it is transported by the wind.

Trajectory models, which describe the paths of air parcels take in the atmosphere, are useful tools for determination of source-receptor relationships of air pollutants. Various trajectory computation methods have been developed based on different assumptions.

In most of the trajectory models, observed or model analysed winds are used to compute horizontal advection component. The vertical component of the trajectories, on the other hand, are computed based on one of the following assumptions:

- Isobaric
- Isentropic
- Kinematic

The trajectory is assumed to follow a constant pressure surface in isobaric assumption and a constant temperature potential in isentropic assumption. In kinematic assumption, the trajectory is assumed to move with the vertical velocity wind fields generated by diagnostic or prognostic meteorological model.

Due to the significant amounts of moisture and diabatic factors that play an important role in the growth and dissipation of boundary layer, transport in boundary layer is difficult to model. In kinematic model assumption, all adiabatic and diabatic components contribute to the 3-D velocity fields.

The isobaric trajectory models have been used in several studies in the past. However, it has been found that the significant vertical motions were ignored in isobaric assumption (Harris and Kahl, 1994). Nowadays, the isentropic trajectory models are widely used in trajectory calculations. Isentropic models are advantageous due to not requiring vertical motion data. The vertical motions occur implicitly as air parcels move along sloping isentropic surfaces (Fuelberg et al., 1996).

The long-range transport of pollutants has been examined in the past for several receptor sites. The studies involving back trajectory models reported in literature were for Vienna (Stohl and Kromp-Kolb, 1994), Barrow-Alaska (Harris and Kahl, 1994), Oki Island (Mukai and Suzuki, 1996) for receptor sites in Mediterranean basin (Miller et al., 1987; Güllü, 1996) and in Black Sea basin (Karakaş, 1999).

Accuracy of trajectories has improved in the last decade; however, trajectories still cannot represent the "ground truth". Trajectories are often uncertain, which lead to misinterpretation of flow situation. The errors associated with trajectory calculations mainly result from the interpolation from a regular grid to actual trajectory position in time and space; assumptions of vertical wind component; analysis and forecasting of wind fields (Stohl, 1998).

Since the spatial and temporal resolution of meteorological observations limit the accuracy of trajectory calculations, it is necessary to verify the trajectory models. The assessment of errors involved in trajectory calculations can be performed by determination of a true reference trajectory. A reference trajectory can only be determined by allowing an air parcel into the atmosphere along with a tracer that is

conserved along trajectory. The most commonly used tracers are balloons, material and dynamical tracers.

Trajectories, which are derived from balloon flights, are useful tools to validate the computed trajectories. Numerous studies were performed by using the constant level balloons, which remain on constant density surface (Pack et al., 1978; Kahl et al., 1991). Balloon tracks are not representative of the three dimensional air mass trajectories since the vertical displacement of balloons is controlled by the pilot rather than the vertical wind field component. Thus, balloon tracks help us to determine the trajectory errors resulting only from the horizontal wind component errors (Baumann et al., 1997).

There are also material tracers such as smoke plumes or inert tracer gases. An inert tracer must be chemically stable, not subjected to washout or dry deposition, and its background concentration must be near zero. Sulphur hexafluoride ($SF_6$) in local scale, and perfluorocarbons in continental scale, were the commonly used tracers (Draxler, 1991). Additionally, any material that is conserved along trajectory such as pollen (Raynor et al., 1983), Saharan dust (Martin et al. 1990), and radioactive materials (Klug, 1992) can be used as tracer.

In the last decade, several tracer studies were conducted to test the accuracy of trajectories. Among all, three of them were taken most of the interest. These are Cross Appalachian Tracer Experiment (CAPTEX), conducted during September and October 1983, Across North America Tracer Experiment (ANATEX) during January to March 1987 and European Tracer Experiment (ETEX) during October to November 1994. In addition to these experiments, the gas balloon tracks during Gordon Bennett Cup in 1995 were also used for the verification of trajectory models (Baumann and Stohl, 1996).

During the Gordon Bennett Cup 95, Baumann and Stohl were tested isobaric trajectories calculated with European Centre for Medium Range Weather Forecast

(ECMWF) wind field data. In this study, the path length of the forecasted and analysed trajectories and the absolute horizontal transport deviations (AHTD) were considered to be the characteristics of the trajectories. The absolute horizontal transport deviations have been extensively used in literature to quantify the inaccuracy associated with calculated trajectories. (Kuo et al., 1985; Rolph et al., 1990; Stohl et al., 1995) The AHDT was determined by the following formula;

$$AHTD(t) = \frac{1}{N}\sum_{n=1}^{N}\left\{[X_n(t) - x_n(t)]^2 + [Y_n(t) - y_n(t)]^2\right\}^{1/2} \quad \text{.....(2.1)}$$

where; X and Y are the locations of balloon trajectory, x and y are the locations of calculated trajectory. The path length of forecast and analysed trajectory at the end of the first 52 hours and also their corresponding AHTD's were given in Table 1.

Table 1. AHTD's versus pressure levels

| Pressure Level (hPa) | Forecast Trajectory path length (km) | Analysed Trajectory path length (km) | AHTD (km) |
|---|---|---|---|
| 1000 | 877 | 910 | 327 |
| 900 | 502 | 1298 | 1338 |
| 800 | 1583 | 1291 | 992 |
| 700 | 2674 | 1644 | 1039 |
| 600 | 3681 | 2265 | 1982 |

Baumann and Stohl have found the errors of 4-45% of the distance travelled after 46 to 92 hours.

In another balloon study the trajectories calculated from ECMWF analyses were checked (Knudsen, 1996). The results showed that the typical difference of travel distances between balloon and trajectories were 20%.

The results of CAPTEX, ANATEX and ETEX were used in several studies. Haagenson et al.,(1986) derived tracer trajectories using the data available after CAPTEX to make a comparison between NCAR isentropic trajectory model and a more conventional isobaric trajectory model. The parameter they have used to make

comparison between tracer trajectories with the model trajectories was the root mean square (RMS) separation.

Table 2. The RMS deviation observed between tracer and model trajectories

| Trajectory Type | 1000 mb | 950 mb | 900 mb | 850 mb |
|---|---|---|---|---|
| Isentropic | 148 | 177 | 245 | 314 |
| Isobaric | 246 | 193 | 260 | 332 |

Draxler et al., used the data obtained during ANATEX and calculated the back trajectories using the tracer centroid positions. They found that the trajectory errors were 20-30% of the distance travelled.

Reiff and Forbes were studied the African dust transport to North western Europe to verify the trajectory calculations based on ECMWF wind analyses. They have found agreement between calculated and observed trajectories. The horizontal displacement of observed and model trajectories were at most 200 km.

Trajectory calculations still require further developments to be able to interpret them the accurate pathways of air parcels. Nowadays, the isentropic trajectory models are believed to be the most accurate models and should be preferred

# CHAPTER 3

# METHODOLOGY

In this study the Air Resources Laboratories Branching Atmospheric Transport model (ARL-BAT), National Oceanic and Atmospheric Administration's (NOAA) Hysplit (Hybrid Single Particle Lagrangian Transport) model and European Centre Medium Range Weather Forecast (ECMWF) trajectory model are compared.

## *3.1. Branching Atmospheric Transport Model*

The ARL-BAT (Heffter et al., 1983) is an isobaric model, which simulates the air parcel transport by Eulerian advection technique using the transport winds averaged over a fixed or variable layer.

A new puff is generated at each 3 hour time step and placed in a proper vertical layer according to day/night occurrence. This model divides the lower troposphere into 3 layers;

- surface layer (300 m above surface)
- Boundary Layer (from surface up to critical inversion during daytime, from the top of surface layer to the critical inversion)
- Upper layer (from critical inversion to 3000 m)

The critical inversion criteria are:

1. $\Delta\theta / \Delta Z \geq 0.005$ °K/m
2. $\theta_T - \theta_B \geq 2$ °K

where $\Delta\theta / \Delta Z$ is the potential temperature ($\theta$) change with height (Z), $\theta_T$ and $\theta_B$ are the potential temperature at the top and base of inversion respectively.

Puff trajectories are calculated by using the average winds for each layer. The puffs are branched into numerous ones depending on the day to night transitions, or may vertically mix in the new layer. The new branches generated then follow independent trajectories in accordance with the winds in the layer.

The trajectory of a puff is calculated for 4 days as three hours segments using the wind analysis of 2.5 degrees grid every 6 hours at standard pressure levels.

The meteorological data at different heights are used as the model inputs since the air mass movements at 850 mb level are calculated. The study area of the model is selected as the area between the latitudes of 65°N and 25°N and the longitudes of 10°W and 40°E. The daily data from upper atmospheric measurement stations are required and obtained from both Turkish Directorate of Meteorology and National Centre for Atmospheric Research (NCAR).

The trajectory calculations using BAT model were performed in a previous study for Antalya station (Güllü, 1996), and, therefore, the calculated back trajectories by Güllü were used in comparison.

### *3.2. HYSPLIT Model*

The HYSPLIT is an isentropic model to compute trajectories using the gridded meteorological data on one of the conformal map projections. These are Polar,

Lambert or Mercator. The dispersion rate calculation performed from the vertical diffusivity profile, wind shear, and horizontal deformation of the wind field.

The calculation method of model is a hybrid between Eulerian and Lagrangian approaches. The advection and diffusion calculations are performed by a Lagrangian approach. The meteorological data for computation of trajectories are obtained from gridded outputs of meteorological models.

The minimum requirements of the HYSPLIT model are the horizontal wind components (U,V), temperature (T), height (H), pressure (P) and the pressure at the surface ($P_0$). The advection of a puff is computed from the average of the three dimensional velocity vectors at the particles initial position P(t), and its first guess position P(t+dt). The velocity vectors are then linearly interpolated between time and space.The first guess position is given by the following equation:

$$P(t+dt) = P(t) + V(P,t)d \qquad (3.1)$$

The final position is:

$$P(t+dt) = P(t) + 0.5[V(P,t) + V(P,t+dt] \qquad (3.2)$$

The trajectory calculations by HYsplit model was performed by using the model code on the website of Air Resources Laboratory. The required meteorological data were also obtained from the archive available on this website. The trajectory of a puff was calculated as 1-hour segments and 4 days long duration.

### *3.3. ECMWF Trajectory Model*

The ECMWF trajectory model is based on a parcel advection code used in the contour dynamics/advection algorithm of D. Dritschel and W. A. Norton. The horizontal advection on a sphere is performed in Cartesian coordinates. The vertical

advection can be included. Time stepping uses a fourth order Runge-Kutta scheme. The winds are interpolated onto parcel positions at the current time by linear interpolation. The order of the time and space interpolations depends on the number of parcels being advected by the model.

The model uses analysed wind field components; u (zonal) and v (meridional), and the vertical velocities available in the archive of the center (MARS) in the form of a special, on-line database gridded every 6h (00, 06, 12, 18 UT) for standard pressure levels. The grid space is 1.875° for latitude and longitude. The position of an air parcel is recalculated at each 15-min. time step by utilising linear spatial and temporal interpolations. All calculations are carried out on a regular latitude-longitude grid, with a resolution selected by the user. In this study a resolution of 1.5x1.5 degrees has been used. The parcel positions resulting as latitude and longitude, the wind components and pressures are written hourly as characters to a resultant file.

The publicly available operational model on the CRAY C90/UNICOS super computer at the European Centre for Medium-Range Weather Forecast (ECMWF, Reading, U.K.) was utilised to obtain the three dimensional (3-D), three and half days long back trajectories. A request file for a trajectory of specific date and region was initialised via Internet. A sample of trajectory request file and the resultant data file are given in Appendix A and B respectively.

Table 3.1. The trajectory models and their essential considerations

| Model | Basic Assumption | Calculation Scheme |
|---|---|---|
| BAT | Isobaric | Eulerian advection approach |
| HYSPLIT | Isentropic | Hybrid between Eulerian and Lagrangian approaches |
| ECMWF | Isentropic | Lagrangian approach |

### *3.4. Trajectory Statistics*

Back trajectories, as they give information about the history of an air parcel in previous days before reaching to a receptor location, are helpful tools to determine the sources of air pollutants.

One of the major application areas of back trajectories is environmental science. Back trajectories and air pollution measurements at a receptor site are used in combination to determine the source-receptor relationships of air pollutants.

In the past, trajectories were used to investigate the transport processes of individual air pollution events. However, the development of sophisticated methods nowadays enables us to determine air pollution climatology of a region using large sets of trajectories.

The multivariate statistical methods developed until now together with the most recent methodologies are elucidated in the following part in an historical order.

#### 3.4.1. Flow Climatology

This is the earliest statistical method for identification of the sources of air pollutants. Flow climatology is often used to determine the pollution input from distant sources to a selected region and also allows understanding of airflow patterns.

The approach of flow climatology is the collection of several years of trajectories ending at a selected receptor site and classification of them according to their transport speed and direction.

The transport sectors associated with high pollutant concentrations at the receptor site are identified by flow climatology studies. The countries, which fall in to the

sectors associated with high pollutant concentrations at the receptor site, are pronounced as the source regions of air pollutants.

Although roughly identifies the source regions and can not detect individual source areas, flow climatology was applied to several remote locations such as Mauna Loa, Hawaii (Miller, 1981); Bermuda (Miller and Harris, 1985), Barrow, Alaska (Harris and Kahl, 1994); Norway (Saltbones et al., 1999), Aliartos, Greece (Katsoulis and Whelpdale, 1992; Katsoulis, 1999) and for some receptor locations in the Mediterranean region (Miller, 1987; Güllü, 1996)

### 3.4.2. Single Layer PSCF Analysis

Potential Source Contribution Function was developed Ashbaugh (1983) to identify the source areas of pollutants individually. PSCF is receptor–oriented method that uses the chemical measurements of pollutants at the receptor site and meteorological information. The objective of PSCF is to identify the geographic locations that have higher probability of being source areas of pollutants.

The PSCF construction can be described by as follows; a trajectory is assumed to collect the emitted pollutants in the cell (i,j) if the trajectory segment endpoint falls into that cell. Once incorporated into the air mass, the pollutants can be transported to the receptor site along the trajectory.

The PSCF value for a grid cell (i,j) is calculated by counting the 1 hr trajectory segment endpoints that fall into that grid cell. If N is the total number of trajectory segment endpoints for the study period, and $n_{ij}$ is the number of trajectory segment endpoints that terminates in the ij-th cell, then the cumulative probability of these endpoints $P[A_{ij}]$ throughout the study period, which is also known as the residence time of air parcels over that subregion, is given by

$$P[A_{ij}] = \frac{n_{ij}}{N} \qquad (3.3)$$

If there are $m_{ij}$ counts among $n_{ij}$, for which the measured pollutant concentration exceeds a selected criterion value, then the probability of event $B_{ij}$ that is related to the high concentration at the receptor site is given by

$$P[B_{ij}] = \frac{m_{ij}}{N} \tag{3.4}$$

Then the PSCF is as follows;

$$PSCF = \frac{P[B_{ij}]}{P[A_{ij}]} = \frac{m_{ij}}{n_{ij}} \tag{3.5}$$

The PSCF is conditional probability, which gives the spatial distribution of the possible source locations. The cells with high PSCF value are the potential source areas of pollutants. It is important to notify that the grid cell size must be sufficiently large for the assimilation of reasonable trajectory segments endpoint.

The value of PSCF ranges between 0 and 1. Any grid cell having PSCF of 0 is unlikely to be the source region, while the opposite is true for PSCF of 1. One important feature of PSCF is that, if $m_{ij}$and $n_{ij}$ are equal to each other, the PSCF ends up equal to unity. For large values of $n_{il}$, the results are statistically stable. It is necessary to reduce the effect of small values of $n_{ij}$ by developing a weight function.

The PSCF of Grand Canyon (Ashbaugh et al., 1985); Eastern France (Colin et al., 1988); Canada (Cheng and Hopke, 1993); Rubidoux CA (Gao et al., 1992); Eastern Mediterranean (Güllü, 1996); Barrow, Alaska (Polissar et al., 1999) were studied.

### 3.4.3. Three Layer Integrated PSCF Analysis

Three layer PSCF analysis is a new method, which incorporates the material transfer from multiple vertical heights.

If A1, A2 and A3 are the events for three different pressure levels, and B is the subset of events Ai, i=1,2,3, which is defined as the polluted events.

The theory of the total PSCF (TPSCF) is summarised as;

$$P[B] = P[B/A1]P[A1] + P[B/A2]P[A2] + P[B/A3]P[A3] \quad (3.6)$$

Where, P [B] ie the total probability of occurrence of event B, P [$B/A_i$, i=1,2,3] is the conditional probability of event B as event $A_i$ occurs. The TPSCF is defined to be;

$$TPSCF = \frac{P[B]}{\sum_{i=1}^{3} P[A_i]} \quad (3.7)$$

### 3.4.4. Concentration Fields Method

Concentration fields is a new method of establishing source-receptor relationships of air pollutants developed by Seibert et al., (1994) to overcome the uncertainties associated with PSCF analysis.

The logarithmic mean concentration for a grid cell is calculated by the following formula:

$$C_{mn} = \frac{1}{\sum_{l=1}^{M} \tau_{mnl}} \sum_{l=1}^{M} \log(c_l) \times \tau_{mnl} \quad (3.8)$$

where m, n are the grid cell indices, l is the trajectory index, M is the total number of trajectories, $c_l$ is the concentration observed on arrival of trajectory l at the receptor site and $\tau_{mnl}$ is the residence time of air masses in grid cell (m,n) by the trajectory l.

The air parcels passing over a grid cell of high log-mean concentration, results in high concentration at the receptor site. The concentration fields method does not give the exact source locations since the measured concentration at the receptor site is equally attributed to all segments of related trajectory.

The procedure developed by Seibert et al. was applied to determine the source locations of particulate sulphate for Sevettijarvi (Stohl, 1996) and acidity of precipitation at Morvan, France (Charron et al., 2000).

### 3.4.5. Redistributed Concentration Fields Method

In order to construct the method, a set of trajectories, one of which is polluted and the rest are clean, are imagined to pass over a specific gird cell. Therefore, it can be said that there are no major pollutant sources located along the paths of clean trajectories and not in the grid cell where they share with polluted trajectory. Thus, the polluted trajectory must have taken up the polluted material from its path before reaching that grid cell.

Using this information, a new method of trajectory statistics is developed. The log-mean concentrations calculated by concentration field method is used as a first guess concentration and it is redistributed.

Let $c_l$ is the concentration measured upon arrival of trajectory l to the receptor site, $X_{il}$ is the mean concentration of the grid cells where the 1 hr segments of trajectory l terminates in. Then $X_{il}$ is as follows:

$$X_{il} = 10^{C\ MN} \qquad (3.9)$$

The average of the mean concentrations, $X_l$ is given by

$$X_l = \frac{\sum_{j=1}^{N_l} X_{jl}}{N_l} \qquad (3.10)$$

Then the redistributed concentrations along trajectory l is given by:

$$C_{il} = \frac{X_{il}}{X_l} \qquad (3.11)$$

Equation (16) can be applied to all individual trajectories. The new concentration field can be calculated after finishing the redistribution by the following formula;

$$C_{mn} = \frac{1}{\sum_{l=1}^{M}\sum_{i=1}^{N_l} \tau_{mnl}} \sum_{l=1}^{M}\sum_{i=1}^{N_l} \log(c_l) \times \tau_{mnl} \qquad (3.12)$$

where $\tau_{mnl}$ is the residence time of segment i of trajectory l in grid cell (m,n).

The concentration field and redistributed concentration field methods were applied to determine the sources of particulate sulphate at the receptor site Kosetice (Stohl, 1996). The results showed that each method pronounced the same maxima and also agreed well with the emission inventories.

# CHAPTER 4

# RESULTS AND DISCUSSION

## *4.1. Comparison of Trajectory Models*

Models that are used to calculate movements of air masses at various altitudes, which are commonly called "backtrajectory models", are used to evaluate the transport of chemical constituents in the atmosphere. The development of backtrajectory models enabled us to study the path followed by air masses during their travel before reaching a receptor site, and this information can be used to understand : (1) How atmospheric constituents (mostly pollutants) are transported in the atmosphere and (2) the source regions of a pollutant or pollutants effecting a particular receptor site.

Currently there are various backtrajectory models available for the computation of trajectories based on different assumptions. Isobaric models assume transport of air masses and pollutants at a constant pressure levels assuming that they do not change altitude during transport. Isentropic models, on the other hand, assume motions of air parcels along fixed temperature surfaces. Naturally, air masses do change altitude in isentropic models. Isobaric models are the first models that were used to assess pollution transport. Although, currently isentropic models are believed to be more reliable, it had been frequently shown in the past that the reliability of trajectory calculations is of great importance in establishing the source-receptor relationships

since the accuracy of the established relationship is at least determined by the accuracy of the trajectory calculations.

Approximately 2000 aerosol and precipitation samples collected at permanent stations along the Mediterranean and Black Sea coasts of Turkey were analyzed by various researchers in our group (Güllü, 1996; Al-Momani, 1995; Karakas, 1998; Al-Agha, 2000). The main objective in all these studies was to understand the source regions in Europe and Turkey that are responsible for the observed concentrations of measured elements along Turkish coasts. Such objective obviously requires extensive trajectory calculations. Approximately 5 years ago, the only trajectory model available was ARL-BAT which is a one dimensional isobaric code. However, currently two additional backtrajectory models that can be used for the same purpose became available. These are HYSPLIT model developed by the NOAA (USA) and ECMWF model used fairly extensively in the literature. Since the reliability of conclusions reached in source apportionment studies in our group strongly depends on the accuracy of calculated backtrajectories, intercalibraiton of the available models is highly important.

In this study, Air Resources Laboratory Branching Atmospheric Transport Model (ARL-BAT), National and Oceanic Administration's HYSPLIT Model and the European Centre Medium Range Weather Forecast (ECMWF) Model are evaluated to be able to observe whether each model determines similar paths of air masses. The HSPLIT and ECMWF models are 3D isentropic models, whereas BAT is an isobaric model. Additionally, it will be possible to see the differences between the isobaric and isentropic models by this comparison. The comparison of models was performed in two levels. First, models are qualitatively compared. For this, the backtrjectories calculated by the three models using the same meteorological input data were visually inspected to see similarities and differences between them. In the second step, a quantitative comparison were performed by calculating fractions of

trajectories falling in the same wind sector and residence times of trajectories in various subregions by the three models.

The main difficulty encountered in the model intercomparison is the availability of data for all models for the same time period. The BAT model was used in our group between 1992 and 1995. The meteorological input data for BAT at that time were obtained from the General Directorate of Meteorology. The ECMWF code was used for source apportionment studies after 1995. No meteorology data was necessary for ECMWF runs; because ECMWF computers at Reading (UK) was used for trajectory calculations and meteorology data were available in their archives. Since BAT was not used after 1995, met data collection by the General Directorate of Meteorology was terminated. Consequently, BAT trajectories are available only for the period between 1992 and 1995.

The HYSPLIT is a publicly available model developed by the NOAA (USA), which can be run only on the NOAA computers by using meteorological data stored NCAR archives. The model was placed for public use in 1998, but unfortunately only 6 month-long old meteorological input data were made available to users. Consequently, HYSPLIT trajectories were available after August 1998.The ECMWF model were run on the ECMWF computers and since historical data were accessible in their archives, the ECMWF trajectories did not have the time limitations that were encountered in trajectories calculated by the other two models. Since there was no time period at which both BAT and HYSPLIT trajectories were simultaneously available, both models were compared against ECMWF code for different time periods. Comparisons between BAT and ECMWF trajectories were done for a period in 1995 and the comparisons between the HYSPLIT and ECMWF trajectories were done for after 1998.

### 4.1.1. Qualitative Comparison

Trajectories prepared by different codes are expected to follow the same path when the same meteorological input data are used. However, this may not be the case for every single trajectory since different formulations and different assumptions are involved in each model. Individual trajectories calculated by different models may not be exactly identical, but they may produce similar results when averaged over long periods such as one year. If that is the case both trajectories can be considered "reliable" because trajectory statistics which is used for the source region apportionment studies uses long-term average trajectory information. In this study similarities and differences in individual trajectories calculated by each of the three models using the same meteorological information were compared qualitatively. The long-term average results, which is more important for source apportionment, is investigated quantitatively in the following sections.

The qualitative comparison of trajectory models was performed by testing the similarities between the trajectories for a selected time period. For this purpose, 1-month data of each trajectory model was evaluated to determine whether the routes of trajectories to the selected receptor site are the same.

The BAT and ECMWF trajectories are compared for the time period of July 1992 for the receptor site Antalya. During the 24% of the days, both ECMWF and BAT trajectories are followed the same path. Rest of the time, the trajectories are observed to be followed not exactly the same routes to the receptor site. It should be noted that, although the paths followed are not exactly the same, they both start at the points that are very close to each other and show the same wind sector. During only two days of this one month time period, BAT and ECMWF trajectories are originated from different wind directions. Although there are similarities between BAT and ECMWF trajectories, almost all BAT trajectories are shorter. ECMWF trajectories generally come from longer distances and do not follow identical routes with the BAT trajectories most of the time.

A similar assessment was also performed for the HYSPLIT and ECMWF trajectories. The test period selected is August 1998. Considering the first, the second and the third days of the trajectories of HYSPLIT and ECMWF models, it can be said that 40% of the 850 mb level trajectories resemble to each other in terms of the paths followed and length. Although the rest of the trajectories are seem to be different, all of them originate from the regions, which are very close to each other. There is only one exception during this 1-month period in which the ECMWF and HYSPLIT trajectories originated from opposite wind directions. A similar comparison is also performed by using 700 mb level trajectories. The routes of the 50% of the 700 mb ECMWF and HYSPLIT trajectories are observed to be different from each other, but again their origins and general directions are the same. For the 1 month periods selected for the comparison, trajectories of each models are depicted in Appendix C.

As a result of such comparison, it can be said that, the HYSPLIT and ECMWF trajectories are fairly similar to each other as expected since both models are isentropic. The BAT model, as it is isobaric, showed differences from ECMWF trajectories as a result of this visual evaluation.

Another qualitative way to obtain information on the reliability of trajectory models is to find a strong source in the study area and to test whether trajectories passing over the source resulted in high concentrations of pollutants in the corresponding samples. In this study we have selected Istanbul as the strong source and calculated the percentage of days with HYSPLIT and ECMWF trajectories passing over the source, which results in high concentration of $SO_4^{2-}$ and $NO_3$, which are the selected test pollutants. Concentrations of $NO_3$ and $SO_4^{2-}$ higher than their average concentration in the indicated study period were considered as "high concentration". It should be noted that both $SO_4^{2-}$ and $NO_3$ are log normally distributed in the data set used and number of data points above arithmetic mean concentration is approximately 30% of population.

The time period selected for testing of HYSPLIT and ECMWF trajectories was between August 1998 and May 1999, because only for this period there were data of $SO_4^{2-}$, $NO_3$ and trajectories of both models. There are a total of 25 days in the study period when either HYSPLIT or/and ECMWF trajectories at either 850 mb or/and at 700 mb passed over the city of Istanbul. 12 of these days correspond to high concentrations of $NO_3$, and 8 corresponded to high concentrations of $SO_4^{2-}$, which means that success of both trajectories combined was approximately 50% for predicting high $NO_3$ and 20% for predicting high $SO_4^{2-}$ concentrations. But the main objective of this exercise is to compare the performance the two trajectory models used.

There are 10 850 mb level HYSPLIT trajectories, which pass over the Istanbul. Four (40%) of these matches with high concentration of $NO_3$ and five (50%) matches with high concentration of $SO_4^{2-}$. There were twelve 700 mb HYSPLIT trajectories passing over Istanbul. Six of them (50%) correspond to high $NO_3$ and four (33%) of them matched with high $SO_4^{2-}$ concentrations. There are total (either 850 and/or 700 mb) of 17 HYSPLIT trajectories passing over the city of Istanbul. Nine (53%) corresponded high $NO_3$ and six (35%) corresponded to high $SO_4^{2-}$ concentrations

The same calculations were also performed for the ECMWF model predictions. There are 13 850 mb level ECMWF trajectories, which pass over the Istanbul 4 (31%) of these matches' w/high concentrations of $NO_3$ and 3 (23%) matches with high concentrations of $SO_4^{2-}$. There were 7 – 700 mb ECMWF trajectories passing over Istanbul. Three of them (43%) correspond to high $NO_3$ and 1 (15%) matched w/high $SO_4$ concentrations. There are total (either 850 and/or 700 mb) of 16 ECMWF trajectories passing over the city of Istanbul. Six (37%) corresponded high $NO_3$ and 3 (19%) corresponded to high $SO_4^{2-}$ concentrations.

Similar comparison was also performed for ECMWF and BAT trajectories. The test period selected to compare the BAT and ECMWF trajectories was between May to

August 1992. Pb is selected as the test element and the percentage of days with BAT and ECMWF trajectories passing over the Istanbul, which results in high concentration of Pb were counted.

There are 10-850 mb level ECMWF trajectories, which pass over the Istanbul. The 3 (33%) of these matches resulted in high concentrations of Pb. Since only the 850 mb trajectories of BAT are available, the 700 mb trajectories of ECMWF are not included. There are 9- 850 mb BAT trajectories passing over Istanbul , 4 of which (44 %) matched with high Pb concentration.

The percentages calculated above suggests that the NOAA's HYSPLIT model performs better in relating Istanbul to high $SO_4^{2-}$ and $NO_3$ levels in Antalya, and BAT model performs better than ECMWF in relating Istanbul to high concentration of Pb in Antalya. It should be pointed that this approach in testing the performance of two trajectory models is qualitative. There is probably a significant uncertainty in the results due to short period involved in the analysis, which is due to lack of simultaneous pollutant and trajectory data

On the average Istanbul is approximately 1 trajectory day away from Antalya, at such a distance the horizontal uncertainty in model calculations should be approximately 50 km. Consequently, a trajectory (either one) which is assigned as passing over Istanbul can be anywhere between 50 km east to 50 km west of the city. If the air mass is located between the city and 50 km east of it picks up emissions from Istanbul Kocaeli industrial region and will be loaded with $SO_4^{2-}$ and $NO_3$ when it reaches to our station. But if an air mass is located between the city and 50 km west of it will not pick up any emissions as the region is not industrialised. When such an air mass reaches to our station concentrations of pollutants will not be high. Over a long period of time, since chances of an air mass to be on the east and west of the city is equal, these will cancel each other and Istanbul can be correctly related to the pollutant concentrations in Antalya. But this exercise covers only 10 months in

which each trajectory have passed over the city for only 16 or 17 times. This is one of the reasons why only small percentages 50% at most of the trajectories passing over Istanbul is bringing high loads of $SO_4^{2-}$ and $NO_3$. Because of the same reason, the reliability of calculated percentages is limited. Consequently, the better performance of the NOAA's HYSPLIT model and BAT have to be taken cautiously.

### *4.1.2. Quantitative Comparison*

For quantitative comparison of trajectory results, the air mass backtrajectories ending at Antalya (36°08 N 8°40E) at 850 mb level were calculated using ECMWF trajectory model for the time period between August and December 1998, during which the HYSPLIT trajectories are available. Comparison between ECMWF and BAT models were performed for the time period during January and February 1995.

#### 4.1.2.1. Wind Sector Contribution

Two different comparisons were performed to assess the similarities and differences in the assignment of certain regions by different models. In the first set of calculations flow climatology, frequency of flow from each wind sector, were calculated using each model. In the second set of calculations, residence time of air masses in arbitrary sub-regions in the study area was again calculated by each model and results are compared.

In the calculation of flow frequencies from each of the eight wind sectors, the backtrajectories calculated by HYSPLIT and ECMWF models were divided into1 hr segment, whereas the ones calculated by BAT model were divided into 3 hr segments, since the BAT model computes the air mass coordinates at 3 hr time intervals. The trajectory segment endpoints in each of the eight wind sectors are computed by using the each model trajectories and depicted in Figures 4.1 and 4.2.

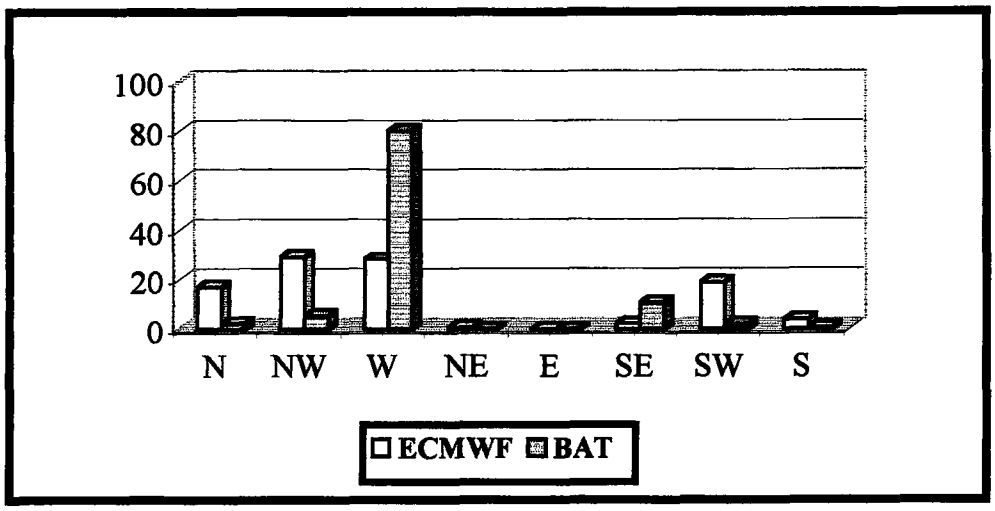


Figure 4.1. Flow frequency (%) from wind sectors calculated using ECMWF and BAT backtrajectories

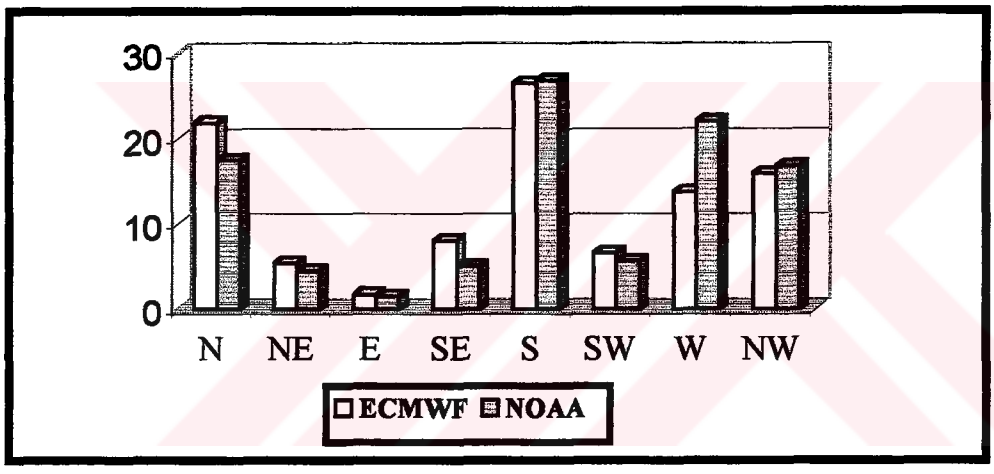


Figure 4.2. Flow frequency (%) from wind sectors calculated using ECMWF and NOAA (HYSPLIT) backtrajectories

As can be seen from Figure 4.1, the flow frequency to Antalya from N, NW, S and SW sectors are higher when the ECMWF backtrajectories are used. During two months period, air mass backtrajectories calculated by BAT model suggested higher frequency of flow from W and SE sectors, compared to ECMWF trajectories. In general the agreement between flow patterns calculated by BAT and ECMWF codes are not encouraging. Fairly large differences in calculated patterns exist in most of the wind sectors.

Fairly comparable results were obtained when flow patterns are calculated using ECMWF and HYSPLIT models. Both models calculated similar flow frequencies from E, S, SW and NW sectors. The flow frequency from N and SE sectors are higher when ECMWF trajectories are used, probably due to short period of time used in calculations. As a result of this comparison, it can be concluded that, both model results in fairly similar frequency distributions.

#### 4.1.2.2. Residence Time Analysis

Another selected quantitative method of comparing the trajectory models is the residence time analysis. To perform this analysis, the study area that extends from west of the UK to the east of Iran, and from Siberia to the centre of Africa was divided into various sub-regions. The sub-regions were tentatively assigned based on emission intensities, and frequency of air mass transport. They were kept large if there are no significant known emission sources, or if the upper atmospheric flow is not frequent in that general direction. The boundaries of subregions were assigned based on the EMEP grid system, which covers whole Europe. The grid system was extended in order to include Turkey, North Africa and Middle East. Based on these criteria each country in Europe was assigned as an individual sub-region, the only exception to this was Netherlands and Belgium which together was assigned as one sub-region, because they were so small that, number of trajectory segments in each of them were not large enough for a reasonable statistical uncertainty. Former USSR countries were assigned one sub-region. Turkey was divided into four sub-regions as northwestern Turkey, western Turkey, central Turkey, and eastern Turkey. Although emissions in central, and eastern parts of Turkey was not large enough to varrant such division, the number of trajectory segments in each of them were sufficiently large for the results to be statistically significant. The countries in the Middle East were assigned as one large sub-region, because emissions were not high and transport frequency was low from the E sector. North Africa was divided into three sub-regions By this way 30 subregions were assigned as depicted in Figure 4.3.

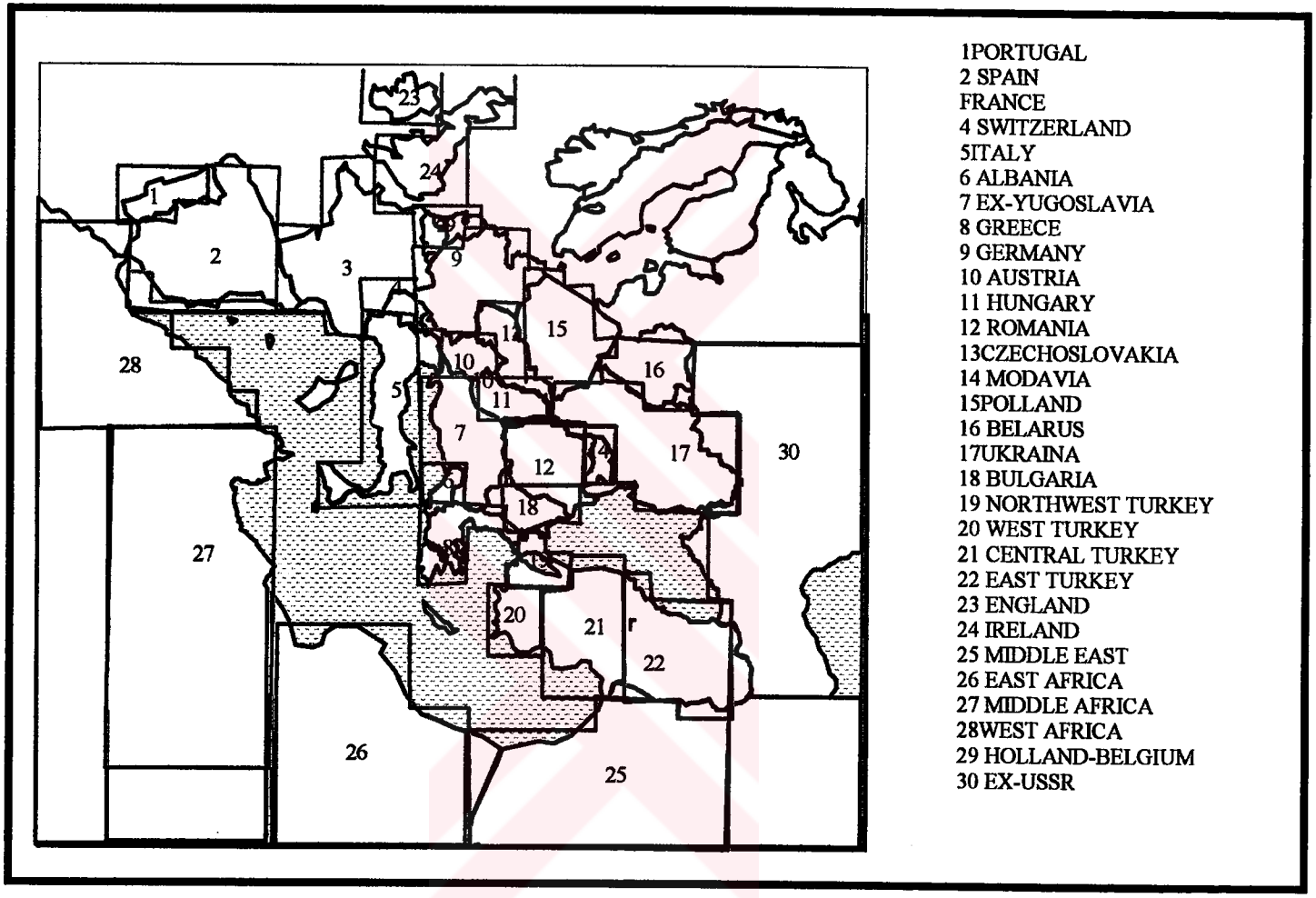


Figure 4.3. Subregions

The residence times of air masses over subregions were computed by each model by counting the trajectory segment end points in each subregion. The ECMWF and HYSPLIT trajectories were divided into 1 hr segments and the trajectories of BAT model were divided into 3 hr segments since the coordinates of the trajectories available at 3 hr time intervals for the BAT model. The calculated residence times using ECMWF and BAT model trajectories are given in Figures 4.4 and 4.5.

As can be seen from Figures 4.4 and 4.5, there are significant differences in the residence times of air masses in different subregions when they are calculated by ECMWF and BAT codes. Air masses spent most of their time in middle and West Africa and to a lesser extent in Middle East and central Turkey when the BAT trajectories are used. One important feature observed is the lower residence times over European countries calculated using BAT trajectories. The residence times of air masses calculated by ECMWF backtrajectories are higher in central Turkey, east Africa, whereas the air masses over these subregions computed by BAT trajectories are quite small. The air masses spent significant fraction of their times over European countries such as Italy, Greece and Hungary when ECMWF trajectories are used, whereas these countries do not seem to be origins of air masses in BAT model. In addition to these, the air masses should spend their time over nearby subregions like central and western parts of Turkey before reaching Antalya station as observed in ECMWF case. The conclusion that 3 months long average trajectories calculated by BAT and ECMWF codes are not the same agrees with the similar conclusion reached in flow pattern calculations.

The residence times over the subregions calculated considering both ECMWF and HYYSPLIT trajectories depicted in Figures 4.6 and 4.7,approximately resulted in a similar distribution with high residence times over western and central parts of Turkey and Ex-USSR. It is also observed that, the time spent computed by using both ECMWF and HYSPLIT trajectories over west, central and east Africa, east Turkey, northwest Turkey, Middle East and Greece are approximate to each other. There also small differences noticed. The orders of France and Italy in the residence

time distribution over the subregions are higher when the HYSPLIT trajectory data is used, whereas the residence time of air masses over these countries calculated with the ECMWF trajectory data are lower. The opposite is true for former Yugoslavia and Romania. When the two figures are compared, it is clearly understood that, the residence times of air masses over subregions computed by both trajectory models resulted in an approximate distribution. The calculated residence times over nearby regions are very close to each other, however, differences are observed on the residence time distribution over the distant subregions. This can be due to small period used in the comparison study.

None of the trajectories available today are exact, they all possess certain uncertainty. The uncertainty in trajectory calculations increase as one goes backwards in time. For the most sophisticated trajectory codes, such as ECMWF and HYSPLIT, the horizontal uncertainty is believed to be approximately 150 km after 3-days. The uncertainty is naturally smaller for shorter time intervals. But since the horizontal and vertical uncertainties are random, they are supposed to cancel out if sufficiently long time intervals are used in segment computations. The computation in this comparison study was performed for 5 months in 1998. This period is not long enough to get rid of all errors due to trajectory uncertainties. Both models resulted in identical residence times in subregions close to the starting point of trajectories, because uncertainties in these short trajectory durations are not large. Probably if computations were performed for one year or longer the same results would be obtained not only in subregions close to starting point of trajectories, but also at distant subregions.

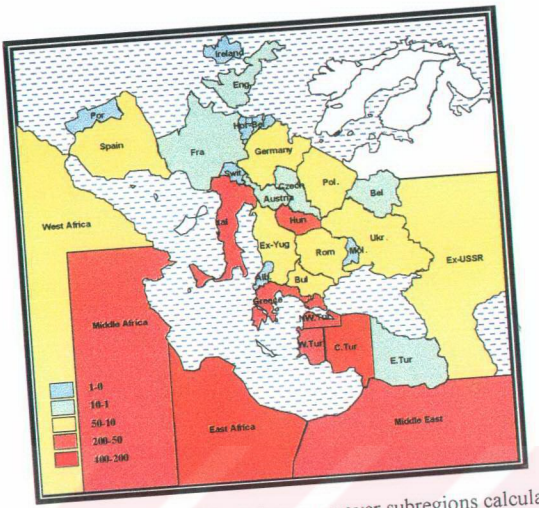


Figure 4.4. Residence time (hr) of air masses over subregions calculated by using ECMWF trajectory data between January – February 1995

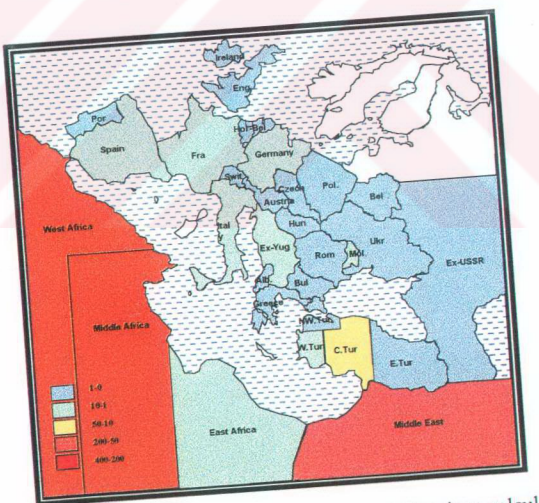


Figure 4.5. Residence time (hr) of air masses over subregions calculated by using BAT trajectory data January – February 1995

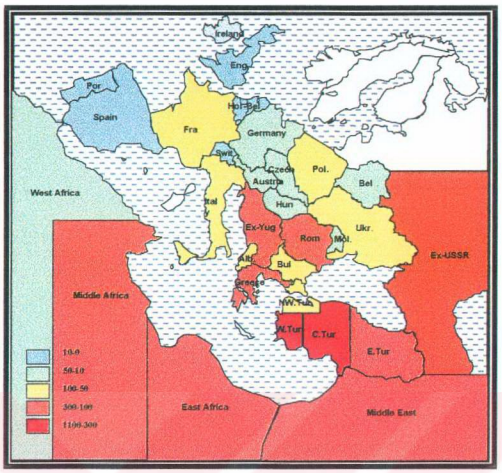


Figure 4.6. Residence time (hr) of air masses over subregions calculated by using ECMWF trajectory data between August –December 1998

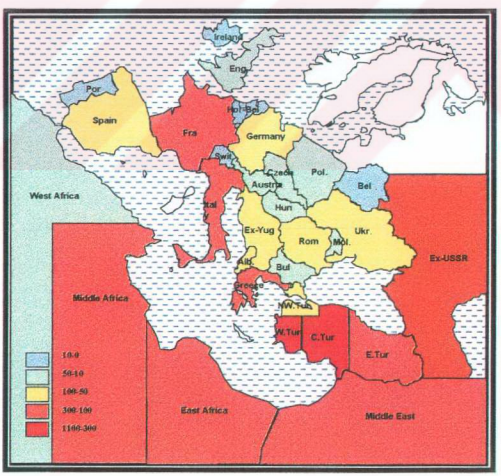


Figure 4.7. Residence time (hr) of air masses over subregions calculated by using HYSPLIT trajectory data August –December 1998

The comparison of BAT, HYSPLIT and ECMWF trajectories using residence time and sectoring technique showed that, HYSPLIT and ECMWF trajectories more or less yielded approximately similar results, on the contrary, BAT trajectories resulted in different wind sector contributions and residence times than the ECMWF trajectories. This is an expected result, as the BAT is an isobaric model, whereas, both HYSPLIT and ECMWF models are isentropic. Therefore, it is convenient to use either of ECMWF or HYSPLIT trajectory data rather than BAT trajectories. From logistics point of view the use of ECMWF trajectory model is more convenient because, one can calculate the trajectories with ECMWF model using historical meteorology data extending several years in the past, whereas special arrangements have to be made to use HYSPLIT model to calculate old trajectories. It should also be noted that ECMWF model is not publicly available, whereas HYSPLIT can be used by everyone simply by giving the starting date and coordinates of the trajectory through internet. But technically, both models are equally reliable.

### *4.2. Trajectory statistics*

Receptor oriented source apportionment techniques, which is commonly known as receptor modelling, have been used extensively in last decade to identify types, locations and contributions of sources effecting air pollution at a given receptor site. These techniques were developed as an alternative to conventional source oriented emission inventory and dispersion modelling approach to obtain more accurate and reliable results that can be used for regulatory enforcement.

Receptor modelling approach, which involves using chemical information, obtained at the receptor site as tracers of sources proved very useful since its development to determine contribution of sources at urban and industrial areas. The results obtained was much more accurate than results obtained using modelling approach. However,

these studies, which can be considered as first-generation receptor modelling applications, was not as successful in regional scale.

There are substantial differences in terms of their purpose in local (urban – industrial) and regional scale applications of receptor modelling. In local scale applications the purpose is to determine the contributions of known sources. The key point in these applications is that the locations of sources are known or can be easily determined. However, in regional scale applications the aim is to identify source regions rather than contributions of individual sources. Since the emissions from various sources are well mixed during long-range transport from source to receptor areas, identification of individual sources or determination of contributions of individual sources is not possible. Contributions of different source regions on the observed levels of pollutants at a given receptor can be quantified to a certain extend, but generally the purpose is qualitative assessment of different source regions and their relative contributions. The first generation receptor modelling applications which included chemical information and statistical tools, but lacked geographical information was naturally not very successful in determining source regions in the regional scale.

More recent applications of receptor modelling, which can be considered as second generation receptor models incorporated chemical as well as geographical information. The geographical information in these regional scale receptor-modelling applications is provided by backtrajectory analysis.

In a simplest way, one can combine the backtrajectories and the observed concentrations of pollutants at a receptor site to determine the geographic locations of source regions. Such methods involving both statistics and trajectory information are called trajectory statistics.

There are a few (four) different techniques that are being used in trajectory statistics. They all use chemical information obtained at the receptor, by analysis of collected samples and trajectory information that is obtained by using one of the many backtrajectory models. In all methods used in trajectory statistics the trajectory information is incorporated to the model by dividing each of the 3 – 4 day long trajectory into hourly segments. Each of the segments represent to location of the air mass at a given time. The techniques differ in the statistical tools that handle to trajectory segments and in the methods that relate these segments to chemical data.

Normally all methods used in trajectory statistics should identify the same source areas when used with the same data and trajectory sets. However, since these techniques are being widely used in only last 5-6 years the data on the intercomparison of these techniques is very scarce.

In our group we are generating large volumes of data on the chemical composition of aerosols and precipitation in the Black Sea and Mediterranean coasts of Turkey. One of the major objectives in most of the studies in our group is to identify source regions which effects chemical composition of particles and rain in the Eastern Mediterranean basins. Such an assessment naturally requires the use of trajectory statistics. In order to be able to make reliable assessments on the potential source regions we must use a method that is reliable. This forced us to evaluate the performance of existing methods that are being used in trajectory statistics.

In this study, four different methods of trajectory statistics were used to identify the source areas of pollutants affecting a selected receptor site, Antalya. These approaches are "single layer potential source contribution function", "3-layer potential source contribution function", "concentration fields approach" and redistributed concentration fields approach". The ability of each method to identify the potential source areas are tested using the same chemical and trajectory data and

the contributions of source areas to the receptor site calculated by each method are compared.

### 4.2.1. Study Area and Backtrajectory Data

The back trajectories were computed for Antalya station between the period March 1992 and December 1993, using the ECMWF isentropic 3D trajectory model during which the concentration data of trace elements and ions are available. The detailed description of data retrieval from ECMWF data centre is given in section. A sample trajectory data file obtained from the centre is given in Appendix B. The first two column of the data matrix are the coordinates as latitude and longitude computed for each 1 hr time interval backward.

Using the backtrajectory data, the residence times of air masses over the subregions, were computed using homemade software, which counts the 1 hr trajectory segment endpoints in each of these subregions in every trajectory day. The assignment of subregions was explained in Section 4.1.2.2. For the whole study period, which is the days for which the concentration data available, the number of 1 hr trajectory segment endpoints were computed and summed up. The summation of these segments was performed for each subregion during the study period, and considered to be the residence time of air masses over each subregion. Calculation of the residence time (or the number of 1 hr trajectory segment endpoints over the subregions) is the basis for all trajectory statistics methods evaluated in this study.

The chemical information data consist of measurements of trace elements in aerosols between March 1992 and December 1993 (Güllü, 1996). Samples were collected on a daily basis using a high volume sampler and analyzed for approximately 35 elements and ions by a combination of ion chromatography, atomic absorbtion spectrometry and instrumental neutron activation analysis techniques. Details of the sampling, analysis and data quality assurance procedures are given elsewhere (Güllü, 1996; Güllü et al., 1998). The species Al, Pb and $SO_4^{2-}$ are selected to be

investigated by different trajectory statistics methods in this study. The Al is selected because the source regions for Al for eastern Mediterranean is well documented. The main source regions for Al is either the local region around the station and North Africa and Middle east where dust bearing Al is being consistently transported to the eastern Mediterranean. The techniques that are being intercompared should reproduce these source regions. The $SO_4^{2-}$ and Pb are selected as they are important pollutant parameters and their sources are roughly known to be at the north and northwest of the study area.

### *4.2.2. Single and Three Layer Potential Source Contribution Function (PSCF)*

To calculate the PSCF, the 1 hr trajectory segments in each subregion during the study period ($n_j$) and the 1 hr trajectory segments corresponding to the days of high concentration at the receptor site ($m_j$), are counted. The high concentration of pollutants is a tentative term and is being used differently by different researchers. In this study we have selected concentrations of a test element that are above the annual arithmetic average of that element as high concentration. Since the data used in this study is log-normally distributed (Güllü et al., 1998) most of the data population centers around the geometric mean value. The values that are above the arithmetic average in a log-normally distributed data set are approximately 30% of the data points. In this sense, roughly 30 percentile values of elements are being used as the cut point for high concentrations.

The PSCF is simply the ratio of polluted segments ($m_j$) to the total number of segments ($n_j$) at each subregion. This ratio is a measure of the fraction of trajectory segments in the subregion, which results in high pollutant concentration at the receptor site. Therefore, PSCF can be used to identify the source regions, which may have potential to contribute on the observed concentrations of the pollutants.

PSCF can be calculated as single layer, using the trajectories at only 850 mb level, or as three layer, including also 700 and 900 mb level trajectories. When, three layer

PSCF is to be computed, the residence time of air masses over each subregion at 700 and 900 mb levels are also calculated using the coordinates of the air mass at 700 and 900 mb level as input to the software.

The three layer PSCF (TPSCF) is then becomes the following ratio

$$TPSCF = \frac{mj_{(700mb)} + mj_{(850mb)} + mj_{(900mb)}}{nj_{(700mb)} + nj_{(850mb)} + nj_{(900mb)}} \quad (4.1)$$

A subregion with a PSCF of 0 is unlikely to be a source region, while the ones with PSCF of 1 is likely to indicate a potential source region for the receptor site under investigation. It is important to note that, the PSCF ends up equal to unity, when the counts of total segments ($n_j$) are equal to the counts of pollutant segments ($m_j$), which means every time a trajectory pass over that particular subregion, high concentration of the test elements observed at the receptor. As the number of polluted trajectory segment endpoints terminating in a subregion increases, the emitted material from that subregion is more probably affect the receptor site. The uncertainty of PSCF value for a subregion depends on the number of trajectory segments in that subregion. The reliability of the estimates increases with increasing number of segments in that particular subregion, therefore the sizes of grids or the subregions should be kept sufficiently large to increase the number of segments in that subregion and thus reduce uncertainty. In this study, to reduce the uncertainty due to the small number of trajectory segments, the subregions over which the trajectories have passed less than 20 days were ignored in the PSCF calculations

It should be noted that, PSCF identifies the source areas having higher probabilities to contribute to high concentrations observed at receptor site, and does not yield quantitative estimates of source contributions, Therefore, PSCF can not be interpreted as substitute for emission inventories.

### *4.2.3. Concentration Fields (CF) and Redistributed Concentration Fields (RCF)*

The concentration and redistributed concentration field methods also require the computation of residence times over the subregions assigned as PSCF. After calculating residence time, the following formula is used to establish the concentration field maps

$$C_{mn} = \frac{1}{\sum_{l=1}^{M} \tau_{mnl}} \sum_{l=1}^{M} \log(c_l) \times \tau_{mnl} \qquad (4.2)$$

In this formula, $\tau_{mnl}$ is representing the residence times of air masses, that is the number of trajectory segment endpoints during the study period, and the $c_l$ is the observed concentration at the receptor site. The details about the formula are also given in Section 3.4.4.

The high concentration fields calculated means that on average, air parcels passing over the subregion (i,j), result in high concentration at the receptor site. The sources of pollutants in the concentration field procedure are concentrated in hot pots, however, the gradients of true source fields are underestimated in this procedure, since the measured concentration at the receptor site is equally attributed to all trajectory segments.

In the method developed by Stohl et al. (1996) this uncertainty is overcome by an iterative redistribution of the concentrations along trajectories. The formulas and details of the redistributed concentration field method are given in Section 3.4.5.

### *4.2.4. Comparison of Source Regions of Pollutants Identified by Each Method*

For the computation of source regions affecting eastern Mediterranean atmosphere, among the available aerosol data, Al, $SO_4^{2-}$ and Pb were selected.

Since the sources of aluminium are well known both in Turkey and Africa, it is a good element to test. The source regions of Al calculated by each of the 4 methods, are given in Figures 4.8, 4.9, 4.10 and 4.11.

As can be seen from the figures, the main sources of Al, which are west Africa, middle Africa and east Africa, Middle East and Turkey are identified by all approaches. This indicates that, the main source regions of Al in eastern Mediterranean aerosols are correctly identified by all three techniques. Additionally, the contributions of other regions are low in all approaches.

Both CF and RCF approaches have resulted in identical ordering of source areas. The contribution of all subregions are very close to each other in CF approach, whereas, in RCF approach, the contributions cover a wider range, indicating a better resolution of RCF method. Romania, Bulgaria, northwest Turkey, Middle East, Czechoslovakia and are the second order sources in RCF method, however, they are in the third order in CF method.

Single layer PSCF have also identified Africa, Middle East and Turkey as the main source areas for Al, which is identical with the main conclusions of the CF and RCF approaches. In addition to these major areas, Italy and Greece are identified by single layer PSCF as the secondary source regions, which can affect the eastern Mediterranean atmosphere.

The results of the three layer PSCF for Al is similar with the results obtained in the CF, RCF and single layer PSCF. But it should be noted that the distant sources are more important in three layer PSCF. When single layer and three layer PSCF approaches are compared, it is observed that the contribution of distant sources like France, Germany, West Africa, Austria and Holland-Belgium differs from each other. The contribution of France and West Africa is one order higher in three layer PSCF .Similarly, Germany, Austria and Holland-Belgium are second order sources

in three layer PSCF, whereas their contributions to the eastern Mediterranean atmosphere are the lowest in single layer PSCF. As a result, it can be said that the distant sources are more important in three layer PSCF, due to longer transport at 700 mb level.

The source areas of Pb calculated by each of the four methods are depicted in Figures 4.12, 4.13, 4.14 and 4.15. Romania, Belarus, western Turkey, middle and east Africa and are identified as primary and Bulgaria, Central Turkey and Greece, as secondary source regions for the Pb measured in Eastern Mediterranean aerosols by PSCF approach.

The Middle East, Italy, Belarus, West Turkey, Greece and East Africa are the primary source areas identified by three layer PSCF. One important difference observed between the results obtained by single and three layer PSCF, is the contribution of west Africa, which is rather unexpected source of Pb in eastern Mediterranean. As it is mentioned before, the subregions where the air masses passed through less than 20 days were ignored for each method to reduce the uncertainty. Therefore, the air masses passed through west Africa more than 20 days during the study period at three barometric levels and observed contribution can not be linked to statistical uncertainty in assessment. The observed concentration of west Africa subregion which appear in three layer PSCF but not in single layer PSCF should again due to the inclusion of 700 mb level trajectories, coming from longer distances. The three layer potential source contribution function have the general agreement with single layer PSCF for Pb, but more distant sources such as former Yugoslavian countries, Italy and Austria have more contribution in three layer PSFC.

When the CF, and RCF methods are compared, it is seen that the ordering of the source regions are identical. The range of values in RCF method is covering a wider range compared to the range of values obtained in CF methods.

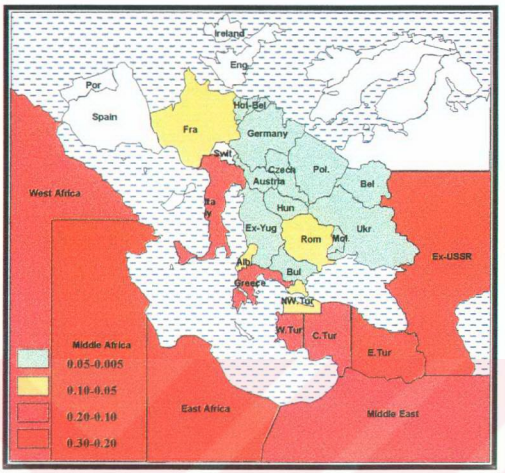


Figure 4.8. Single Layer PSCF for Al

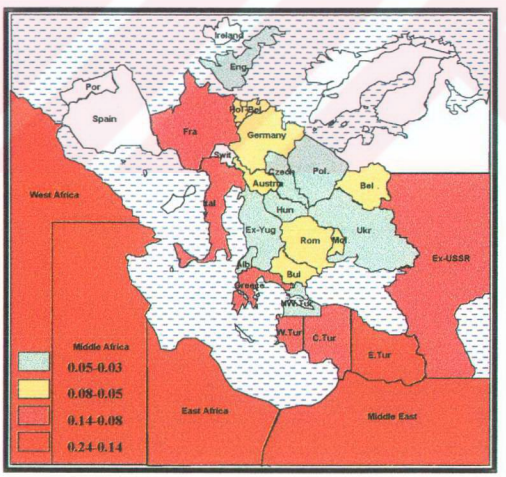


Figure 4.9. Three Layer PSCF for Al

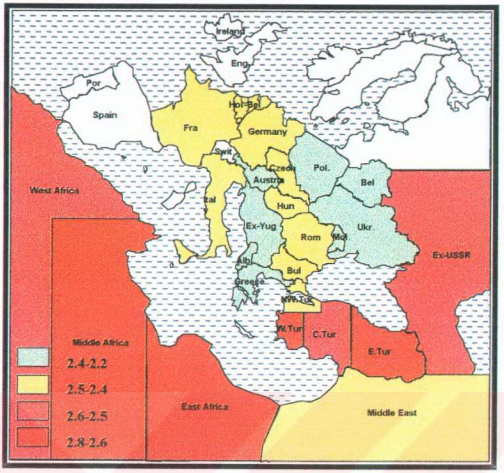


Figure 4.10. Concentration Fields (log, ng/m$^3$) for Al

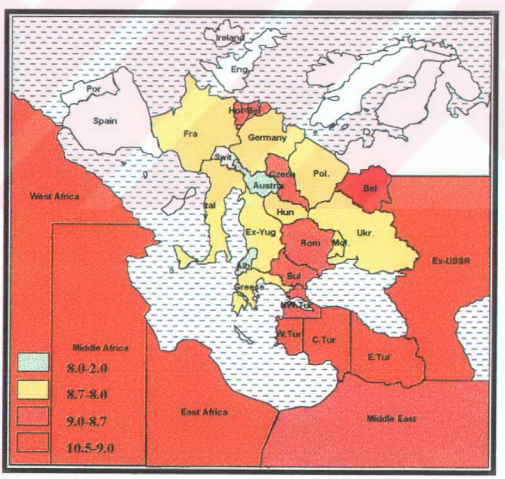


Figure 4.11. Redistributed Concentration (log, ng/m$^3$) Fields for Al

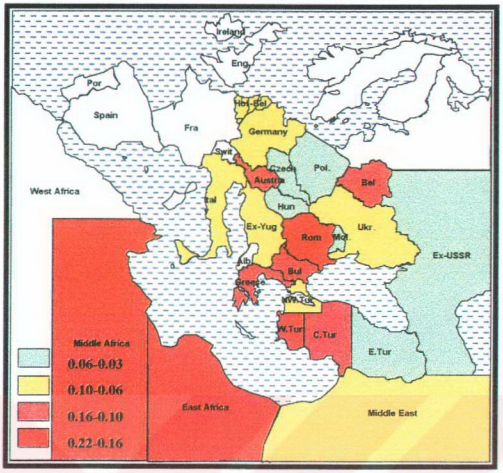


Figure 4.12.Single Layer PSCF for Pb

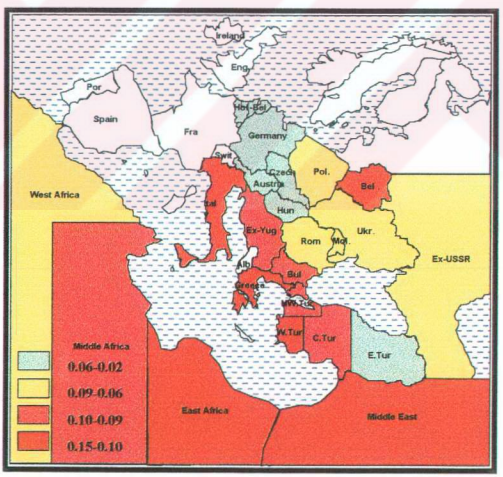


Figure 4.13. Three Layer PSCF for Pb

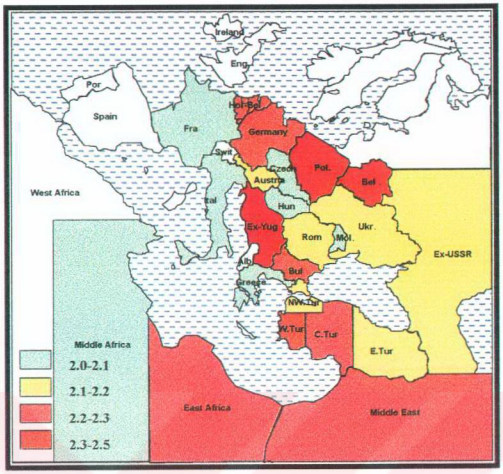


Figure 4.14. Concentration Fields (log, ng/m$^3$) for Pb

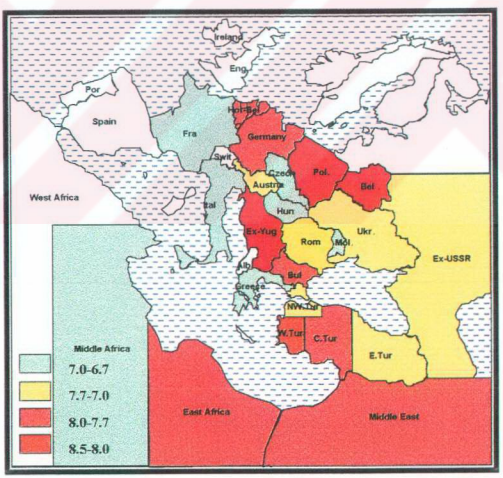


Figure 4.15. Redistributed Concentration (log, ng/m$^3$) Fields for Pb

The distributions of Pb source areas obtained by PSCF and concentrations field methods have some similarities and differences. Source areas close to the receptor such as subregions in Turkey, Balkan countries, Middle East and Africa are equally well predicted by all methods used. It may be a little misleading to divide the subregions as primary and secondary source regions due to small range of values obtained in most of the tested methods. But, the distant source regions predicted by PSCF and CF approaches are significantly different. Although White Russia appears as an important source in all approaches, Germany, Poland and to a certain extent France appears as more important source regions for eastern Mediterranean in CF and RCF techniques then they are in PSCF calculations.

It appears that CF and RCF approaches are more heavily weighted by distant source regions than single layer PSCF. The source regions of $SO_4^{2-}$ calculated by each method were depicted in Figures 4.16,4.17,4.18 and 4.19. The primary source regions of $SO_4^{2-}$ identified by CF and RCF methods similar. The primary source regions for $SO_4^{2-}$ are western Turkey, northwest Turkey, Greece and Bulgaria The Central Turkey, Romania, former Yugoslavia and Italy are as secondary source regions identified by both approaches. The only difference observed between the two approaches, is that France appeared as a secondary potential source region in RCF. However, the contribution of France is smaller in CF approach. On the contrary, Ex-USSR is a secondary potential source region in CF, whereas it does not contribute significantly in RCF approach. These are minor differences and do not change the conclusion stated at the beginning of the paragraph.

The subregions identified as potential source regions by PSCF approach have general agreement with the results obtained in CF and RCF methods. However, there are some differences between them. The contribution of Middle Africa seems higher in PSCF, although its contribution calculated by CF and RCF methods is low.

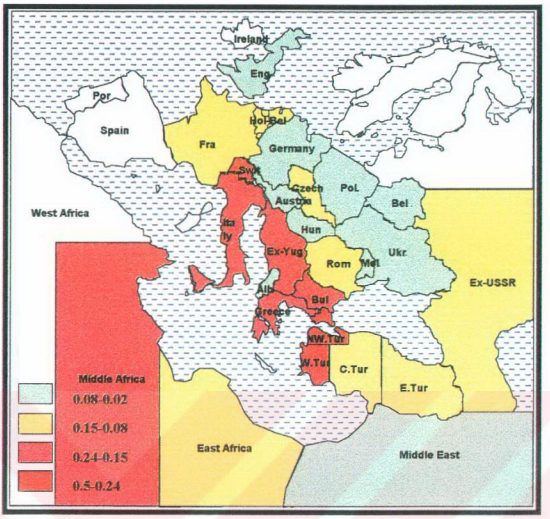


Figure 4.16.Single Layer PSCF for $SO_4^{2-}$

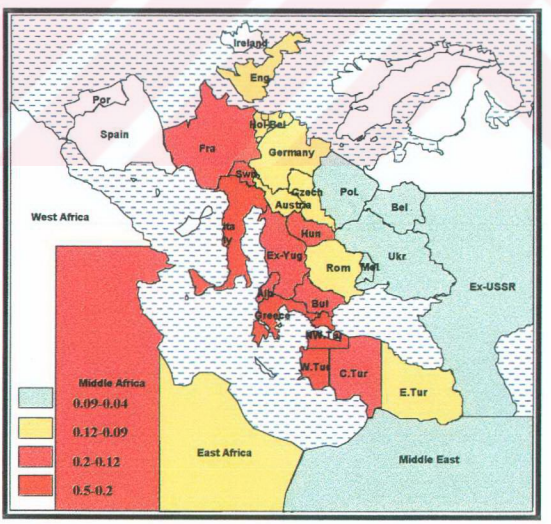


Figure 4.17.Three Layer PSCF for $SO_4^{2-}$

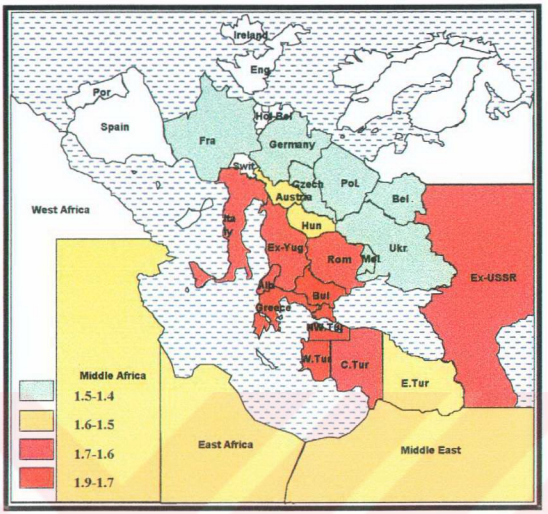


Figure 4.18. Concentration Fields (log, ng/m$^3$) for $SO_4^{2-}$

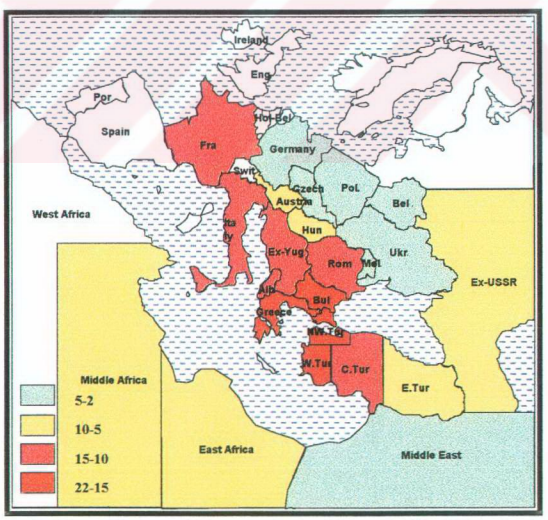


Figure 4.19. Redistributed Concentration (log, ng/m$^3$) Fields for $SO_4^{2-}$

The western and northwestern parts of Turkey, Greece, Bulgaria, Italy are the primary source areas identified by three layer PSCF. Former Yugoslavia, Hungary, France and Middle Africa are the secondary source regions of $SO_4^{2-}$.These are the source regions are that also identified by the CF and RCF techniques. Although the results obtained by each approach look similar to each other, there are some differences between the three layer PSCF and RCF methods. Western Turkey, northwestern Turkey and Greece are identified as the primary potential source areas by all three techniques used. But, Bulgaria which appeared as the primary source region in both CF and RCF methods is a secondary region in both single and three layer PSCF. Italy, which is a secondary source region, is CF and RCF approaches, is a primary source region in three layer PSCF approach.

In order to see the effect of 700 and 900 mb level transport on the CF and RCF methods, also the trajectory data at these levels are included in the source evaluation in addition to 850 mb level data. The calculations was only performed for $SO_4^{2-}$ using CF approach, since both CF and RCF methods result in similar ordering of source areas. The three layer CF's calculated are depicted in Figure 4.20.

When the source regions determined by single layer and three layer CF approaches, the contribution of the source areas that are closer to the receptor site are the same. The northwestern and western Turkey, are the primary sources in three layer CF method. Again, the higher contribution of distant sources are definitely distinguished, due to the incorporation of 700 mb trajectory data. France, Germany, Middle Africa, Poland and Czechoslovakia have higher contributions when the 700 and 900 mb level trajectories are used to calculate the residence times of air masses over the subregions.

The potential source regions identified by these trajectory statistics techniques, namely CF, RCF and PSCF (single and three layer) approaches show a general

agreement. This agreement is encouraging, suggesting that any of the three approaches will give fairly reliable qualitative information.

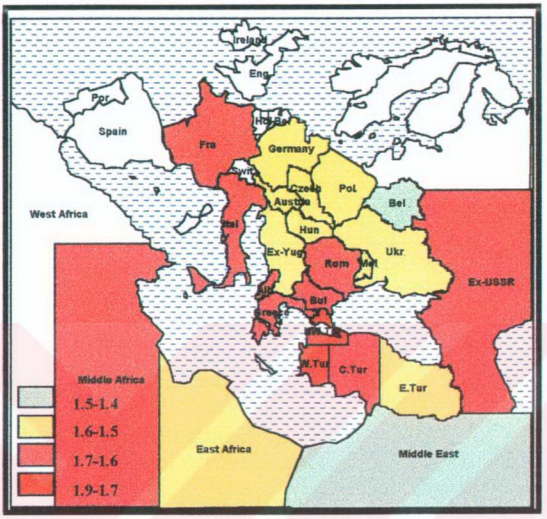


Figure 4.20. Concentration (log, ng/m$^3$) Fields for $SO_4^{2-}$ (Three layer)

The source areas that are close to the receptor site are reliably identified by all techniques used. However, there are some differences in the magnitudes of contributions of distant source regions such as Germany, France and Italy. These distant sources are more heavily weighted in the RCF and three layer PSCF approaches, compared to CF and single layer PSCF approaches. Generally, the distant sources identified as primary in RCF and three layer PSCF, as secondary in CF and single-layer PSCF.

Although single-layer and three layer PSCF approaches have identified the same source regions, the distant sources have more contribution in the three layer PSCF. This is expected, because single-layer PSCF includes only 850 mb trajectories,

whereas three layer PSCF approach use both 900,850 and 700 mb trajectories. 700 mb trajectories are generally longer, and transport in this higher altitude is not affected from wet scavenging as much as transport at 850 mb level.

The CF and RCF approaches are expected to produce fairly similar results. They use similar type of statistical tools. Similarly single layer and three layer PSCF approaches use similar formulations, only the level of trajectories used in the analysis differ from each other. But, the statistics used in CF-RCF and single layer three layer PSCF are totally different. Consequently, identification of same potential source regions by the two groups of trajectory statistics is highly encouraging.

The intercomparison discussed in this section have also highlighted the importance of 3D trajectory calculations. In most of the studies in this area 850 mb level is considered as standard, assuming the transport altitude is roughly 1500 m which corresponds to 850 mb level. However, there are no experimental evidence, which shows that transport does not occur at 700 mb level (3000 m). If annual averages of trajectories in these two levels are the same then such an assumption and use of only 850 mb level trajectories in sour region assessment would not be a problem. But most of the evaluations in this study have demonstrated that 700 mb level trajectories are longer than 850 mb level trajectories. Furthermore, since the pollutant wet scavenging is an important process that determines the temporal behaviour of pollutants at eastern Mediterranean and Black Sea atmospheres, and since wet scavenging occurs more extensively at 850 mb level compared to 700 mb, then exclusion of 700 mb trajectories from statistics would underestimate the significance of distant sources and overestimates the importance of nearby sources. Consequently, whenever possible 700 mb level trajectories should be included in statistics. This can be done by making all segment statistics at both 850 mb and 700 mb levels as described previously in this section.

### *4.3. Flow Climatology*

Flow climatology is the earliest method of source identification of pollutants. The basic of this approach is the classification of several years of backtrajectories ending at a receptor site according to their transport directions. By this method, it is possible to determine potential source regions of pollutants as the transport sectors associated with high pollutant concentrations are identified.

In this study, atmospheric transport patterns of pollutants to the eastern Mediterranean, western Mediterranean and Black Sea basins were determined by flow climatology method. The three receptor sites selected at each of the basin were Antalya for eastern Mediterranean (36°08 N 30°60 E), Cape Cavallo at Corsica Island for western Mediterranean (42°31 N 8°40 E) and Bartın for Black Sea basin (41°47 N 32°29 E). The 3.5 days long back trajectories ending at 12 00 UT at each receptor sites were calculated for every day during the years 1992, 1993, 1994 and 1995 using isentropic 3D European Centre Medium-Range Weather Forecast trajectory model at 700 and 850 mb barometric levels.

The air mass transport patterns to the each of the basin were calculated by sectoring technique based on the eight wind sectors. The calculated back trajectories were divided into 1 hr long segments and the air mass transport frequency from each of the wind sectors were determined by counting the number of these trajectory segment endpoints falling into each sector during 4 year time period. By this method, 4 year average and also seasonal air mass transport frequency distributions were determined for each monitoring site.

Upper atmospheric annual wind roses, which show percent contribution of air mass transport from each wind sector on annual air mass transport to the each of the

selected receptor sites, are given in Figure 4.21 and 4.22, for 850 and 700 mb levels, respectively

Trajectory roses at all three receptor sites at both levels have similar general features with higher frequency of flow from NW, N and NE sectors compared to E, SE, S and SW sectors.

Although the general features of the frequency distribution at each monitoring site at 850 mb level are the same, there are some differences between them. The flow frequency form N and NE sectors in the eastern and western Mediterranean are similar, but the NW flow in the eastern Mediterranean is approximately a factor of two higher than that in the western Mediterranean

The Black Sea basin does not receive as much N and NE flow. The contribution of these sectors to air mass transport to the Black Sea basin is approximately half of that observed in the eastern and western Mediterranean. NW flow to the Black Sea is 30% and 60% higher than the flows in the same sector to the eastern Mediterranean and western Mediterranean, respectively.

The air mass transport frequency at 700 mb level are similar in eastern Mediterranean, western Mediterranean and Black Sea basins with higher flow contribution from NW and N sectors, and smaller contribution from SE, E and S sectors. Similar to the 850 mb level transport, the flow frequency from S and SE sectors to the each of the basins are small at 700 mb level. In contrast to eastern Mediterranean and Black Sea basins, the western Mediterranean basin also receives high NE and E flow.

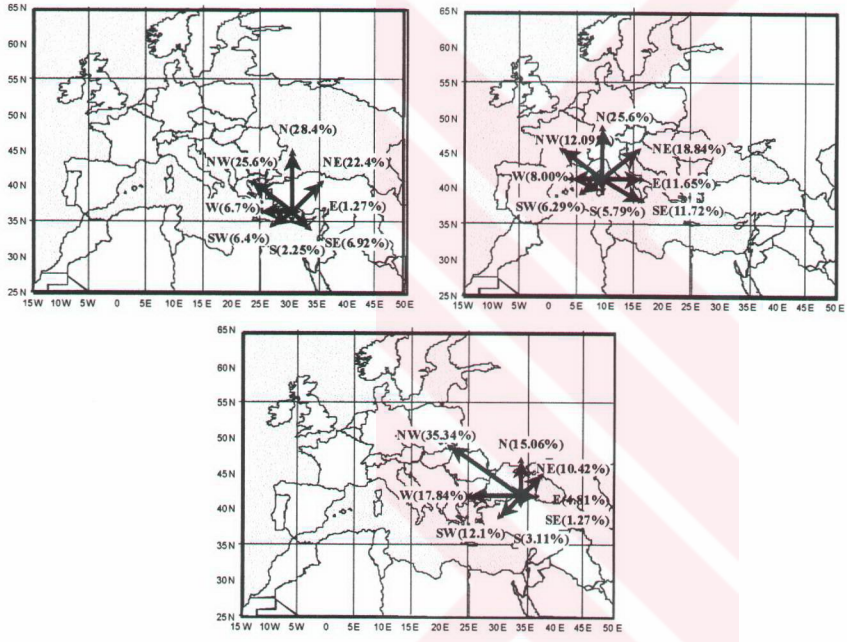


Figure 4.21. Air mass flow frequency to the tree receptor sites at 850 mb level

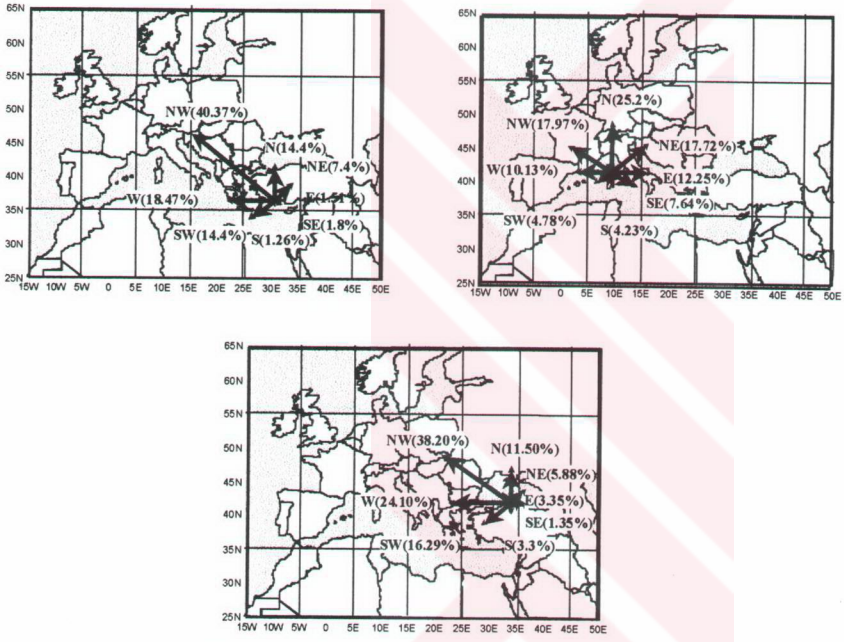


Figure 4.22. Air mass flow frequency to the three receptor sites at 700 mb level

The SW contribution to Black Sea basin at 850 mb is a factor of 2 higher than the flow contribution to the western and eastern Mediterranean. The flow frequency from NW, and W sectors to the eastern Mediterranean at 700 mb level are approximately a factor of two higher than in 850 mb level and the opposite is true for N and NE sectors. Additionally, the SW contribution at 700 mb level is also higher than in 850 mb level to the eastern Mediterranean basin, implying a higher flows from eastern parts of North Africa. Similarly, the air mass transport frequency at 700 mb level to the Black Sea basin from W and SW sectors are higher than in 850 mb level, whereas NE contribution is lower.

The differences observed in the air mass transport frequencies to each of the basins have some implications in terms of pollution transport. Although similarities in the N and NE flows in the western and eastern parts of the Mediterranean basin gives an impression that pollution transport from these two sectors are the same to the both parts of the Mediterranean basin, it should be noted that the sectors from which pollutants are expected to be transported to the eastern, and western Mediterranean atmospheres are not the same. Pollution transport to the eastern Mediterranean, and Black Sea atmospheres are expected to occur from NE, N, NW, and W sectors, whereas sectors, which include high emission areas for the western Mediterranean, are SE, E, NE, N, and NW. Smaller contributions of SE and E sectors on annual flow pattern in the western Mediterranean indicate a smaller contribution of central European, and former USSR countries on the chemical composition of aerosols and precipitation in the western Mediterranean basin, and implies a difference in the potential source regions affecting western and eastern Mediterranean atmospheres. Significantly higher NW flow in the Black Sea suggests stronger impact of central European sources to the Black Sea atmosphere compared to their impact on the Eastern Mediterranean basin.

Although there are some differences also in the E, and SE sector contributions, these differences are not significant in terms of pollution transport, because (1) contributions of E, and SE sectors on annual flow patterns are very small, and (2) Most of the countries lying to the E, and SE of the eastern Mediterranean, and Black Sea basins are not heavily industrialized, and hence they do not have high emission intensities.

### *4.4. Comparison of Flow Climatologies at eastern and western Mediterranean Basins*

Different researchers have studied flow climatology in the Mediterranean region in the past. However, these studies were not evaluated in terms of pollution transport to the region. The four sector flow patterns (north-northwest, west-southwest, south-southeast and east-northeast) computed for the western, and eastern Mediterranean basins in different studies are given in Figure 4.23. The mean feature that is common in all studies performed so far is the more frequent flow from N, and W, and smaller flow frequency from S, and E sectors. Although, these general features of upper atmospheric flow appears in all studies, there are some differences between them. Frequencies of flow from each of the major wind sectors calculated in this study for the eastern Mediterranean atmosphere (Antalya) agrees remarkably well with the flow patterns derived by Kubilay (1996) for the Erdemli site, which is located approximately 400 km to the east of our site and agrees fairly well with the flow pattern calculated by Katsoulis and Whelpdale (1993) for the Crete island which is located approximately 400 km to the SW of our site. However, flow patterns calculated for a site on the Israel coast by Dayan et al. (1986), which is also in the eastern Mediterranean basin, has approximately 30% smaller contribution of the N sector. Four-year average flow pattern calculated in this study for the western Mediterranean atmosphere (Corsica) have approximately 60% lower contribution of the W sector, and 90 %higher contribution of the E sector compared to flow pattern obtained in the GESAMP (1985) study for the western Mediterranean region.

The observed differences in the flow patterns in the Black Sea, eastern and western Black Sea can be real due to relatively large distances between these basins. However, the patterns obtained in four studies in the eastern Mediterranean are expected to be similar, also the patterns obtained for the western Mediterranean in the GESAMP study in 1985 should be similar to the flow pattern obtained in this study for the Corsica. The differences obtained in these studies are probably due to different software used in back trajectory calculations, different methods used to assign back trajectories into wind sectors, different locations and different time-slots used for calculations. This comparison demonstrates that although general features of flow climatology in the Mediterranean region are fairly well established, the agreement between different studies is not good enough to differentiate between the flow climatologies of the eastern, and western Mediterranean basins.

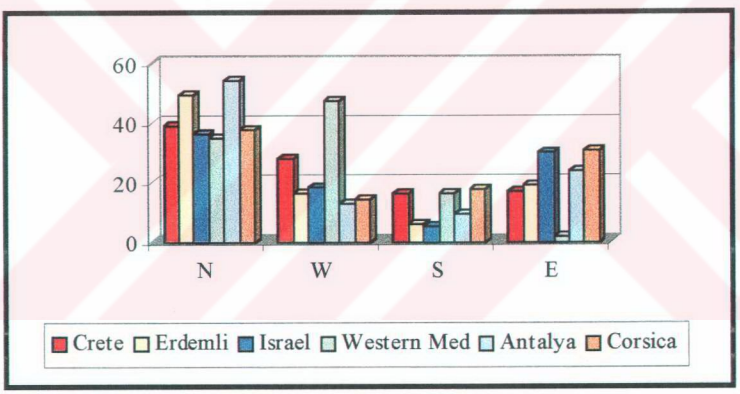


Figure 4.23. The average frequency of air mass transport at different sites in Mediterranean Sea

### *4.5. Seasonal Flow Patterns*

The seasonal variations in the flow patterns due to the seasonal differences in the climate may affect the contribution of source regions to the chemical composition of

aerosols and precipitation in the Black Sea, eastern, and western Mediterranean basins. Therefore, the seasonal variations of air mass transport frequencies to the each monitoring site are required to be determined.

In order to determine the seasonal transport patterns, the year is divided into two period. The summer (dry) season covers the period between May and October, and winter (wet) season covers the rest of the year. Such division of the year into summer and winter seasons is based on occurrence of precipitation in the eastern Mediterranean and found to be convenient to explain seasonal variations in the chemical composition of both particles and rain water in the region (Al-Momani et al., 1998; Güllü et al., 1998). Based on such division, summer is the dry period when only 20% of the annual precipitation occurs, and winter is the wet period during which 80% of the annual rainfall occurs. Summer and winter flow patterns calculated at 850 mb level for the eastern Mediterranean, Black Sea and western Mediterranean are given in Figure 4.24.

At the receptors in the eastern and western Mediterranean basins, flow frequency from NE sector is higher during summer, and flows from S, SE, E, SW, and W sectors are more frequent during winter. The contribution form N sector to the eastern and western Mediterranean basins in summer and winter seasons are close to each other. The flow frequency from NW sector at eastern Mediterranean is higher in winter season, in contrast to western Mediterranean, where the NW sector contribution is approximately factor of 2 higher in summer season. Seasonal variations in the flow patterns, similar to those found in this study were also observed in previous climatological studies in the region (GESAMP, 1985; Katsoulis and Whelpdale, 1993; Dayan et al., 1986; Kubilay, 1996).The flow frequency to Black Sea basin from N, NE and E sectors are higher in winter season, whereas the contribution from SE, SW and W sectors are higher during the summer season. The air mass transport from NW sector during both summer and winter seasons are very close to each other.

a. Antalya (eastern Mediterranean)

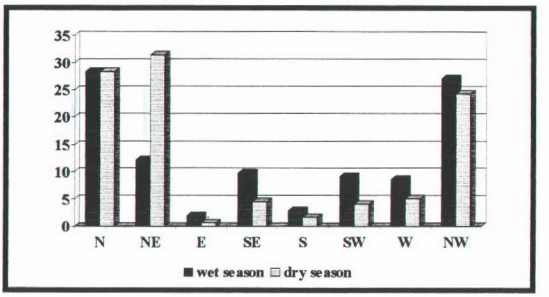


b. Bartın (Black Sea)

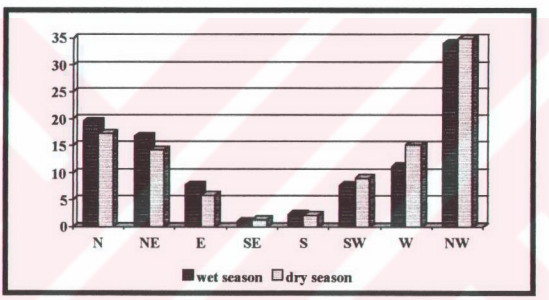


c. Corsica (western Mediterranean)

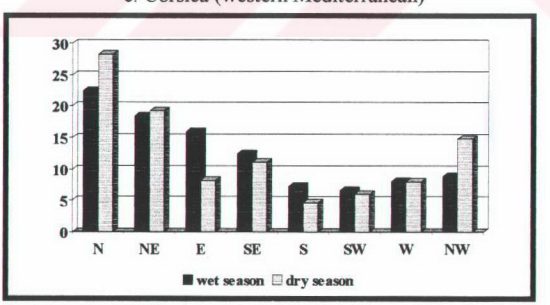


Figure 4.24. The seasonal flow patterns at three-receptor site investigated in this study

Seasonal differences in the frequencies of air mass transport from each sector varies between 5 % and 15% both in this work as shown in Figure 4.24 and in other studies discussed previously. Since large number of back trajectories and trajectory segments were involved in all of these studies, reported differences, no matter how small, are statistically significant. However, the main question that is important in terms of pollution transport to the region is whether these differences can explain observed seasonal variations in the chemical compositions of aerosols and precipitation in the Mediterranean atmosphere. Concentrations of pollution-derived trace elements and ions in the Mediterranean atmosphere (both in aerosols and in precipitation) are approximately a factor of 2 to 3 higher during summer season. This general feature is repeatedly demonstrated in all aerosol and precipitation measurements, both in the eastern, and western Mediterranean regions (Güllü et al., 1998; Al-Momani et al., 1998; Kubilay and Saydam, 1995; Dulac et al., 1987; Bergametti et al., 1989). When seasonal differences in the concentrations of pollutants are compared with the magnitude of seasonal differences in the flow frequenceis from each sector which is at most 15%, it can be concluded that seasonal variations in the flow patterns are not large enough to explain observed seasonal variations in the concentrations of pollution derived parameters in the western, and eastern Mediterranean atmospheres. Observed seasonal variations in the concentrations of pollutants in the Mediterranean basin should be explained by other factors such as different scavenging efficiencies in different seasons.

### *4.6. Residence Time Analysis*

The trajectory rose approach discussed previously is convenient to understand flow patterns in the Black Sea, and Mediterranean atmospheres, and to compare these flow patterns with results obtained from other climatological studies in the region where trajectories are always grouped into wind sectors. However, the trajectory rose approach is not the best one to evaluate potential source regions affecting chemical composition of particles and precipitation at the selected sites, because

several different source regions which occur in the same wind sector can not be evaluated separately. Consequently, the trajectory rose approach have fairly poor resolution to evaluate source regions from where pollutants are transported to the Black Sea, eastern, and western Mediterranean atmospheres.

A different approach was used to determine the influence of flow patterns on the transport of emissions from source areas to the three selected basins.

The 1 hr trajectory segments at 850 mb level over the subregions assigned before, for each day during 4 years time period were counted using a home made software. The sum of these trajectory segments that fall into each subregion were considered to be the measure of the residence times of air masses over subregions before reaching to the selected receptor sites in the Black Sea, eastern, and western Mediterranean basins.The 4-year-long residence times (hr) of air masses over subregions at 850 mb level are given in Figure 4.25, 4.26 and 4.27 for eastern, western Mediterranean and Black Sea basins respectively.

Air masses spent most of their time over France, Italy, Spain, and UK, and to a lesser extend over Germany and other central European countries, and western parts of the North Africa before they reach to the selected receptor in the western Mediterranean basin. France and Italy are particularly important potential source regions, because air masses affecting western Mediterranean spent approximately 50% of their time over these two countries.

For the eastern Mediterranean, approximately 58% of the hourly trajectory segments were found to occur at western, and central Turkey, and air masses spent smaller but significant fraction of their time over Eastern part of Africa, Ex-USSR, Middle East,

Ukraine, Greece and Italy. These countries totally account for approximately 27% of the hourly segments, meaning that air masses that reach to the eastern Mediterranean have spent 27% of their time over these subregions. Remaining 22 subregions account for the rest of the trajectory segments (15%). Consequently, Turkey itself, Balkan countries and nearby regions in the east and south are the regions where air masses reaching to the eastern Mediterranean spent most of their time.

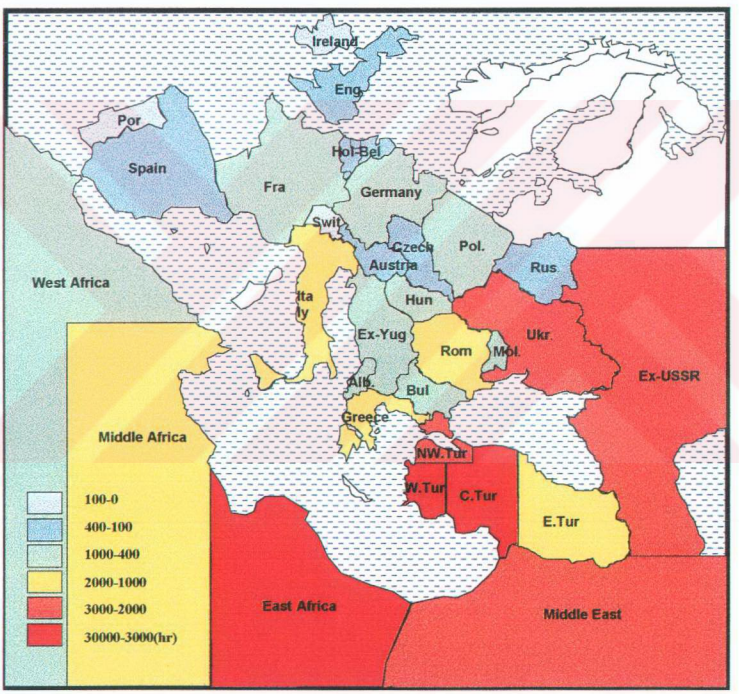


Figure 4.25. Residence time of air masses before reaching Antalya at 850 mb level

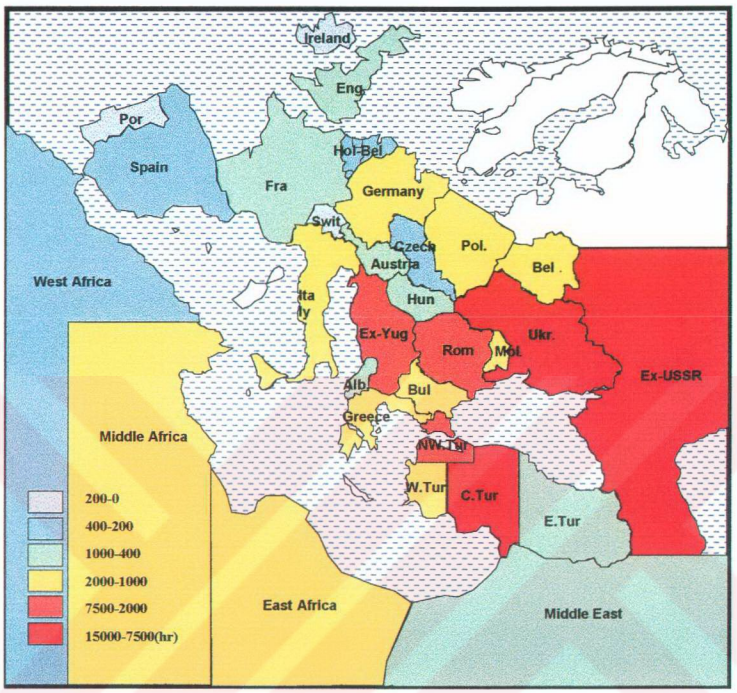


Figure 4.26. Residence time of air masses before reaching Bartın at 850 mb level

Air masses that arrive to the Black Sea spent most of their time over central Turkey, EX-USSR and Ukraine. These three countries account for the 52% of the trajectory segments. Romania, Bulgaria, Greece, Italy, western parts of Turkey are the other potential source regions in terms of air mass residence time.

The residence times of air masses over subregions at 700 mb level before reaching at Antalya station were also calculated to be able to perform a comparison between the 850 mb and 700 mb level transport patterns. The calculated residence times for Antalya are given in Figure 4.28.

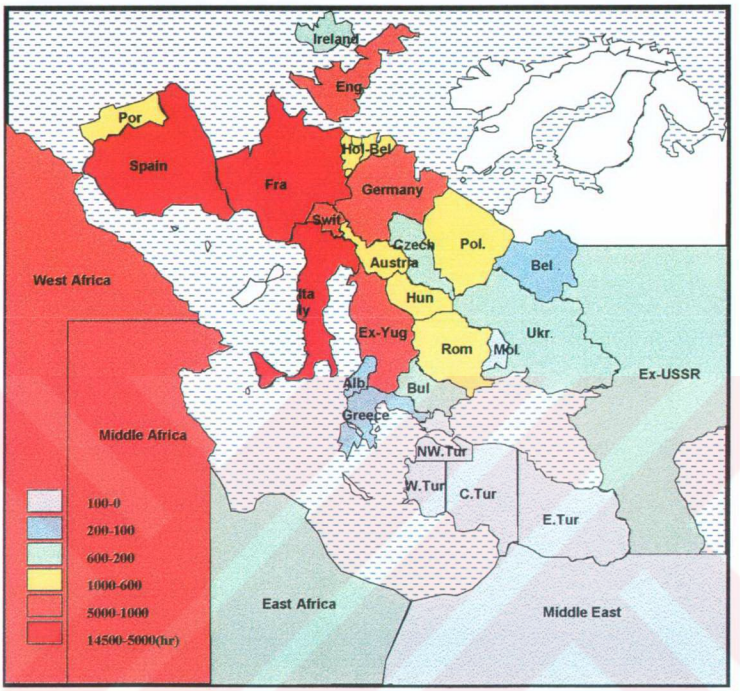


Figure 4.27. Residence time of air masses before reaching Corsica at 850 mb level

The 700 mb level air masses arriving at the receptor site at eastern Mediterranean spent approximately 46% of their time in central Turkey, eastern and central parts of the North Africa. Italy, Greece, ex-USSR, Ukraine, west and northwest Turkey and Middle East totally account for the 27 % trajectory segments at 700 mb level.

As it is seen from figure 4.25 and 4.28, the flow at 850 and 700 mb levels are similar to each other with higher residence times at central Turkey, Italy, Ukraine, and eastern parts of North Africa. The only observed difference between 700 mb and

850 mb level transport is that the residence times of air masses over distant subregions such as France, Spain, Germany, Italy, West Africa are higher in 700 mb level than in 850 mb level, whereas the residence times over nearby sources like Middle East, Turkey and Ex-USSR are lesser. This indicates that the air mass transport at 700 mb level mostly occurs from distant sources.

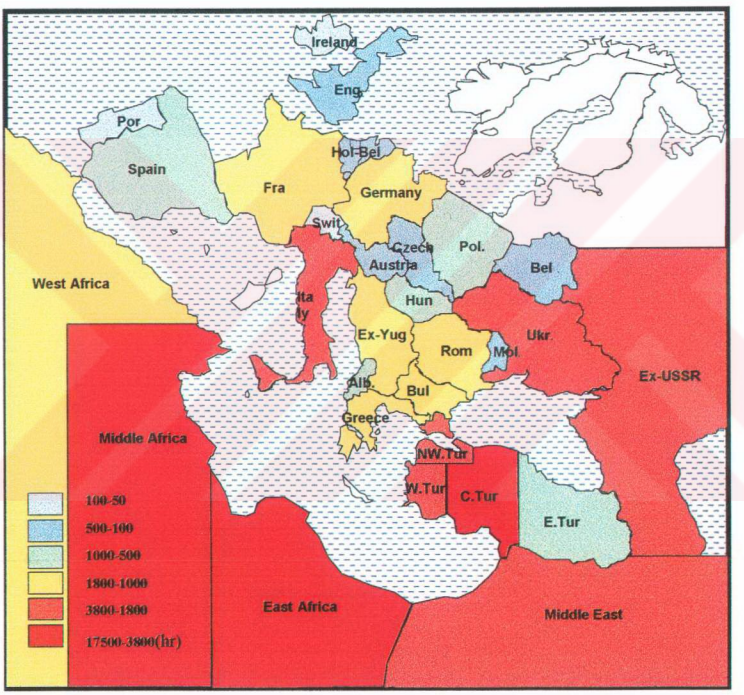


Figure 4.28. Residence time of air masses before reaching Antalya at 700 mb level

In all three basins residence times of air masses are the highest in the countries closest to the selected receptor site. This is due to the fact that no matter where they

originate from, all of the back trajectories pass over these subregions before they reach to the receptor site. Consequently, the countries closest to the selected receptor sites are the most likely candidates to be potential source regions affecting chemical composition of particles and precipitation. However, air mass movements alone cannot produce complete picture on the potential source regions, because a trajectory can stay over a region for most of its time, but still do not carry pollutants to the receptor site if there are no emissions in that region. Consequently, emissions of pollutants in each subregion should also be taken into account to determine potential source regions.

In order to take into account both air-mass residence-times over subregions and emissions in determining the potential source regions, the residence times over each subregion were multiplied with the emissions from that subregion. In this treatment, the calculations were performed for the three selected sites, and for S, N, Zn, Pb, and As for which the emission data were available.

Country-based emissions for trace elements and ions were obtained from an EMEP modeling study (UNEP, 1994), and shown in Figure 4.29 and 4.30 for As and Pb. Pb and As emissions are high in countries (subregions) such as, Ukraine, Belarus, Poland, Germany, Italy, France, Spain, and UK which lies to the west and north of the study area. With minor differences, similar distributions of emissions were also observed for S, N, Zn are given in Table 4.1. Countries that lie to the east, and south of the study area are characterized with their low pollutant emissions.

In order to calculate the relative contributions of the emission sources on the observed pollutant concentrations at the three selected receptor sites, the emissions in each subregion (ton/yr) and the residence time over that subregion (hr) were multiplied. This product was considered to be giving the relative pollutant contributions of each subregion and termed as residence time – emission intensity index of each subregion.

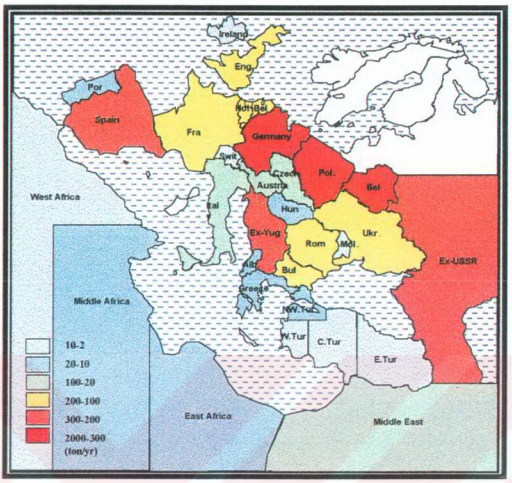


Figure 4.29. Country based As emission

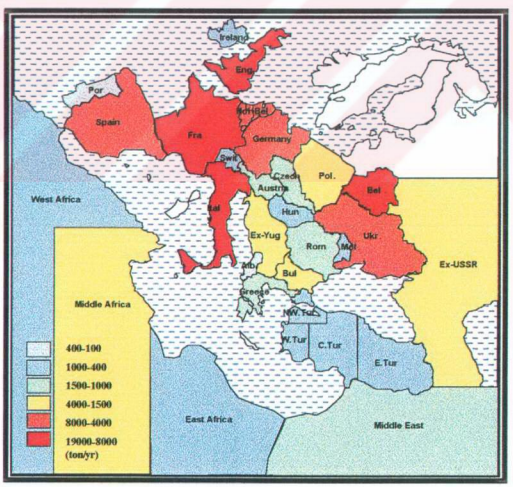


Figure 4.30. Country based Pb emissions

Table 4.1. Country based emissions of S, N, Zn

| | $SO_2$- S | $NH_3$+$NO_x$ | Zn |
|---|---|---|---|
| | (tons/yr) | (tons/yr) | (tons/yr) |
| PORTUGAL | 102000 | 95000 | 100.5 |
| SPAIN | 1158000 | 305000 | 3982.5 |
| FRANCE | 685000 | 1187000 | 3311.5 |
| SWITZERLAND | 31000 | 103000 | 64 |
| ITALY | 1090000 | 874000 | 1949 |
| ALBANIA | 55000 | 37000 | 37 |
| EX-YUGOSLAVIA | 740000 | 302000 | 1804 |
| GREECE | 250000 | 291000 | 175.5 |
| GERMANY | 2870000 | 2045000 | 4538 |
| AUSTRIA | 49000 | 134000 | 175 |
| HUNGARY | 505000 | 212000 | 203 |
| ROMANIA | 900000 | 424000 | 645 |
| CZECHOSLOVAKIA | 1222000 | 467000 | 756 |
| MOLDAVIA | 82000 | 55000 | 12 |
| POLLAND | 1498000 | 785000 | 4023 |
| BELARUS | 2233000 | 2186000 | 75.66 |
| UKRAINE | 1391000 | 1036000 | 2150.4 |
| BULGARIA | 633000 | 151000 | 1724 |
| NW. TURKEY | 80000 | 182400 | 244.64 |
| W. TURKEY | 40000 | 91200 | 122.32 |
| C. TURKEY | 40000 | 91200 | 122.32 |
| E. TURKEY | 40000 | 91200 | 122.32 |
| ENGLAND | 1887000 | 1216000 | 2296 |
| IRELAND | 95000 | 178000 | 43.5 |
| HOLLAND-BELGIUM | 308000 | 547000 | 1004 |
| MIDDLE EAST | 185000 | 137000 | 268.1 |
| E. AFRICA | 125000 | 48000 | 114.8 |
| M. AFRICA | 180000 | 138000 | 251 |
| W. AFRICA | 76000 | 49000 | 117.8 |
| EX-USSR | 201000 | 237000 | 2786.6 |

The results of this treatment which show relative contribution of emissions from subregions on the chemical composition of particles and precipitation in the eastern Mediterranean, Black Sea and western Mediterranean atmospheres are given in Figures 4.31, 4.32 and 4.33 for As, and 4.34, 4.35 and 4.36 for Pb, respectively, and in Table 4.2 for the remaining species. Potential source regions affecting the western and eastern Mediterranean atmospheres are significantly different. Turkey

(particularly the central parts), Ukraine, Italy and central parts of Turkey, Belarus, ex-USSR and Germany are the potential source regions that can affect the chemical composition of aerosols and precipitation in the eastern Mediterranean basin.. The chemical composition of particles and rainwater in the western Mediterranean, on the other hand, are strongly effected by emissions in France, Germany, Italy, Spain, and UK.

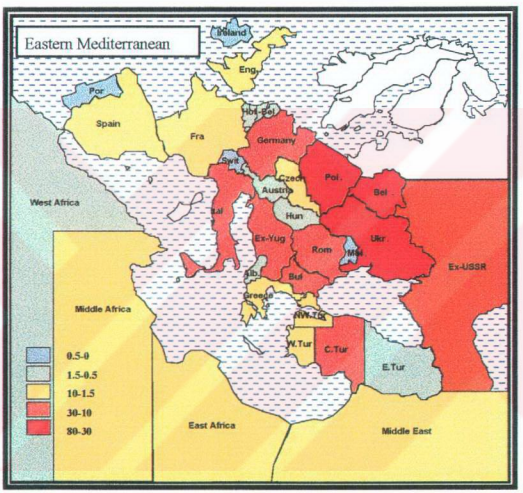


Figure 4.31. Residence time-emission intensity index of As for eastern Mediterranean (ton)

Table 4.2. Emission intensity-residence time index of S,N and Zn calculated for eastern Mediterranean, western Mediterranean and Black Sea basins ($10^3$ ton )

| | Eastern Mediterranean | | | Western Mediterranean | | | Black Sea | | |
|---|---|---|---|---|---|---|---|---|---|
| | S | N | Zn | S | N | Zn | S | N | Zn |
| PORTUGAL | 0.24 | 0.23 | 0.00 | 8.63 | 8.04 | 0.01 | 0.15 | 0.14 | 0.00 |
| SPAIN | 22.87 | 6.02 | 0.08 | 652.37 | 171.82 | 2.24 | 26.83 | 7.07 | 0.09 |
| FRANCE | 35.19 | 60.98 | 0.17 | 1130.25 | 1958.55 | 5.46 | 67.72 | 117.34 | 0.33 |
| SWITZERLAND | 0.10 | 0.32 | 0.00 | 4.40 | 14.63 | 0.01 | 0.26 | 0.86 | 0.00 |
| ITALY | 207.67 | 166.52 | 0.37 | 1368.72 | 1097.49 | 2.45 | 236.54 | 189.67 | 0.42 |
| ALBANIA | 3.09 | 2.08 | 0.00 | 1.18 | 0.79 | 0.00 | 3.08 | 2.07 | 0.00 |
| EX-YUGOSLAVIA | 79.74 | 32.54 | 0.19 | 159.15 | 64.95 | 0.39 | 170.81 | 69.71 | 0.42 |
| GREECE | 55.42 | 64.51 | 0.04 | 4.57 | 5.32 | 0.00 | 46.20 | 53.78 | 0.03 |
| GERMANY | 173.97 | 123.96 | 0.28 | 861.98 | 614.20 | 1.36 | 466.87 | 332.66 | 0.74 |
| AUSTRIA | 1.07 | 2.92 | 0.00 | 4.96 | 13.55 | 0.02 | 2.34 | 6.41 | 0.01 |
| HUNGARY | 23.98 | 10.07 | 0.01 | 45.60 | 19.14 | 0.02 | 55.80 | 23.43 | 0.02 |
| ROMANIA | 152.05 | 71.63 | 0.11 | 62.47 | 29.43 | 0.04 | 319.62 | 150.58 | 0.23 |
| CZECHOSLAVAKIA | 24.13 | 9.22 | 0.01 | 59.98 | 22.92 | 0.04 | 46.73 | 17.86 | 0.03 |
| MOLDAVIA | 3.90 | 2.62 | 0.00 | 0.28 | 0.19 | 0.00 | 10.48 | 7.03 | 0.00 |
| POLLAND | 107.90 | 56.55 | 0.29 | 125.35 | 65.69 | 0.34 | 297.21 | 155.75 | 0.80 |
| BELARUS | 95.85 | 93.83 | 0.00 | 47.67 | 46.66 | 0.00 | 391.79 | 383.55 | 0.01 |
| UKRAINA | 409.52 | 305.01 | 0.63 | 67.33 | 50.14 | 0.10 | 1230.94 | 916.79 | 1.90 |
| BULGARIA | 69.30 | 16.53 | 0.19 | 20.81 | 4.96 | 0.06 | 130.07 | 31.03 | 0.35 |

Table 4.2. Continued

| | | | | | | | | | |
|---|---|---|---|---|---|---|---|---|---|
| ENGLAND | 677.04 | 436.29 | 0.82 | 352.84 | 227.38 | 0.43 | 116.75 | 75.24 | 0.14 |
| IRELAND | 19.27 | 36.11 | 0.01 | 4.12 | 7.72 | 0.00 | 1.51 | 2.82 | 0.00 |
| HOLLAND-BELGIUM | 17.26 | 30.66 | 0.06 | 21.13 | 37.53 | 0.07 | 8.75 | 15.55 | 0.03 |
| MIDDLE EAST | 56.45 | 41.80 | 0.08 | 0.00 | 0.00 | 0.00 | 8.93 | 6.62 | 0.01 |
| E. AFRICA | 55.81 | 21.43 | 0.05 | 5.54 | 2.13 | 0.01 | 18.07 | 6.94 | 0.02 |
| M.AFRICA | 44.22 | 33.90 | 0.06 | 43.73 | 33.52 | 0.06 | 22.85 | 17.52 | 0.03 |
| W.AFRICA | 252.63 | 162.88 | 0.39 | 24.01 | 15.48 | 0.04 | 2.73 | 1.76 | 0.00 |
| EX-USSR | 35.38 | 41.72 | 0.49 | 4.63 | 5.47 | 0.06 | 214.93 | 253.42 | 2.98 |

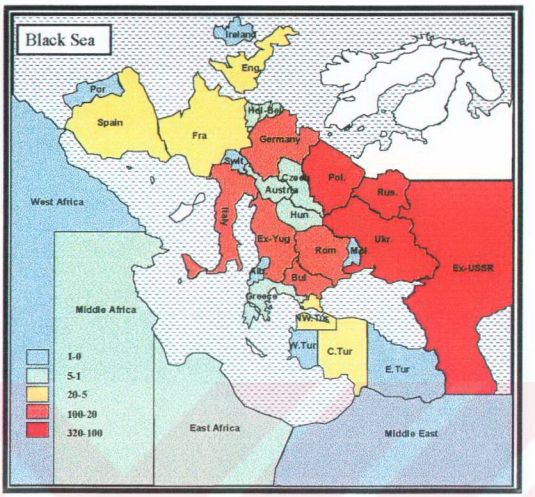


Figure 4.32. Residence time-emission intensity index of As for Black Sea (ton)

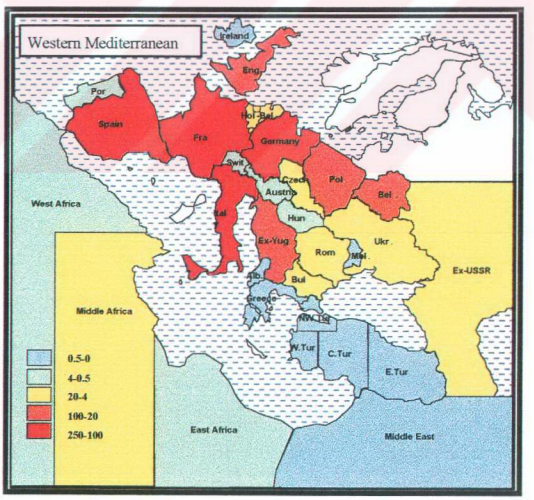


Figure 4.33. Residence time-emission intensity index of As for western Mediterranean (ton)

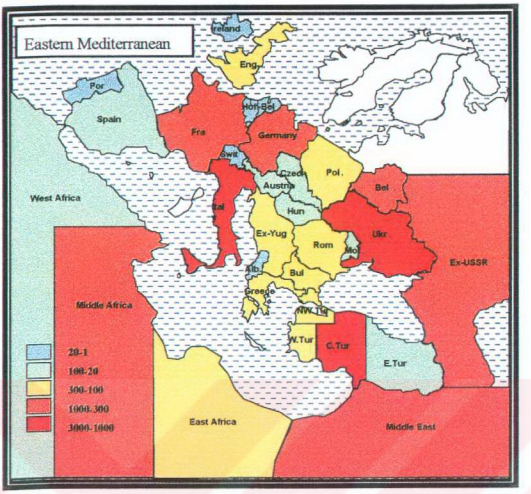


Figure 4.34. Residence time-emission intensity index of Pb for eastern Mediterranean (ton)

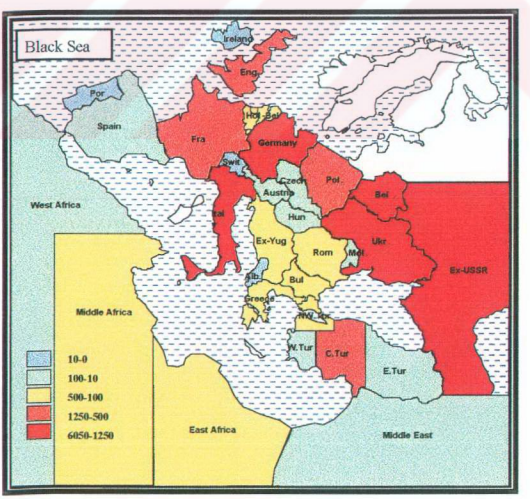


Figure 4.35. Residence time-emission intensity index of Pb for Black Sea (ton)

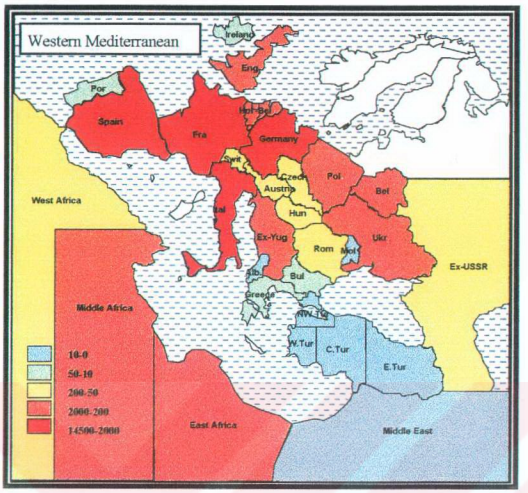


Figure 4.36. Residence time-emission intensity index of Pb for western Mediterranean (ton)

Although distribution of potential source regions around the Black Sea, and eastern Mediterranean looks similar, there are some differences in relative magnitudes of subregion-contributions. The most important potential source areas for the Black Sea are the countries lying to the north of the basin, namely Ukraine, Ex-USSR, Belarus, countries such as Turkey, Poland, Romania, Bulgaria, Italy, Germany and France can also effect the pollutant levels observed in the Black Sea, but their contribution are not as large as the contributions of regions in the first group.

Based on these discussions it can be concluded that the potential source regions that can effect the chemical composition of aerosols and rain in the eastern Mediterranean and the Black Sea are fairly similar, whereas potential source regions for the western Mediterranean basin are significantly different. The western European countries that are the primary sources for the western Mediterranean basin are the secondary

potential source areas for the Black Sea and eastern Mediterranean. Similarly, the countries that lies to the north of the study area such as Ukraine and Ex-USSR region, which are the primary potential source regions for the eastern Mediterranean and Black Sea are not as significant for the western Mediterranean basin.

Although the discussion on the similarities and differences in the emission areas which are affecting chemical composition of anthropogenic component in aerosols and precipitation in the Mediterranean and Black Sea atmospheres were based on S, N, As, Pb and Zn, conclusions reached can be used for the anthropogenic component of aerosols and precipitation in general, because the parameters included in the discussion are good tracers for a variety of industrial processes.

The theoretical potential source regions affecting eastern Mediterranean atmosphere are compared with the PSCF's of elements calculated for the eastern Mediterranean (Antalya). Since the PSCF discussed previously in the text bases on measured concentrations of elements, calculated PSCF's of elements can be considered as experimentally determined actual source regions affecting eastern Mediterranean atmosphere.

The potential source contribution functions of elements and major ions for the eastern Mediterranean were computed using data from approximately 300 daily aerosol samples (Güllü,.1996) and their corresponding back trajectories. The PSCF's of As and Pb in subregions for the eastern Mediterranean atmosphere are given in Figure 4.37 and 4.38 respectively and the PSCF of the remaining species are given in Table 4.3.

When subregions with high PSCF values are compared with potential source areas derived from emission-segment product, it can be concluded that emission segment product approach predicts potential source regions close to the receptor site, such as

Turkey, Middle East, Balkan countries and Italy, but overestimates the significance of distant potential source regions such as Ukraine. Ex-USSR and western European countries. Similar differences between theoretical and experimental potential source regions were also observed for $NO^{3-}$, $SO_4^{2-}$, Zn.

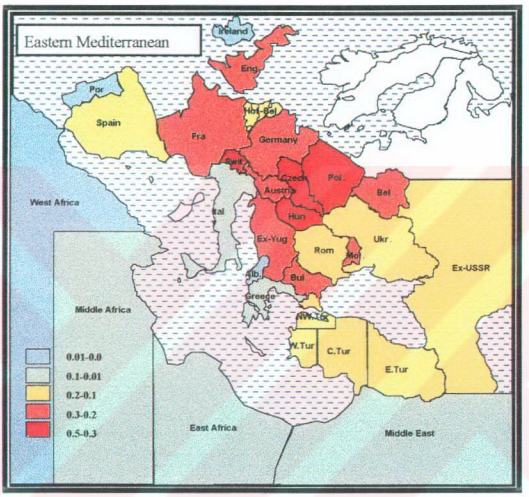


Figure 4.37. PSCF of As

The reason for differences between theoretical and experimental source regions for the eastern Mediterranean atmosphere is the scavenging of particles during transport from their source areas to the receptor site in the eastern Mediterranean, which is a parameter that was not taken into account in theoretical calculation of potential source regions. Although it is not possible to differentiate between wet and dry deposition as the scavenging mechanism which is responsible from observed differences, the wet deposition mechanism is expected to have a dominating effect over dry deposition as the transport over hundreds-to-thousands of kms from source regions to the eastern Mediterranean occur in the free troposphere, and most of the large particles for which dry deposition is an effective scavenging mechanism are

removed from the atmosphere before they escape from boundary layer to the free troposphere. Both precipitation events on the path of the trajectories, which bring pollutants to the receptor and the precipitation events at the receptor site can effect atmospheric concentrations at the receptor. Since the rain is not frequent at the eastern Mediterranean (annual rainfall 500 mm), approximately 75% of the particle scavenging is due to distant rain events during transport of particles and 25% of the scavenging is due to local rain events at the receptor site (Güllü et al., 1998).

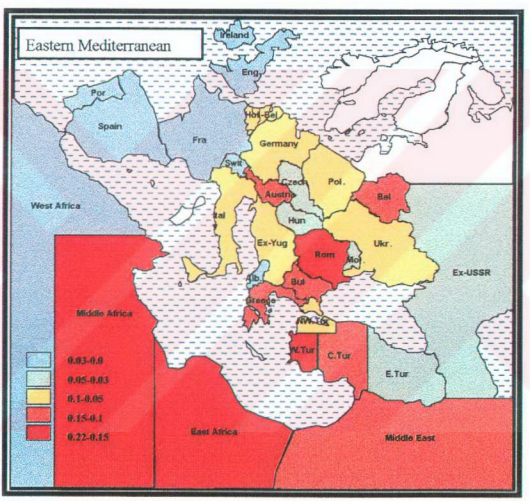


Figure 4.38. PSCF of Pb

Wet scavenging of particles from the atmosphere becomes more important as the distance between the source and receptor increases, due to higher probability of an air mass to encounter precipitation event as it travels long distances toward the receptor. Consequently, rain events removes particles from distant source regions such as France, Germany, Poland more efficiently compared to particles from source regions close to the receptor, hence increasing the importance of the nearby subregions, and reducing the importance distant subregions as potential source

regions affecting the eastern Mediterranean atmosphere. Higher contribution of countries surrounding the Mediterranean basin on deposition of $SO_4^{2-}$, $NO_3^-$ and heavy metals to the Mediterranean Sea was also reported in modelling exercises for the region (EMEP report, AVICENNE report).

Potential source contribution function calculations performed in the western Mediterranean suggest Italy, UK, France and Germany as source regions affecting major ion and heavy metal composition of particles (Mateu et al., 1996) and precipitation (Plaisance et al., 1996). The same source regions were also cited in other experimental studies where PSCF is not used (Bergametti et al., 1989; Dulac et al., 1987). These countries, namely UK, Spain, Italy, France and to a lesser extend Germany are identical with the subregions which were found to be potential source areas affecting chemical composition of particles and precipitation in the western Mediterranean atmosphere as shown in Figure 4.37 and 4.38 for As and Pb. Consequently, unlike in the eastern Mediterranean basin, theoretical potential source regions affecting the western Mediterranean atmosphere which were calculated using emissions and transport are identical with the source regions determined using experimental data. This difference between the eastern and western parts of the Mediterranean basin can be attributed to closer proximity of high emission regions to the receptor sites in the western Mediterranean. Since the distance that is traveled by the particles between high emission areas and receptor sites is shorter for the receptor sites located at the western part of the basin compared to those located at the eastern Mediterranean, particles bearing pollution-derived elements and ions are not scavenged during their transport to the western Mediterranean as much as they do during their transport from the same emission areas to the receptors in the eastern Mediterranean. This scenario also agrees well with significant role of local precipitation events at the receptor site relative to distant ones for the scavenging of particles in the western Mediterranean (Bergametti et al., 1989), whereas distant rains are the ones that are responsible for 75% of particle scavenging in the eastern Mediterranean (Güllü et al.. 1998).

Table 4.3. PSCF of $NO_3^-$, $SO_4^{2-}$, and Zn

| | $NO_3^-$ | $SO_4^{2-}$ | Zn |
|---|---|---|---|
| PORTUGAL | 0.00 | 0.00 | 0.00 |
| SPAIN | 0.00 | 0.00 | 0.00 |
| FRANCE | 0.04 | 0.12 | 0.42 |
| SWITZERLAND | 0.00 | 0.21 | 0.62 |
| ITALY | 0.14 | 0.23 | 0.43 |
| ALBANIA | 0.14 | 0.07 | 0.22 |
| EX-YUGOSLAVIA | 0.07 | 0.17 | 0.44 |
| GREECE | 0.17 | 0.21 | 0.37 |
| GERMANY | 0.05 | 0.04 | 0.26 |
| AUSTRIA | 0.05 | 0.05 | 0.26 |
| HUNGARY | 0.05 | 0.07 | 0.32 |
| ROMANIA | 0.06 | 0.09 | 0.40 |
| CZECHOSLOVAKIA | 0.04 | 0.00 | 0.11 |
| MOLDAVIA | 0.00 | 0.00 | 0.11 |
| POLLAND | 0.01 | 0.00 | 0.05 |
| BELARUS | 0.01 | 0.04 | 0.12 |
| UKRANIA | 0.04 | 0.02 | 0.12 |
| BULGARIA | 0.11 | 0.18 | 0.38 |
| ENGLAND | 0.00 | 0.07 | 0.27 |
| IRELAND | 0.00 | 0.00 | 0.00 |
| HOLLAND-BELGIUM | 0.08 | 0.12 | 0.43 |
| MIDDLE EAST | 0.15 | 0.06 | 0.10 |
| EAST AFRICA | 0.23 | 0.12 | 0.19 |
| MIDDLE AFRICA | 0.19 | 0.15 | 0.21 |
| WEST AFRICA | 0.27 | 0.24 | 0.58 |
| EX-U.S.S.R | 0.07 | 0.08 | 0.24 |
| WEST TURKEY | 0.37 | 0.50 | 0.86 |
| NORTHWEST TURKEY | 0.20 | 0.24 | 0.43 |
| CENTRAL TURKEY | 0.16 | 0.13 | 0.34 |
| EAST TURKEY | 0.05 | 0.14 | 0.27 |

Similar assessment of the role of particle scavenging on chemical composition of particles and precipitation in the Black Sea atmosphere is not possible for the time being because an extensive data set, which is needed for trajectory statistics, is not available for any receptor site in the Black Sea basin.

# CHAPTER 5

# CONCLUSION AND RECOMMENDATION FOR FUTURE STUDIES

## 5.1. Conclusion

In this study various trajectory models and trajectory statistics techniques were intercompared to assess the most accurate approach to determine the potential source regions affecting pollution levels in different parts of Turkey. The study proved to be more important than anticipated when it is started, because recently it is fairly well established that the eastern Mediterranean and Black Sea atmospheres are among the most heavily polluted regions around whole Europe. Obviously, assessment of source regions responsible for the heavy atmospheric pollution observed in rural areas in Turkey is very important.

In this study, three trajectory models were compared both qualitatively and quantitatively. For a qualitative comparison, trajectories of each model were evaluated visually. 24 % of the BAT and ECMWF trajectories, 40% of HYSPLIT and ECMWF trajectories resembled to each other during the selected time period. BAT trajectories were generally shorter than the ECMWF trajectories and observed to be originating from different sources. No such differences were investigated when ECMWF and HYSPLIT trajectories were compared.

Moreover, selecting the trajectories passing over İstanbul, percentage of the days resulting in high concentration of pollutants at Antalya was calculated. As a result of this treatment, it was observed that 53% of HYSPLIT trajectories corresponded high $NO_3$ and 35% corresponded to high $SO_4^{2-}$ concentrations, whereas, 37% of ECMWF trajectories corresponded high $NO_3$ and 19% corresponded to high $SO_4$ concentrations. The comparison of BAT and ECMWF trajectories indicated that, 44% of the BAT trajectories and 33% of the ECMWF trajectories corresponded to high Pb concentration observed at Antalya. This qualitative comparison suggested that HYSPLIT and BAT models' performance was better in relating the high concentrations observed at the receptor site.

Trajectory models were also compared by performing sectoring and residence time analysis. The frequency of air mass transport from each wind sectors calculated by using HYSPLIT and ECMWF trajectories resulted in approximate contributions from each sector, however, the contributions computed by BAT and ECMWF trajectories were totally different from each other. The calculated residence times using HYSPLIT and ECMWF trajectories showed similar distributions over subregions, however, the residence time distributions over the study area were totally different from each other when BAT and ECMWF trajectories were used.

The potential source regions of pollutants affecting eastern Mediterranean were identified by four different techniques that are being used in trajectory statistics. The performances of these four methods of trajectory statistics were evaluated for the receptor site Antalya, using test elements Al, Pb and $SO_4^{2-}$ during March 1992 to December 1993.

The potential source regions of Al were determined as west, middle and east Africa, Turkey, Middle East by all approaches. The source regions of Pb were found out as east and middle Africa, west Turkey, and White Russia by single and three layer PSCF. Ex-Yugoslavia, Poland, White Russia were identified as the source regions of Pb by CF and RCF approaches. The main source regions of $SO_4^{2-}$ affecting eastern Mediterranean were western and northwestern Turkey, Greece, Bulgaria, and Italy and identified by all techniques.

The potential source regions identified by each approach indicated a general agreement, although there are little differences in the ordering of the source areas between each technique. The contributions of nearby sources were observed to be similar by each approach, however, the distant sources were more heavily weighted in three layer PSCF and RCF approaches.

To be able to understand the transport patterns to eastern Mediterranean, western Mediterranean and Black Sea basins, the flow climatology approach using the 850 and 700 mb level backtrajectories of 3D isentropic ECMWF model during the years 1992,1993,1994 and 1995 was applied. This analysis demonstrated that the most frequent air mass flow to the each of the basins were mainly from NW, N and NE sectors compared to the E, SE and S sectors.

In addition to the sectoring technique, potential source regions of pollutants for each of the basins were investigated by emission intensity-residence time product using the emission data of As, Pb, $SO_4^{2-}$, $NO_3^{2-}$ and Zn in each subregion. This treatment identified the central parts of Turkey, Ukraine, Italy and east Africa as the primary source regions affecting eastern Mediterranean basin. The source regions identified for the Black Sea basin were found out as Ukraine, Ex-USSR, Turkey, Poland, Romania and Bulgaria .The

primary source regions of pollutants affecting western Mediterranean basin were France, Italy, Germany, Spain and UK.

In addition to the theoretical source regions identified by emission intensity-residence time product, Potential Source Contribution Function, which incorporates the observed concentration data at the receptor site into the evaluation, was also applied. The nearby source regions were also predicted by PSCF approach. However, the significance of the distant sources was overestimated. The difference between the theoretical and experimental source regions was determined to be the result of scavenging of particles during transport.

### 5.2. Recommendations For Future Studies

In this study, the four different techniques used in trajectory statistics were compared. RCF, which is the newest method of trajectory statistics, is more reliable since the uncertainties of PSCF and CF methods were overcome.

The subregions used for the residence time analysis in this study were determined by the combination of 150 km x 150 km EMEP grids in each country. Application of RCF method to each EMEP grids using the 3D trajectory data can result in a higher resolution in identification of source regions of pollutants. Incorporation of rain fields as a factor into the evaluation of source regions can also result in better agreement between experimental (RCF, PSCF, etc.) and theoretical potential source regions.

The techniques used to apportion source regions provide information on relative contributions of source regions. However, there are other trajectory statistics approaches such as that used by Vossler et al. (1996) which produces % contribution of wind sectors. These can be modified to include subregions defined in this study to obtain

information on the % contribution of each subregion on the pollution load at a given receptor.

There had been various studies in Turkey, mostly by our group where source regions contributing different locations in Turkey were evaluated. Single layer PSCF were used in most of the assessments. Since it is shown in this study that the 3D RCF approach appears to be more promising, these data set has to be recalculated in terms of potential source regions using 3D RCF.

## REFERENCES


Al-Momani, I.F., 1995. "Long Range Atmospheric Transport of Pollutants to Eastern Mediterranean Basin", PhD Thesis, Department of Environmental Engineering, Middle East Technical University.

Al-Momani, I. F., Güllü, G., Ölmez, İ., Eler, Ü., Örtel, E., Şirin, G., Tuncel, G., 1997. "Chemical composition of eastern Mediterranean aerosol and precipitation: Indication of long range transport", *Pure and Applied Chemistry*, Vol.69, No:1, pp.41-46.

Al-Momani, I. F., Aygun, S., Tuncel, G., 1998. "Wet deposition of major ions and trace elements in the eastern Mediterranean basin", *J. Geophys. Res.*,Vol.103, pp. 8287-8299.

Al-Momani, I. F., Güllü, G., Eler, Ü., Örtel, E., Şirin, G., Tuncel, G., 1999. "Long range transport of pollutants from Europe to the eastern Mediterranean", *Fresenius Envir. Bull.*, Vol.8, pp. 249-256.

Ashbaugh, L.L., Malm, C., Sadeh, W. Z., 1985. "A residence time probability analysis of sulfur concentrations at Grand Canyon National Park", *Atmospheric Environment*, Vol.19., No.8, pp.1263-1270.

Baumann, K., Stohl, A., 1997. "Validation of a long range trajectory model using gas balloon tracks from Gordon Bennett Cup 95", *Journal of Applied Meteorology*, Vol.36, pp.711-720.

Bergametti, G., Dutot, A.L., Buat-Menard, P., Losno, R., Remoudaki, E., 1989. "Seasonal variability of the elemental composition of atmospheric aerosol particles over the northwestern Mediterranean", *Tellus*, Vol. 41B, pp.353-361.

Charron, A., Plaisance, H., Sauvage, S., Coddeville, P., Galloo, J., Guillermo, R., 2000. " A study of the source receptor relationships influincing the acidity of precipitation collected at a rural site in France", *Atmospheric Environment*, Vol.34, pp.3665-3674.

Cheng, M., Hopke, P. K., Barrie, L., Rippe, A., Olson, M., Landsberger, S., 1993. "Qualitative determination of source regions of aerosol in Canadian High Arctic", *Environmental Science and Technology*, Vol.27, pp. 2063- 2071.

Cognetti, C., 2000. "Environmental Control in Mediterranean: A Renewed Commitment to International Co-operation", *Marine Pollution Bulletin*, Vol.40, No.5, pp.361-362.

Dayan, U., 1986. " Climatology of Back Trajectories from Israeal Based on Synoptic Analysis", *Journal of Climate and Applied Meteorology*, Vol.25, pp. 591-595.

Dayan, U., Miller, J.M., 1989. "Meteorological and Climatological Data from Surface and Upper Air Measurements for the Assessment of Atmospheric Transport and Deposition of Pollutanats in the Mediterranean Basin: A Review", MAP Technical Report Series No:30. UNEP, Athens.

Dorling, S.R., Davies, T.D., Pierce, C.E., 1992. "Cluster analysis: a technique for estimating the synoptic meteorological controls on air and precipitation chemistry-results from Eskdalemuir, S. Scotland", *Atmospheric Environment*, Vol.26A, pp .2575-2581.

Dorling, S.R., Davies, T.D., 1995. "Extending cluster analysis-synoptic meteorology links to characterise chemical climates at six Northwest European monitoring stations", *Atmospheric Environment*, Vol.29, pp.145-167.

Draxler, R.R., 1991. "The accuracy of trajectories during ANATEX calculated using dynamic model analyses versus rawinsonde observations", *Journal of Applied Meteorology*, Vol.30, pp.1446-1467.

Draxler, R.R., 1998. "Description of the HYSPLIT4 modelling system", NOAA Technical Memorandum ERL, ARL-224.

Dulac, F., Buart-Menard, P., Arnold, M., Ezat, U., Martin, D. 1987. Atmospheric Input of Trace Metals to the Western Mediterranean Sea: 1. Factors Controlling the Variability of Atmospheric Concentrations, *J. Geophys. Res., 92, 8437-8453.*

Fernau, M.E., Samson, P.J., 1990. "Use of cluster analysis to define periods of similar meteorology and precipitation chemistry in Eastern North America. Part 1: Transport Patterns", *Journal of Applied Meteorology*, Vol.29, pp.735-750.

Fernau, M.E., Samson, P.J., 1990. "Use of cluster analysis to define periods of similar meteorology and precipitation chemistry in Eastern North America. Part 2:Precipitation patterns and pollutant deposition", *Journal of Applied Meteorology*, Vol.29, pp.751-761.

Fuelberg, H. E., Loring, R.O., Watson, M.V., Sinha, M.C., Pickering, K.E., Thompson, A.M., Sache, G.W., Blake, D.R., Schoeberl, M.R., 1996. "TRACE A Trajectory intercomparison 2. Isentropic and kinematic methods", *Journal of Geophysical Research*, Vol.101, No. D19, pp.23,9278-23,939.

Gao, N., Cheng, M., Hopke, P.K., 1993. "Potential source contribution function analysis and source apportionment of sulfur spevcies measured at Rubidoux, CA during Southern California Air Quality Study, 1987", *Analytica Chimica Acta*, Vol.277, pp. 369-380.

GESAMP (Joint Group of Experts on the Scientific Aspects of Marine Pollution), 1985. "Atmospheric transport of contaminants into Mediterranean region", *Reports and Studies*, No.26,53, WMO, Geneva.

Güllü, G. 1996. "Long Range Transport of Aerosols", PhD Thesis, Department of Environmental Engineering, Middle East Technical University.

Güllü, G.H., Olmez, I., Aygun, S., Tuncel, G., 1998. "Atmospheric concentrations of trace elements over the eastern Mediterranean Sea: factors affecting temporal variability", *J. Geophys. Res.*,Vol.103, D17, pp. 21943-21954.

Hacısalihoğlu, G., 1989. "Trace Elements in the Black Sea Atmosphere: Concentration and Variations", MSc Thesis, Department of Chemistry, Middle East Technical University.

Harris, J.M., Kahl, J.D.W., 1994. "Analysis of 10-day isentropic flow patterns for Barrow, Alaska:1985-1992", *Journal of Geophysical Research*, Vol.99, NO.D12, pp.25845-25855.

Heffter, J.L., 1983. "Branching Atmospheric Trajectory (BAT) Model, NOAA Technical Memorandum NRL ARL-121.

Kahl, J.D., Schnell, R.C., Sheridan, P.J., Zak, B.D., Church, H.W., Mason, A., Heffter, J.L., Harris, J.M., 1991. "Predicting atmospheric debris transport in real time using a trajectory forecast model", *Atmospheric Environment*, Vol.25A, pp.1705-1713.

Kalkstein, L.S., Tan, G., Skindlov, J.A., 1987. "An evaluation of three clustering procedures for use in synoptic climatological classification", *Journal of Climate and Applied Meteorology*, Vol.26, pp.717-730.

Karakaş, D., 1999. "Determination of the European Contribution on the Aerosol Composition in the Black Sea Basin and Investigation of Transport Mechanisms", PhD Thesis, Department of Chemistry, Middle East Technical University.

Katsoulis, B.D., Whelpdale, D.M., 1993. "A climatological analysis of four day back trajectories from Aliartos, Greece", *Theory of Applied Climatology*, Vol.47, pp.93-103.

Katsoulis, D.B., 1999. "The potential for long-range transport of air pollutants into Greece: a climatological analysis", *The Science of the Total Environment*,Vol.231, pp. 101-113.

Klug, W., Graziani, G., Grippa, G., Pierce, D., Tassone, C. W., 1992. "Evaluation of Long Range Atmospheric Transport Models Using Environmental Radioactivity Data from the Chernobyl Release", Elsevier, Amsterdam.

Knudsen, B.M., Rosen, J.M, Kjome, N.T., Whitten, A.T., 1996. "Comparison of analysed stratospheric temperatures and calculated trajectories with long duration balloon data" *Journal of Geophysical Research*, Vol.101, pp. 19137-19145.

Kubilay, N., Saydam, A.C., 1995. "Trace elements in atmospheric particulates over the eastern Mediterranean: concentrations, sources, and temporal variability", *Atmospheric Environment*, Vol.29, pp. 2289-2300.

Kubilay, N.1996. "The composition of atmospheric aerosol over the eastern Mediterranean; concentrations, sources, and temporal variability",Ph.D. Thesis, METU Institute of Marine Sciences.

Kubilay, N., Nickovic, S., Moulin, C., Dulac, F., 2000. "An illustration of the transport and deposition of mineral dust onto eastern Mediterranean", Atmospheric Environment, Vol.34, pp. 1293-1303.

Kuo, Y., Skumanich, M., Haagenson, P.L., Chang, J.S., 1985. "The accracy of trajectory models as revealed by the observing system simulation experiments", *Monthly Weather Review* , Vol.113, pp. 1852-1867.

Martin, D., Bergametti, G., Strauss, B., 1990. "On the use of synoptic vertical velocity in trajectory model: validation by geochemical tracers, *Atmospheric Environment*, Vol.24A, pp.2059-2069.

Mateu, J., Forteza, R., Cerda, V., Colomaltes, M., 1996. "Particle size distribution and long-range transport of metals in atmospheric aerosols fromthe Alfabia station (Majorca, Spain), *Journal of Environmental Sci. Health*, Vol. A31(1), pp. 31-54.

Miller, J. M., 1981. "A five year climatology of back trajectories from the Mauna Loa observatory, Hawaii", *Atmospheric Environment*, Vol.15, pp.1553-1558.

Miller, J. M., Harris, J., 1985. "The flow climatology to Bermuda and its implications for Long-Range Transport ", *Atmospheric Environment*, Vol.19, pp.409-414.

Miller, J.M., Martin, D., Strauss, B., 1987. "A Comparison of the Results from two Trajectory Models Used to Produce Flow Climatologies to the Western Mediterranean", NOAA Tech. Memo.ERL ARL-151, Air Resources Laboratory, Silver Spring, MD, 11 pp.

Mukai, H., Suzuki, M., 1996. "Using air trajectories to analyse the seasonal variation of aerosols transported to the Oki Islands", *Atmospheric Environment*, Vol.30, No.23, pp.3917-3934.

Pack, D.H., Ferber, G.J., Heffter, J.L., Telegadas, K., Angell, J.K., Hoecker, W.H., Machta, L., 1978. "Meteorology of long-range transport", *Atmospheric Environment*, Vol.12, pp.425-444.

Plaisance, H., Coddeville, P., Roussel, L., Guillermo, R., 1996. A quantitaive determination of the source locations of precipitation constituents in Morvan, France, *Environmental Technology*, Vol.17, pp.977-986.

Polissar, A.V., Hopke, P.K., Paatero, P., Kaufmann, Y.J., Hall, d.k., Bodhaine, B.A., Dutton, E.G., Harris, J.M., 1999. "The aerosol at Barrow, Alaska: long term trends and source locations", *Atmospheric Environment*, Vol.33, pp.2441-2458.

Raynor, G.S., Hayes., J.V., Lewis, D.M., 1983. "Testing of Air Resources Laboratories trajectory model on cases of pollen wet deposition after long distance transport from known source regions", *Atmospheric Environment*, Vol.17, pp.213-220.

Rolph, G.D., Draxler, R.R., 1990. "Sensitivity of three dimensional trajectories to the spatial and temporal densities of the wind field", *Journal of Applied Meteorology*, Vol.29, pp.1043-1054.

Saltbones, J., Foss, A., Bartnicki, J., 2000. "Threat to Norway from potential accidents at the Kola nuclear power plant. Climatological trajectory analysis and episode studies", *Atmospheric Environment*, Vol.34, pp.407-418.

Sandroni, V., Migon, C., 1997. "Significance of trace metal medium-range transport in the western Mediterranean", *The Science of the Total Environment*, Vol.196, pp.83-89.

Stohl, A., Kromb-Kolb, H., 1994. "Origin of ozone in Vienna and surroundings, Austria", *Atmospheric Environment*, Vol.28, pp.1255-1266.

Stohl, A., Wotawa, G., Seibert, P., Kromb-Kolb, H., 1995. "Interpolation errors in wind fields as a function of spatial and temporal resolution and their impact on different types of kinematic trajectories" *Journal of Applied Meteorology*, Vol.34, pp.2149-2165.

Stohl, A., 1996. "Trajectory statistics- A new method to establish source receptor relationships opf air pollutants and its application to the transport of particulate sulfate in Europe" *Atmospheric Environment*, Vol.30, pp.579-587.

Stohl, A., 1998. "Computation, accracy and applications of trajectories- A review and bibliography", *Atmospheric Environment*, Vol.32, No.6, pp.947-966.

United Nations Environment Program, World Meteorological Organization (WMO,UNEP), 1989. "Airborne pollution of the Mediterranean Sea", Report and Proceedings of a WMO/UNEP Workshop, Map Technical Report Series No.31, Athens, UNEP.

United Nations Environment Program, World Meteorological Organization (WMO,UNEP), 1994. "Assessment of airborne pollution of the Mediterranean Sea", Report and Proceedings of a WMO/UNEP Workshop, Map Technical Report Series No.31, Athens, UNEP, 304.

Wotawa, G., Kröger, H., 1999. "Testing the ability of trajectory statistics to reproduce amission inventories of air pollutants in cases of negligible measurement and transport errors", *Atmospheric Environment*, Vol.33, pp.3037-3043.

# APPENDIX A

## THE JOB UTILIZED FOR RETRIAVAL OF BACKTRAJECTORIES FROM ECMWF CENTRE

An example of a request file to run the publicly available operational model on the CRAY C90/UNICOS super computer at the European Center for Medium Range Weather Forecast Center (ECMWF, Reading, U.K.) to compute 3.5 days backtrajectories at three barometric levels for 2 July, 1994 is given in Table A.1.

Table A.1. Trajectory request file example

```
#########################################################################
#!/bin/csh -f
#QSUB -q mars              # mars request
#QSUB -lM 20mb             # sets overall memory limit
#QSUB -eo                  # the stderr (error) file is combined with
#QSUB -me                  # mail message is sent when job has executed
#QSUB
#set +v

mkdir /scratch/ms/tr/tug
mkdir /scratch/ms/tr/tug/1
setenv SCRATCH /scratch/ms/tr/tug/1

# put coordinates and heights of trajectory end points here, store in file
#  tre
cat>tre<<eof
36.780 30.570 900.
36.780 30.570 850.
36.780 30.570 700.
36.780 30.570 500.
eof

foreach ym (9407)
foreach dy (02)

#replace scratch file with your own scratch directory / path
```

Table A.1. (Continued)

```
set ymd="$ym""$dy"
set dats="$ymd"12
set datt=`cay<<eof \
$dats \
eof 00
echo $dats ... $dat
# echo $SCRATCH
/home/ms/ie/dur/traj/gettraj -S $dats -T $datt \
-t 213 -x tre -w -b > $SCRATCH/dump3
# ln -s /scratch/ms/tr/tua scratch
# mv scratch/trajout scratch/trajout."$dats"
mv $SCRATCH/trajout $SCRATCH/trajout."$dats"
mail gamze@bergama.enve.edu.tr< $SCRATCH/trajout."$dats"
\rm -f $SCRATCH/19"$datt"_19"$dats"_19"$dats"
\rm -f $SCRATCH/dump3
end
\rm -f $SCRATCH/trajout.*
end
##########################################################################
```

# APPENDIX B

## TRAJECTORY DATABASE OBTAINED FROM THE REQUEST FILE GIVEN IN TABLE A.1.

The trajectory database obtained from the request file for 2 July, 1994 is given in Table B.1.

Table B.1. Trajectory data file obtained from the request file given in Table A.1.

TRAJECTORY NUMBER 1

START: LAT 36.8 DEG N PRESSURE LEVEL 900 HPA
LON 30.6 DEG E TIME 12 UTC ON 2. 7.94

END: TIME 0 UTC ON 29. 6.94

ANALYSIS FIELDS FROM TIME 12 UTC ON 2. 7.94

| HOURS | LAT | LON | LEVEL | U-WIND | V-WIND | W-WIND | PS |
|---|---|---|---|---|---|---|---|
| 0 | 36.80 N | 30.60 E | 900.0 | 1.2 | 6.3 | -0.19 | 908.8 |
| 1 | 36.59 N | 30.50 E | 905.2 | 3.1 | 5.6 | -0.08 | 931.0 |
| 2 | 36.44 N | 30.35 E | 905.2 | 4.2 | 3.8 | 0.06 | 940.7 |
| 3 | 36.34 N | 30.17 E | 900.7 | 4.8 | 1.9 | 0.17 | 940.0 |
| 4 | 36.31 N | 29.97 E | 893.1 | 4.9 | 0.0 | 0.25 | 933.8 |
| 5 | 36.34 N | 29.77 E | 882.6 | 4.7 | -1.6 | 0.33 | 925.4 |
| 6 | 36.41 N | 29.59 E | 868.9 | 4.2 | -2.9 | 0.43 | 915.6 |
| 7 | 36.51 N | 29.42 E | 853.1 | 4.1 | -3.5 | 0.44 | 906.1 |
| 8 | 36.63 N | 29.27 E | 837.6 | 3.7 | -3.8 | 0.42 | 899.0 |
| 9 | 36.76 N | 29.13 E | 823.2 | 3.0 | -4.1 | 0.39 | 893.7 |
| 10 | 36.89 N | 29.02 E | 809.7 | 2.3 | -4.2 | 0.36 | 888.3 |
| 11 | 37.03 N | 28.94 E | 797.6 | 1.7 | -4.3 | 0.31 | 883.5 |
| 12 | 37.17 N | 28.88 E | 787.6 | 1.4 | -4.3 | 0.25 | 880.3 |

Table B.1. (Continued)

| | | | | | | | |
|---|---|---|---|---|---|---|---|
| 13 | 37.31 N | 28.80 E | 781.1 | 2.4 | -4.6 | 0.12 | 881.3 |
| ...14 | 37.47 N | 28.68 E | 779.2 | 3.3 | -5.0 | -0.01 | 887.5 |
| 15 | 37.64 N | 28.53 E | 781.2 | 4.1 | -5.5 | -0.10 | 896.8 |
| 16 | 37.82 N | 28.35 E | 785.4 | 4.5 | -6.0 | -0.13 | 907.4 |
| 17 | 38.02 N | 28.17 E | 789.5 | 4.3 | -6.4 | -0.09 | 917.8 |
| 18 | 38.23 N | 28.01 E | 790.6 | 3.5 | -6.4 | 0.03 | 927.1 |
| 19 | 38.42 N | 27.88 E | 790.7 | 2.7 | -5.3 | -0.05 | 933.9 |
| 20 | 38.58 N | 27.79 E | 794.6 | 2.2 | -4.7 | -0.17 | 938.0 |
| 21 | 38.73 N | 27.71 E | 802.7 | 1.7 | -4.5 | -0.29 | 939.9 |
| 22 | 38.87 N | 27.65 E | 814.7 | 1.1 | -4.5 | -0.38 | 940.0 |
| 23 | 39.02 N | 27.62 E | 829.5 | 0.4 | -4.6 | -0.44 | 938.6 |
| 24 | 39.17 N | 27.61 E | 846.7 | 0.0 | -4.6 | -0.50 | 936.3 |
| 25 | 39.31 N | 27.65 E | 862.3 | -1.6 | -4.3 | -0.37 | 934.6 |
| 26 | 39.45 N | 27.76 E | 873.8 | -3.4 | -4.2 | -0.27 | 933.4 |
| 27 | 39.59 N | 27.93 E | 882.0 | -4.9 | -4.2 | -0.18 | 933.0 |
| 28 | 39.72 N | 28.16 E | 886.5 | -6.1 | -4.0 | -0.06 | 932.1 |
| 29 | 39.84 N | 28.45 E | 885.9 | -7.3 | -3.3 | 0.11 | 927.9 |
| 30 | 39.93 N | 28.78 E | 878.4 | -8.4 | -1.9 | 0.32 | 916.6 |
| 31 | 39.98 N | 29.13 E | 865.8 | -7.9 | -1.3 | 0.37 | 901.4 |
| 32 | 40.02 N | 29.46 E | 853.3 | -7.6 | -1.0 | 0.33 | 889.4 |
| 33 | 40.05 N | 29.77 E | 843.3 | -6.8 | -1.0 | 0.22 | 882.9 |
| 34 | 40.09 N | 30.05 E | 837.0 | -6.1 | -1.3 | 0.14 | 881.3 |
| 35 | 40.14 N | 30.29 E | 832.5 | -5.5 | -1.7 | 0.12 | 881.4 |
| 36 | 40.20 N | 30.52 E | 827.5 | -5.1 | -2.0 | 0.16 | 880.8 |

Table B.1. (Continued)

| | | | | | | | |
|---|---|---|---|---|---|---|---|
| 37 | 40.27 N | 30.73 E | 820.4 | -4.9 | -2.6 | 0.24 | 878.3 |
| 38 | 40.37 N | 30.94 E | 810.3 | -4.8 | -3.1 | 0.32 | 874.0 |
| 39 | 40.47 N | 31.14 E | 797.9 | -4.7 | -3.4 | 0.37 | 868.8 |
| 40 | 40.58 N | 31.35 E | 784.5 | -4.8 | -3.4 | 0.37 | 864.5 |
| 41 | 40.68 N | 31.55 E | 771.4 | -4.8 | -3.1 | 0.35 | 861.8 |
| ...42 | 40.77 N | 31.75 E | 759.1 | -4.7 | -2.6 | 0.31 | 859.7 |
| ...43 | 40.84 N | 31.93 E | 749.3 | -3.5 | -2.1 | 0.23 | 859.6 |
| 44 | 40.91 N | 32.06 E | 741.6 | -2.8 | -1.7 | 0.20 | 860.6 |
| 45 | 40.96 N | 32.18 E | 734.2 | -2.4 | -1.5 | 0.21 | 861.4 |
| 46 | 41.00 N | 32.28 E | 726.0 | -2.3 | -1.7 | 0.20 | 862.4 |
| 47 | 41.06 N | 32.38 E | 718.5 | -2.3 | -2.0 | 0.22 | 864.9 |
| 48 | 41.13 N | 32.48 E | 709.7 | -2.5 | -2.1 | 0.27 | 867.7 |
| 49 | 41.21 N | 32.59 E | 700.0 | -2.3 | -3.3 | 0.26 | 871.7 |
| 50 | 41.35 N | 32.68 E | 691.6 | -2.2 | -5.1 | 0.21 | 881.7 |
| 51 | 41.54 N | 32.78 E | 684.4 | -2.3 | -6.7 | 0.18 | 899.3 |
| 52 | 41.78 N | 32.89 E | 678.2 | -2.7 | -8.3 | 0.16 | 924.6 |
| 53 | 42.07 N | 33.01 E | 673.0 | -3.1 | -9.8 | 0.11 | 957.4 |
| 54 | 42.42 N | 33.16 E | 670.4 | -3.6 | -11.8 | 0.03 | 993.4 |
| 55 | 42.82 N | 33.30 E | 669.4 | -2.6 | -12.4 | 0.04 | 1019.4 |
| 56 | 43.23 N | 33.39 E | 665.6 | -1.4 | -13.1 | 0.17 | 1023.8 |
| 57 | 43.67 N | 33.42 E | 656.7 | 0.0 | -14.0 | 0.32 | 1016.2 |
| 58 | 44.14 N | 33.39 E | 643.6 | 1.7 | -15.3 | 0.40 | 1005.7 |
| 59 | 44.66 N | 33.26 E | 628.3 | 3.9 | -17.0 | 0.44 | 997.7 |
| 60 | 45.24 N | 33.02 E | 612.4 | 5.8 | -18.7 | 0.45 | 1005.0 |

Table B.1. (Continued)

| | | | | | | | |
|---|---|---|---|---|---|---|---|
| 61 | 45.87 N | 32.73 E | 597.9 | 6.4 | -19.9 | 0.35 | 1012.2 |
| 62 | 46.52 N | 32.43 E | 587.1 | 6.8 | -20.4 | 0.24 | 1007.5 |
| 63 | 47.18 N | 32.10 E | 580.6 | 6.8 | -20.3 | 0.12 | 1007.0 |
| 64 | 47.83 N | 31.78 E | 578.0 | 6.6 | -19.6 | 0.03 | 996.4 |
| 65 | 48.45 N | 31.46 E | 577.7 | 6.4 | -19.0 | -0.01 | 988.6 |
| 66 | 49.06 N | 31.15 E | 578.3 | 6.2 | -18.5 | -0.03 | 989.4 |
| ...69 | 51.01 N | 30.16 E | 574.8 | 6.7 | -21.8 | 0.08 | 999.8 |
| 70 | 51.73 N | 29.81 E | 571.2 | 6.7 | -22.4 | 0.11 | 1001.3 |
| 71 | 52.46 N | 29.47 E | 566.9 | 6.4 | -22.7 | 0.13 | 1000.8 |
| 72 | 53.20 N | 29.13 E | 561.9 | 6.1 | -23.0 | 0.15 | 998.7 |
| 73 | 53.94 N | 28.78 E | 556.0 | 6.6 | -22.6 | 0.17 | 995.9 |
| 74 | 54.66 N | 28.38 E | 549.6 | 7.7 | -22.1 | 0.18 | 997.3 |
| 75 | 55.37 N | 27.92 E | 543.2 | 8.7 | -21.4 | 0.18 | 998.1 |
| 76 | 56.05 N | 27.38 E | 537.5 | 9.8 | -20.7 | 0.14 | 1000.7 |
| 77 | 56.71 N | 26.78 E | 533.1 | 10.7 | -20.0 | 0.10 | 1002.6 |
| 78 | 57.35 N | 26.11 E | 531.0 | 11.5 | -19.7 | 0.02 | 998.0 |
| 79 | 57.99 N | 25.39 E | 529.8 | 12.1 | -19.3 | 0.05 | 1010.2 |
| 80 | 58.60 N | 24.61 E | 526.8 | 12.9 | -18.4 | 0.12 | 1015.1 |
| 81 | 59.17 N | 23.75 E | 521.3 | 14.2 | -17.0 | 0.19 | 1016.2 |
| 82 | 59.69 N | 22.79 E | 513.9 | 15.7 | -15.1 | 0.23 | 1018.0 |
| 83 | 60.16 N | 21.72 E | 505.2 | 17.3 | -13.7 | 0.26 | 1019.5 |
| 84 | 60.60 N | 20.51 E | 497.9 | 19.5 | -13.9 | 0.20 | 1018.7 |

TRAJECTORY NUMBER 2

Table B.1. (Continued)

LON 30.6 DEG E TIME 12 UTC ON 2. 7.94

START: LAT 36.8 DEG N PRESSURE LEVEL 850 HPA

END: TIME 0 UTC ON 29. 6.94

ANALYSIS FIELDS FROM TIME 12 UTC ON 2. 7.94

| HOURS | LAT | LON | LEVEL | U-WIND | V-WIND | W-WIND | PS |
|---|---|---|---|---|---|---|---|
| 0 | 36.80 N | 30.60 E | 850.0 | 1.8 | 6.6 | -0.33 | 908.8 |
| 1 | 36.61 N | 30.50 E | 857.7 | 3.0 | 5.0 | -0.12 | 928.2 |
| 2 | 36.47 N | 30.36 E | 858.9 | 3.9 | 3.4 | 0.03 | 936.2 |
| 3 | 36.39 N | 30.20 E | 855.8 | 4.5 | 1.9 | 0.13 | 935.5 |
| 4 | 36.35 N | 30.01 E | 849.7 | 4.7 | 0.5 | 0.20 | 930.3 |
| 5 | 36.35 N | 29.82 E | 841.1 | 4.6 | -0.8 | 0.27 | 923.7 |
| 6 | 36.39 N | 29.65 E | 830.1 | 4.2 | -1.8 | 0.34 | 917.2 |
| 7 | 36.46 N | 29.49 E | 817.7 | 3.6 | -2.3 | 0.35 | 911.2 |
| 8 | 36.54 N | 29.36 E | 805.0 | 2.9 | -2.7 | 0.35 | 906.0 |
| 9 | 36.63 N | 29.25 E | 792.2 | 2.1 | -2.9 | 0.35 | 900.1 |
| 10 | 36.72 N | 29.18 E | 779.6 | 1.5 | -3.0 | 0.34 | 893.1 |
| 11 | 36.82 N | 29.13 E | 767.8 | 1.0 | -3.0 | 0.31 | 885.6 |
| 12 | 36.91 N | 29.10 E | 757.3 | 0.6 | -3.0 | 0.27 | 878.1 |
| 13 | 37.02 N | 29.06 E | 748.2 | 1.3 | -3.4 | 0.23 | 872.5 |
| 14 | 37.14 N | 29.00 E | 741.1 | 1.9 | -4.0 | 0.16 | 870.4 |

Table B.1. (Continued)

| | | | | | | | |
|---|---|---|---|---|---|---|---|
| 15 | 37.28 N | 28.92 E | 737.1 | 2.4 | -4.6 | 0.06 | 872.2 |
| 16 | 37.43 N | 28.81 E | 737.0 | 2.9 | -5.2 | -0.06 | 878.0 |
| 17 | 37.61 N | 28.69 E | 740.9 | 3.3 | -5.8 | -0.17 | 887.2 |
| 18 | 37.80 N | 28.55 E | 747.7 | 3.5 | -6.2 | -0.22 | 898.3 |
| 19 | 37.99 N | 28.42 E | 757.3 | 3.2 | -5.4 | -0.33 | 908.7 |
| 20 | 38.15 N | 28.29 E | 770.9 | 3.1 | -4.9 | -0.43 | 917.2 |
| 21 | 38.31 N | 28.16 E | 788.2 | 3.1 | -4.5 | -0.53 | 924.2 |
| 22 | 38.44 N | 28.03 E | 809.0 | 3.0 | -4.0 | -0.62 | 929.8 |
| 23 | 38.57 N | 27.91 E | 832.3 | 3.0 | -3.4 | -0.68 | 934.1 |
| 24 | 38.66 N | 27.78 E | 857.0 | 3.0 | -2.5 | -0.68 | 937.8 |
| 25 | 38.74 N | 27.68 E | 877.3 | 1.9 | -2.0 | -0.46 | 940.6 |
| 26 | 38.80 N | 27.64 E | 890.4 | 0.3 | -1.7 | -0.28 | 941.6 |
| 27 | 38.85 N | 27.66 E | 897.5 | -1.5 | -1.6 | -0.12 | 940.6 |
| 28 | 38.90 N | 27.76 E | 899.4 | -3.2 | -1.5 | 0.01 | 937.5 |
| 29 | 38.95 N | 27.92 E | 897.0 | -4.7 | -1.3 | 0.12 | 933.1 |
| 30 | 38.98 N | 28.14 E | 890.5 | -6.1 | -0.7 | 0.24 | 926.8 |
| 31 | 39.01 N | 28.40 E | 880.8 | -6.3 | -0.8 | 0.30 | 917.5 |
| 32 | 39.04 N | 28.67 E | 868.5 | -6.7 | -0.9 | 0.38 | 904.9 |
| 33 | 39.07 N | 28.96 E | 853.8 | -7.2 | -1.0 | 0.43 | 889.1 |
| 34 | 39.10 N | 29.27 E | 838.8 | -7.7 | -1.1 | 0.39 | 872.9 |
| 35 | 39.14 N | 29.61 E | 828.0 | -8.1 | -1.5 | 0.19 | 861.2 |
| 36 | 39.19 N | 29.97 E | 826.1 | -8.1 | -2.0 | -0.10 | 858.9 |
| 37 | 39.26 N | 30.30 E | 833.6 | -7.3 | -3.0 | -0.30 | 865.9 |
| 38 | 39.38 N | 30.58 E | 844.8 | -6.2 | -4.2 | -0.31 | 876.8 |

Table B.1. (Continued)

| | | | | | | | |
|---|---|---|---|---|---|---|---|
| 39 | 39.53 N | 30.81 E | 853.3 | -5.0 | -5.4 | -0.16 | 884.7 |
| 40 | 39.73 N | 30.99 E | 855.0 | -3.7 | -6.6 | 0.06 | 884.2 |
| 41 | 39.95 N | 31.12 E | 849.8 | -2.7 | -7.5 | 0.22 | 874.5 |
| 42 | 40.20 N | 31.22 E | 841.9 | -2.3 | -7.7 | 0.21 | 862.9 |
| 43 | 40.43 N | 31.32 E | 837.0 | -2.1 | -6.4 | 0.05 | 859.0 |
| 44 | 40.63 N | 31.42 E | 837.8 | -2.0 | -5.6 | -0.11 | 864.4 |
| 45 | 40.81 N | 31.51 E | 844.1 | -1.9 | -5.3 | -0.25 | 877.2 |
| 46 | 40.97 N | 31.58 E | 854.9 | -1.5 | -4.9 | -0.33 | 896.1 |
| 47 | 41.13 N | 31.64 E | 867.2 | -1.0 | -4.6 | -0.35 | 917.7 |
| 48 | 41.27 N | 31.68 E | 879.2 | -0.7 | -4.3 | -0.32 | 939.8 |
| 49 | 41.40 N | 31.73 E | 887.7 | -1.6 | -3.7 | -0.16 | 957.3 |
| 50 | 41.51 N | 31.81 E | 891.5 | -2.2 | -3.2 | -0.06 | 968.2 |
| 51 | 41.61 N | 31.91 E | 893.0 | -2.6 | -2.9 | -0.03 | 974.3 |
| 52 | 41.70 N | 32.03 E | 894.2 | -2.8 | -2.8 | -0.04 | 977.2 |
| 53 | 41.79 N | 32.16 E | 896.0 | -3.0 | -2.7 | -0.06 | 978.1 |
| 54 | 41.88 N | 32.29 E | 898.9 | -3.1 | -2.6 | -0.10 | 977.8 |
| 55 | 41.96 N | 32.43 E | 902.0 | -3.3 | -2.3 | -0.07 | 976.5 |
| 56 | 42.03 N | 32.58 E | 904.2 | -3.6 | -2.0 | -0.05 | 974.5 |
| 57 | 42.09 N | 32.74 E | 905.3 | -3.8 | -1.6 | -0.02 | 971.8 |
| 58 | 42.13 N | 32.92 E | 905.7 | -4.1 | -1.2 | 0.00 | 968.8 |
| 59 | 42.17 N | 33.10 E | 905.6 | -4.2 | -0.8 | 0.01 | 965.5 |
| 60 | 42.19 N | 33.29 E | 905.5 | -4.3 | -0.3 | 0.00 | 961.6 |
| 61 | 42.21 N | 33.45 E | 906.9 | -3.4 | -1.0 | -0.07 | 960.5 |
| 62 | 42.25 N | 33.58 E | 910.5 | -2.7 | -1.8 | -0.12 | 964.8 |

Table B.1. (Continued)

| | | | | | | | |
|---|---|---|---|---|---|---|---|
| 63 | 42.32 N | 33.69 E | 915.4 | -2.2 | -2.7 | -0.14 | 973.9 |
| 64 | 42.42 N | 33.77 E | 920.7 | -1.8 | -3.7 | -0.14 | 986.8 |
| 65 | 42.56 N | 33.85 E | 925.9 | -1.6 | -4.8 | -0.14 | 1001.3 |
| 66 | 42.73 N | 33.92 E | 931.3 | -1.5 | -6.0 | -0.16 | 1014.1 |
| 67 | 42.93 N | 33.98 E | 936.0 | -1.1 | -6.0 | -0.10 | 1020.9 |
| 68 | 43.12 N | 34.02 E | 938.6 | -0.9 | -5.8 | -0.04 | 1021.7 |
| 69 | 43.30 N | 34.06 E | 939.4 | -0.8 | -5.5 | 0.00 | 1019.1 |
| 70 | 43.48 N | 34.10 E | 938.6 | -0.9 | -5.2 | 0.04 | 1015.4 |
| 71 | 43.64 N | 34.14 E | 936.6 | -0.9 | -4.9 | 0.07 | 1011.8 |
| 72 | 43.80 N | 34.19 E | 934.0 | -1.0 | -4.7 | 0.08 | 1008.6 |
| 73 | 43.95 N | 34.25 E | 931.4 | -1.6 | -5.1 | 0.06 | 1005.1 |
| 74 | 44.13 N | 34.33 E | 929.3 | -2.3 | -5.6 | 0.06 | 1001.0 |
| 75 | 44.32 N | 34.45 E | 927.0 | -2.9 | -6.3 | 0.07 | 996.0 |
| 76 | 44.53 N | 34.59 E | 924.9 | -3.3 | -7.2 | 0.05 | 990.2 |
| 77 | 44.78 N | 34.74 E | 924.5 | -3.5 | -8.1 | -0.03 | 985.1 |
| 78 | 45.05 N | 34.90 E | 928.3 | -3.5 | -8.9 | -0.19 | 983.9 |
| 79 | 45.34 N | 35.05 E | 936.4 | -2.8 | -8.8 | -0.26 | 990.0 |
| 80 | 45.62 N | 35.17 E | 945.1 | -2.4 | -8.7 | -0.22 | 1001.1 |
| 81 | 45.90 N | 35.28 E | 950.5 | -2.1 | -8.7 | -0.08 | 1011.2 |
| 82 | 46.20 N | 35.38 E | 950.7 | -2.1 | -9.2 | 0.07 | 1014.4 |
| 83 | 46.51 N | 35.48 E | 946.1 | -2.3 | -10.1 | 0.19 | 1008.7 |
| 84 | 46.85 N | 35.60 E | 938.7 | -2.4 | -10.6 | 0.20 | 1003.8 |

TRAJECTORY NUMBER 3

Table B.1. (Continued)

LON 30.6 DEG E TIME 12 UTC ON 2. 7.94

END: TIME 0 UTC ON 29. 6.94

ANALYSIS FIELDS FROM TIME 12 UTC ON 2. 7.94

| HOURS | LAT | LON | LEVEL | U-WIND | V-WIND | W-WIND | PS |
|---|---|---|---|---|---|---|---|
| 0 | 36.80 N | 30.60 E | 700.0 | 1.3 | -2.4 | -0.26 | 908.8 |
| 1 | 36.86 N | 30.54 E | 711.1 | 1.5 | -1.4 | -0.35 | 896.4 |
| 2 | 36.90 N | 30.48 E | 724.3 | 1.7 | -0.8 | -0.38 | 886.9 |
| 3 | 36.92 N | 30.40 E | 737.7 | 2.0 | -0.4 | -0.36 | 879.1 |
| 4 | 36.94 N | 30.32 E | 750.2 | 2.2 | -0.5 | -0.32 | 871.2 |
| 5 | 36.96 N | 30.23 E | 760.5 | 2.3 | -0.8 | -0.25 | 863.1 |
| 6 | 37.00 N | 30.13 E | 768.2 | 2.4 | -1.5 | -0.18 | 854.1 |
| 7 | 37.05 N | 30.04 E | 774.1 | 2.1 | -1.8 | -0.15 | 845.9 |
| 8 | 37.12 N | 29.96 E | 779.0 | 1.8 | -2.4 | -0.13 | 839.8 |
| 9 | 37.21 N | 29.89 E | 783.3 | 1.8 | -3.0 | -0.12 | 836.2 |
| 10 | 37.32 N | 29.82 E | 787.9 | 1.8 | -3.5 | -0.14 | 835.5 |
| 11 | 37.43 N | 29.75 E | 793.6 | 1.7 | -3.8 | -0.18 | 839.0 |
| 12 | 37.56 N | 29.69 E | 800.8 | 1.3 | -3.9 | -0.22 | 845.9 |
| 14 | 37.78 N | 29.49 E | 824.2 | 3.8 | -3.2 | -0.42 | 864.1 |
| 15 | 37.89 N | 29.31 E | 839.7 | 5.1 | -3.2 | -0.44 | 875.5 |
| 16 | 38.00 N | 29.07 E | 855.0 | 6.4 | -3.6 | -0.41 | 888.6 |
| 17 | 38.12 N | 28.78 E | 868.7 | 7.6 | -4.4 | -0.36 | 902.8 |

Table B.1. (Continued)

| | | | | | | | |
|---|---|---|---|---|---|---|---|
| 18 | 38.28 N | 28.46 E | 880.6 | 8.2 | -5.6 | -0.30 | 916.4 |
| 19 | 38.46 N | 28.16 E | 890.2 | 6.1 | -5.3 | -0.24 | 926.9 |
| 20 | 38.62 N | 27.95 E | 898.3 | 4.4 | -4.7 | -0.22 | 933.6 |
| 21 | 38.76 N | 27.79 E | 905.9 | 3.3 | -3.9 | -0.21 | 937.5 |
| 22 | 38.88 N | 27.66 E | 913.6 | 2.8 | -3.1 | -0.22 | 939.6 |
| 23 | 38.96 N | 27.55 E | 922.0 | 2.7 | -2.3 | -0.25 | 941.4 |
| 24 | 39.02 N | 27.43 E | 931.5 | 2.8 | -1.1 | -0.29 | 943.5 |
| 25 | 39.05 N | 27.33 E | 940.2 | 1.8 | -0.9 | -0.20 | 946.0 |
| 26 | 39.08 N | 27.27 E | 946.0 | 1.0 | -0.9 | -0.12 | 947.4 |
| 27 | 39.12 N | 27.25 E | 946.8 | 0.0 | -1.3 | -0.05 | 947.7 |
| 28 | 39.16 N | 27.26 E | 946.3 | -0.9 | -1.6 | 0.01 | 946.5 |
| 29 | 39.21 N | 27.31 E | 945.1 | -1.5 | -1.7 | 0.06 | 944.0 |
| 30 | 39.27 N | 27.38 E | 942.4 | -2.0 | -2.0 | 0.09 | 941.4 |
| 31 | 39.34 N | 27.45 E | 939.9 | -1.3 | -2.1 | 0.04 | 939.3 |
| 32 | 39.41 N | 27.49 E | 937.7 | -0.8 | -2.4 | 0.00 | 938.4 |
| 33 | 39.49 N | 27.51 E | 937.4 | -0.3 | -2.5 | -0.04 | 938.5 |
| 34 | 39.57 N | 27.51 E | 938.1 | 0.1 | -2.7 | -0.09 | 939.8 |
| 35 | 39.66 N | 27.49 E | 940.0 | 0.4 | -2.8 | -0.14 | 942.2 |
| 36 | 39.74 N | 27.46 E | 943.0 | 0.7 | -2.8 | -0.19 | 945.6 |
| 37 | 39.83 N | 27.43 E | 946.8 | -0.1 | -3.0 | -0.21 | 949.6 |
| 38 | 39.92 N | 27.44 E | 951.2 | -0.9 | -3.3 | -0.23 | 954.5 |
| 39 | 40.03 N | 27.49 E | 956.7 | -2.0 | -3.7 | -0.25 | 960.7 |
| 40 | 40.15 N | 27.59 E | 963.6 | -3.2 | -4.3 | -0.27 | 968.6 |
| 41 | 40.30 N | 27.75 E | 973.1 | -4.6 | -4.9 | -0.26 | 978.2 |

Table B.1. (Continued)

| | | | | | | | |
|---|---|---|---|---|---|---|---|
| 42 | 40.47 N | 27.97 E | 981.4 | -6.1 | -5.8 | -0.20 | 987.7 |
| 43 | 40.66 N | 28.24 E | 986.9 | -6.5 | -5.8 | -0.10 | 994.7 |
| 44 | 40.83 N | 28.50 E | 989.7 | -6.0 | -5.2 | -0.05 | 998.3 |
| 45 | 40.99 N | 28.75 E | 991.7 | -5.2 | -4.5 | -0.06 | 1000.6 |
| 46 | 41.13 N | 28.95 E | 994.6 | -4.3 | -3.8 | -0.10 | 1003.1 |
| 47 | 41.24 N | 29.11 E | 998.8 | -3.3 | -3.2 | -0.13 | 1006.1 |
| 48 | 41.34 N | 29.23 E | 1003.7 | -2.3 | -2.7 | -0.15 | 1009.1 |
| 49 | 41.43 N | 29.32 E | 1008.5 | -1.9 | -2.8 | -0.12 | 1011.4 |
| 50 | 41.52 N | 29.40 E | 1012.1 | -1.6 | -3.0 | -0.08 | 1013.5 |
| 51 | 41.62 N | 29.46 E | 1014.4 | -1.4 | -3.4 | -0.04 | 1015.4 |
| 52 | 41.74 N | 29.52 E | 1015.2 | -1.2 | -3.8 | 0.00 | 1016.5 |
| 53 | 41.87 N | 29.56 E | 1014.7 | -1.0 | -4.4 | 0.03 | 1016.7 |
| 54 | 42.03 N | 29.60 E | 1013.1 | -0.9 | -5.1 | 0.05 | 1015.8 |
| 55 | 42.19 N | 29.64 E | 1011.5 | -0.9 | -4.7 | 0.04 | 1014.4 |
| 56 | 42.33 N | 29.69 E | 1010.4 | -1.1 | -4.3 | 0.02 | 1012.9 |
| 57 | 42.46 N | 29.74 E | 1009.6 | -1.2 | -3.8 | 0.02 | 1011.6 |
| 58 | 42.57 N | 29.80 E | 1008.8 | -1.5 | -3.3 | 0.02 | 1010.4 |
| 59 | 42.67 N | 29.87 E | 1007.6 | -1.9 | -2.8 | 0.04 | 1009.5 |
| 60 | 42.76 N | 29.96 E | 1005.6 | -2.4 | -2.4 | 0.07 | 1008.6 |
| 61 | 42.84 N | 30.08 E | 1002.9 | -2.8 | -3.0 | 0.08 | 1008.4 |
| 62 | 42.95 N | 30.21 E | 1000.2 | -3.1 | -3.6 | 0.08 | 1009.1 |
| 63 | 43.08 N | 30.35 E | 997.8 | -3.4 | -4.4 | 0.06 | 1011.1 |
| 64 | 43.24 N | 30.51 E | 996.4 | -3.5 | -5.3 | 0.02 | 1014.5 |
| 65 | 43.42 N | 30.66 E | 996.1 | -3.1 | -5.8 | 0.00 | 1018.1 |

Table B.1. (Continued)

| | | | | | | | |
|---|---|---|---|---|---|---|---|
| 66 | 43.62 N | 30.78 E | 996.5 | -2.6 | -6.2 | -0.02 | 1020.0 |
| 67 | 43.81 N | 30.89 E | 995.9 | -2.3 | -6.0 | 0.06 | 1019.8 |
| 68 | 44.01 N | 30.99 E | 992.2 | -2.1 | -6.1 | 0.15 | 1018.2 |
| 69 | 44.21 N | 31.08 E | 985.3 | -2.1 | -6.3 | 0.24 | 1016.3 |
| 70 | 44.42 N | 31.18 E | 975.1 | -2.3 | -6.5 | 0.34 | 1015.7 |
| 71 | 44.63 N | 31.30 E | 960.7 | -2.4 | -6.7 | 0.44 | 1016.7 |
| 72 | 44.85 N | 31.41 E | 942.2 | -2.4 | -7.0 | 0.58 | 1019.1 |
| 73 | 45.08 N | 31.51 E | 922.1 | -2.1 | -7.4 | 0.53 | 1021.0 |
| 74 | 45.33 N | 31.61 E | 903.9 | -2.0 | -7.8 | 0.47 | 1021.4 |
| 75 | 45.59 N | 31.70 E | 888.6 | -2.0 | -8.2 | 0.38 | 1019.3 |
| 76 | 45.86 N | 31.80 E | 876.3 | -2.1 | -8.3 | 0.30 | 1015.6 |
| 77 | 46.13 N | 31.90 E | 866.4 | -2.3 | -8.5 | 0.25 | 1012.5 |
| 78 | 46.41 N | 32.01 E | 858.0 | -2.4 | -8.9 | 0.22 | 1011.0 |
| 79 | 46.70 N | 32.11 E | 850.1 | -2.1 | -9.2 | 0.22 | 1010.7 |
| 80 | 47.01 N | 32.21 E | 841.7 | -1.8 | -9.4 | 0.25 | 1010.2 |
| 81 | 47.31 N | 32.29 E | 831.7 | -1.6 | -9.5 | 0.30 | 1008.0 |
| 82 | 47.62 N | 32.36 E | 820.3 | -1.4 | -9.8 | 0.34 | 1004.0 |
| 83 | 47.95 N | 32.42 E | 808.2 | -1.1 | -10.1 | 0.33 | 999.3 |
| 84 | 48.28 N | 32.46 E | 796.8 | -0.9 | -10.3 | 0.32 | 997.6 |

# APPENDIX C

## BACKTRAJECTORIES OF BAT, HYSPLIT AND ECMWF MODELS USED FOR QUALITATIVE COMPARISON IN SECTION 4.1.

The trajectories of the same day for each model, which are differing from each other, are depicted in same colors.

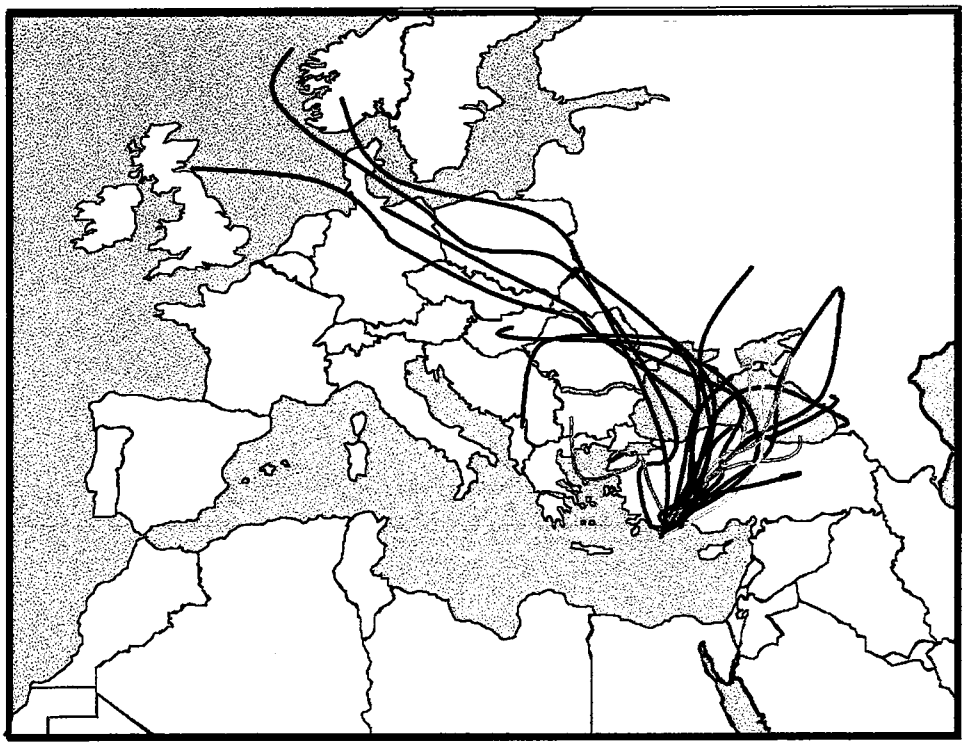

Figure C1. ECMWF trajectories ending at Antalya during August 1998 at 850 mb

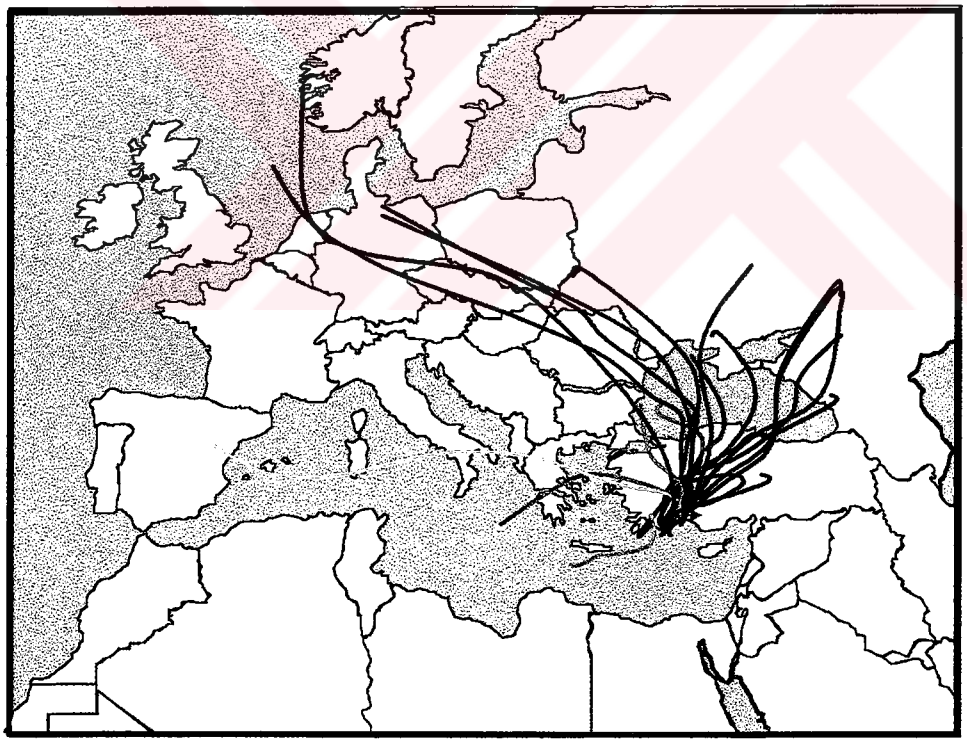

Figure C2. HYSPLIT trajectories ending at Antalya during August 1998 at 850 mb

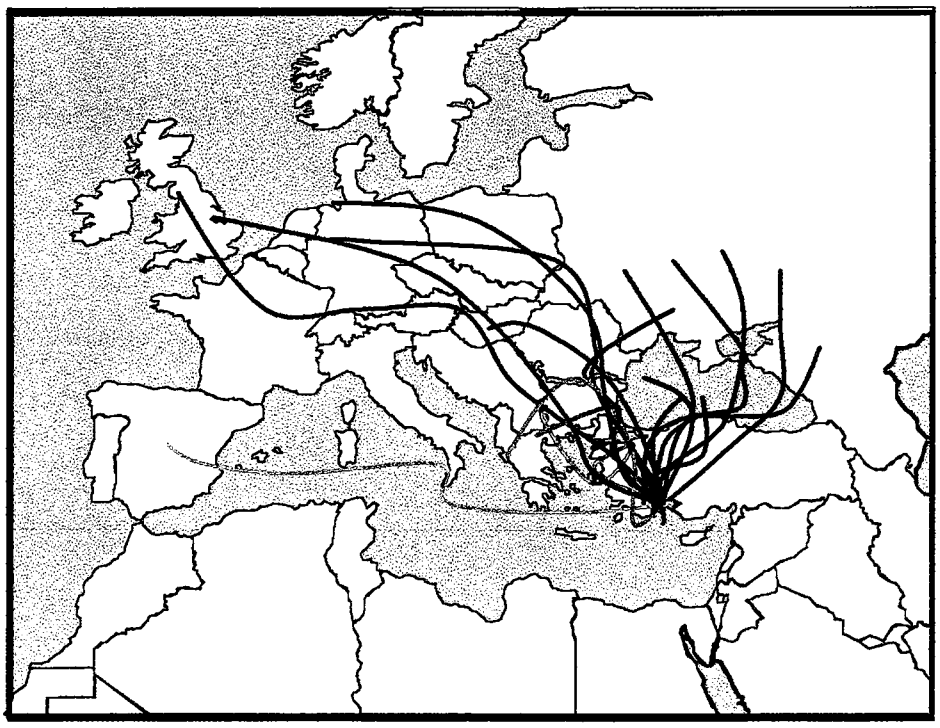

Figure C3. ECMWF trajectories ending at Antalya during August 1998 at 700 mb

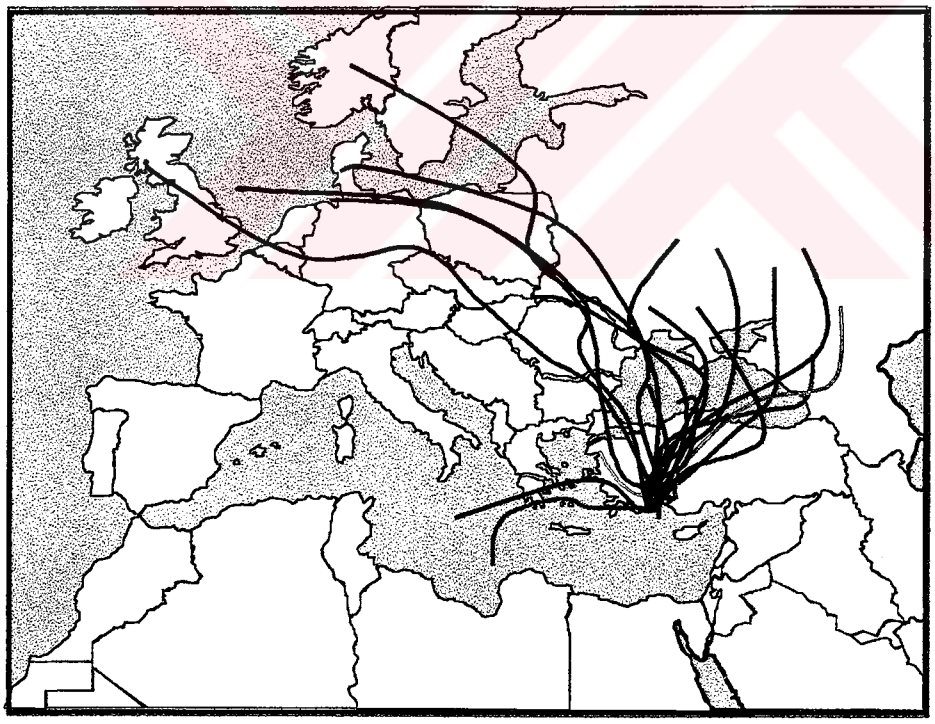

Figure C4. HYSPLIT trajectories ending at Antalya during August 1998 at 700 mb

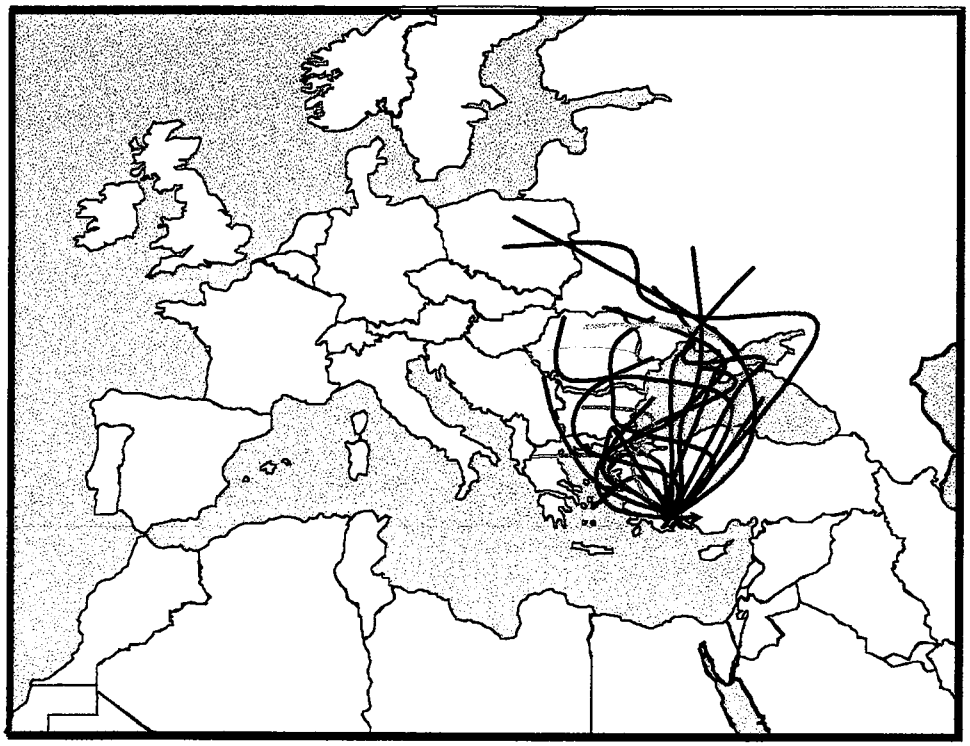

Figure C5. BAT trajectories ending at Antalya during July 1992 at 850 mb

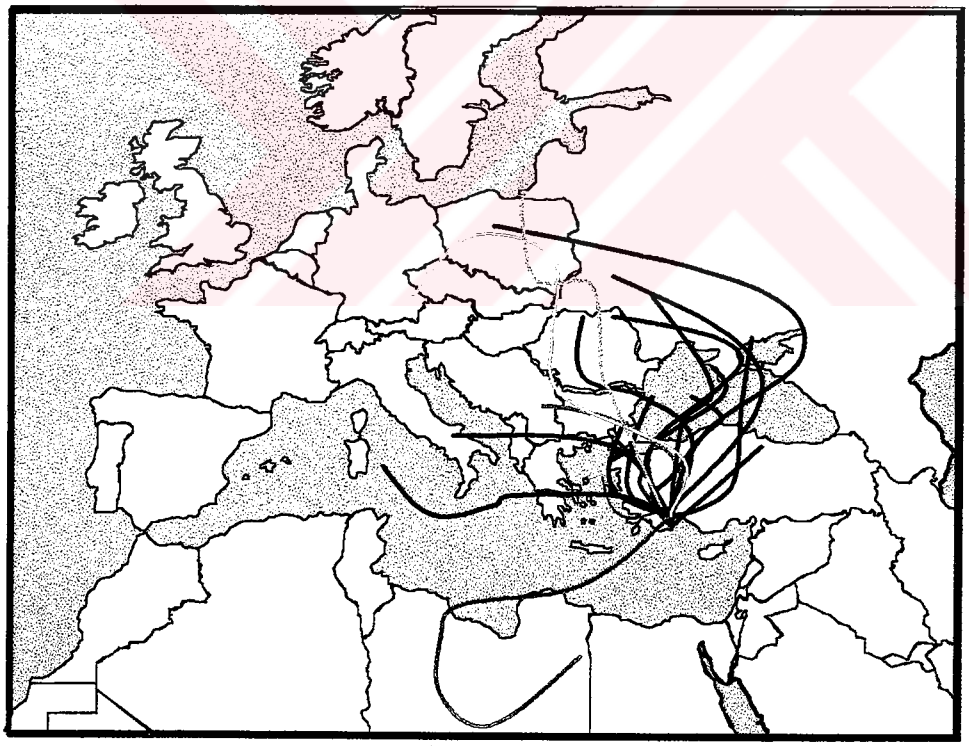

Figure C6. ECMWF trajectories ending at Antalya during July 1992 at 850 mb